UNIVERSIDADE DE LISBOA
FACULDADE DE CIÊNCIAS
DEPARTAMENTO DE ENGENHARIA GEOGRÁFICA, GEOFÍSICA E ENERGIA

Coastal Low-Level Jet and El Niño-like phenomenon at the Benguela coast

Ana Carolina Santos Caldeirinha

Mestrado em Ciências Geofísicas
Especialização em Meteorologia

Dissertação orientada por:
Professor Doutor Pedro M. M. Soares (IDL- Universidade de Lisboa)
Mestre Daniela C. A. Lima (IDL- Universidade de Lisboa)

2017

ACKNOWLEDGEMENTS

First and foremost, I would like to give my most sincere thanks to my co-supervisor Pedro M. M. Soares for his guidance and unending patience, which were essential in the concretization of this thesis.

A special thanks to my co-supervisor Daniela C. A. Lima for the advices and assistance given throughout this work, helping me solve all the obstacles I came across during the whole process.

I would like to express my gratitude to Rita Cardoso for always being available to clear all my doubts.

To Hugo, Miguel and Susana, for standing by my side through my very best and also my most insufferable moments.

The warmest thanks to my lunch squad: Ana, Inês, João, Miguel and Sandra, for receiving me with open arms and for all the high-spirited laughs. Also, to the friends I couldn't mention and accompanied my journey, I give the greatest thanks.

Last, but not once the least, to my parents and brother. Even half an ocean away they are my unfaltering support. Without them, I would not be where I am.

RESUMO

Em determinadas regiões do globo, os ecossistemas costeiros são muito dependentes do afloramento de águas subsuperficiais, mais frias e ricas em nutrientes. Estas regiões são fortemente influenciadas pela interação do vento costeiro na superfície do oceano, pelo que qualquer alteração na frequência e intensidade deste forçamento pode alterar esta dinâmica e pode produzir impactos no clima regional, nos ecossistemas costeiros e, consequentemente, socioeconómicos. A região de Benguela é um destes sistemas de afloramento (*upwelling*) costeiro que se encontram no bordo leste dos oceanos. À semelhança dos seus sistemas homólogos, é influenciada por um jato costeiro de baixa altitude (*coastal low-level jet*, CLLJ). O jato de Benguela é um fenómeno de mesoescala quase-permanente ao longo do ano, caracterizado por dois núcleos de velocidades máximas superiores a 10 m/s, sendo mais intenso durante a primavera austral. O jato está contido na camada limite marítima (*Marine Atmospheric Boundary Layer*, MABL), onde é encontrado tipicamente abaixo dos 500 metros acima do nível do mar. O CLLJ de Benguela ocorre ao longo do flanco leste do sistema de altas pressões do Atlântico Sul, ao longo da corrente fria de Benguela, que se propaga em direção ao Equador. Na região do jato, ventos paralelos à costa sobre o oceano geram correntes para o largo, transportando as águas superficiais, e, consequentemente, provocando o afloramento de águas mais profundas e mais frias. Durante os meses de verão, principalmente, a presença de uma baixa térmica sobre o continente, provocada pelo aquecimento intenso da superfície, vai provocar um gradiente horizontal de temperatura e pressão entre o oceano e o continente. O mecanismo de formação do jato advém da presença do Anticiclone do Atlântico Sul, e é reforçado pela baixa térmica. A ocorrência do jato pode aumentar localmente a intensidade do vento, que por sua vez diminui a temperatura à superfície do oceano (*Sea Surface Temperature*, SST), estabelecendo-se um mecanismo de realimentação entre a atmosfera e o oceano.

Além do CLLJ, outro fenómeno afeta o sistema de *upwelling* de Benguela. Em determinados anos, verifica-se um aquecimento anómalo das águas superficiais na região de *upwelling* de Angola-Benguela, em muito semelhante ao El Niño no Pacífico. Por esta razão, e dada a sua localização, este fenómeno é conhecido como Benguela Niño. Do mesmo modo, os eventos de arrefecimento anómalo da superfície do oceano também verificados na região são denominados Benguela Niña. O Benguela Niño tem vários impactos sobre o clima da região, nomeadamente um aumento da precipitação em Angola, e também sobre os ecossistemas marinhos, provocando, por exemplo, a migração e um aumento da mortalidade de várias espécies. Embora não haja acordo sobre o que provoca estes eventos de aquecimento anómalo do oceano, muitos autores defendem que advém de um enfraquecimento do campo do vento (seja ele local ou de origem remota).

Tanto o CLLJ como o Niño de Benguela têm sido objeto de estudo, embora separadamente. Como tal, a relação entre os dois fenómenos não é de todo conhecida. Dada a importância biológica e socioeconómica desta região de *upwelling* costeiro, é imperativo compreender a ligação entre os dois fenómenos que a afetam.

Pela primeira vez, nesta tese é apresentado um estudo sobre a variabilidade espacial e a estrutura vertical das propriedades físicas da MABL na região de Angola-Benguela, quando sobre a influência de eventos de Benguela Niño e de ocorrência de jato no seu núcleo norte, estabelecendo-se uma relação entre ambos. Para o efeito, utilizou-se a base de dados de alta resolução *NOAA Optimal Interpolation Sea Surface Temperature V2* (OI SST V2), para o período de 1981 a 2016, assim como dados de superfície e de níveis verticais da reanálise *Japanese 55-year Reanalysis* (JRA-55), entre 1980 e 2016. Estudaram-se os campos de temperatura a 2 metros e à superfície do oceano, fluxo de calor latente e sensível, fluxo de momento, subsidência, temperatura potencial, pressão à superfície, humidade específica e vento aos vários níveis.

De modo a estudar o comportamento da MABL quando condicionada por Benguela Niño e Niña, foi desenvolvido um catálogo de eventos baseado na análise de anomalias de SST. Assim, um evento de Niño (Niña) é definido caso as anomalias de SST na região de Angola-Benguela se mantenham superiores a +0.5ºC (–0.5ºC) por um período de, pelo menos, 5 meses consecutivos. Deste catálogo, resultaram 6 eventos de Benguela Niño e 9 de Niña. Os restantes casos foram atribuídos como sendo neutros. A partir do catálogo estabelecido, foram determinados compósitos de SST. Estes consistem no agrupamento de todos os eventos de Niño (e Niña), ao qual foi aplicada uma média. Foi também desenvolvido um catálogo de intensidade de ventos do jato: este foi considerado forte quando a sua anomalia média diária excedia o percentil 90, e fraco quando esta se encontrava abaixo do percentil 10. Os compósitos de vento do jato foram calculados do mesmo modo que os compósitos de SST. As propriedades físicas apresentadas anteriormente foram investigadas com base em cada um destes catálogos de modo a compreender a relação entre o Benguela Niño e o CLLJ.

Este estudo demonstra que o jato é grandemente influenciado pelo campo do vento local. No entanto, uma intensificação do vento à superfície não está necessariamente ligada à ocorrência de jato. Este resultado sugere que a intensificação do vento à superfície depende de outros fatores que não o CLLJ. Assim, o estudo do jato deve ser realizado tendo em conta o vento na altitude do jato, em vez do campo superficial, como foi efetuado em alguns estudos.

Quanto às análises superficiais e verticais das variáveis físicas, existem evidências da relação entre o núcleo norte do jato de Benguela e os eventos de Benguela Niño. Um jato forte (fraco) tem uma assinatura superficial análoga à da Benguela Niña (Niño). De facto, foi demonstrado que o jato é mais forte (fraco) durante Niñas (Niños), face a um caso neutro de anomalia de SST. A análise vertical da estrutura das propriedades físicas da MABL mostra que o jato é menos frequente durante Niños que Niñas. Quanto à sua altitude, o CLLJ é encontrado a maiores altitudes na MABL durante Benguela Niñas. Em Niños, a altitude do jato tem menor variabilidade, encontrando-se entre os 275 m e os 400 m em 50% dos casos. De um modo geral, o jato de Benguela é situado abaixo da altura da camada limite marítima, e tem uma extensão vertical de várias centenas de metros.

Embora os fluxos de calor e de momento influenciem o jato, são verificadas situações em que as propriedades estudadas não apresentam uma relação clara com a ocorrência de jato. Conclui-se que a região de Angola-Benguela tem interações complexas não completamente esclarecidas pela metodologia aqui seguida, pelo que a relação entre o Benguela Niño e o núcleo norte do jato deve ser aprofundada considerando outros fatores no futuro.

Por último, o presente trabalho mostra como uma análise espacial do vento à superfície é insuficiente para estudar o desenvolvimento do jato de baixa altitude, tanto em conjugação com outros fenómenos físicos, como o Benguela Niño, ou por si só. A relação entre os dois é mais complexa do que uma análise superficial demonstra, pois afeta toda a extensão vertical da MABL.

Palavras-chave: camada limite atmosférica, jato costeiro de baixa altitude, Benguela Niño, interação terra-atmosfera-oceano.

ABSTRACT

The Benguela Eastern Boundary Upwelling System (EBUS) is characterised by intense coastal upwelling off the southwestern Africa, and is one of the most productive marine ecosystems in the world's oceans. Its highly nutrient-rich waters make this EBUS an essential habitat to many species and is crucial in supporting the livelihood of the local population. Forced by the wind-driven equatorward Benguela Current, the upwelling system is influenced by the surface winds. In turn, these are associated with the quasi-permanent Benguela Coastal Low-Level Jet (CLLJ), an atmospheric feature characterised by wind speeds superior to 10 m/s and especially intense during the austral spring. Every few years, an El Niño-like phenomenon affects the Benguela coastal region, disrupting the fragile upwelling ecosystems and the regional climate. This anomalous warming of the ocean surface is known as Benguela Niño, and may reach, in average, SST anomalies of 1.5ºC. While the El Niño and some CLLJs have been extensively studied in separate, little has been documented about their respective Benguela counterparts, and the relationship between the two features is rather unexplored. This study uses the high-resolution NOAA Optimal Interpolation Sea Surface Temperature V2 (OI SST V2) dataset and the Japanese 55-year Reanalysis (JRA-55) surface and model-level data for the time period between 1980 to 2016. For the first time, it is shown how the vertical structure of the marine atmospheric boundary layer (MABL) physical properties respond to the influences of both the Benguela Niño and the northern core of the CLLJ, establishing a connection between the two highly-impactful phenomena. Although the period studied is limited and the sampling for the Niño and Niña events is small (6 and 9 identified events for Niño and Niña, respectively), some characteristics of the Benguela jet for SST-based composites of Niño, Niña and "neutral" cases are presented. There is evidence that the physical background associated with the Benguela Niño (Niña) sustains weaker (stronger) manifestations of the Benguela CLLJ, and place it lower (higher) in the MABL. During Niños, the jet is also less frequent than Niñas. It is also shown that a horizontal spatial analysis of the surface wind field is insufficient to study the development of the Benguela CLLJ, and even the study of the vertical structure of the MABL properties cannot relay all the complex interaction between the lower atmosphere and the surface.

Keywords: marine atmospheric boundary layer, coastal low-level jet, Benguela Niño, land-atmosphere-ocean interaction.

CONTENTS

Acknowledgements ..... **i**
Resumo ..... **iii**
Abstract ..... **v**
Contents ..... **vi**
List of Figures ..... **vii**
List of Tables ..... **ix**
List of Acronyms ..... **x**
1. Introduction **1**
2. Fundamental concepts: an overview **2**
2.1 Global Upwelling Systems 2
2.2 The Benguela region 3
2.3 Benguela Niño: an El Niño-like phenomenon 4
2.3.1 Forcing mechanisms 4
2.3.2 Impacts 6
2.4 An overview of Coastal Low-Level Jets 6
2.5 Benguela Coastal Low-level Jet 9
2.5.1 Jet Structure 9
2.5.2 Variability 11
3. Data and methods **12**
3.1 Data 12
3.1.1 NOAA OI SST V2 High Resolution Dataset 12
3.1.2 JRA-55 Reanalysis 12
3.2 Methodology 13
3.2.1 Jet detection algorithm 13
3.2.2 Regions of interest 14
3.2.3 Building the Niños catalogue and SST composites 15
3.2.4 Building the CLLJ catalogue and jet wind composites 16
3.2.5 MABL properties: temporal and spatial analysis 16
4. Results **18**
4.1 Benguela Coastal Low-Level Jet 18
4.2 Surface wind, low-level jet wind and the surface temperature 19
4.3 Relationship between BCLLJ and Benguela Niño 32
5. Summary and conclusions **45**
References **47**
Appendix **51**

LIST OF FIGURES

Figure 2.1 – Schematic of the coastal upwelling due to alongshore wind coupled with Ekman transport, in the Northern Hemisphere. Source: Talley et al., 2011. 2
Figure 2.2 – Mean surface pigment concentrations from the SeaWiFS ocean color sensor, averaged over its full mission (September 1997–December 2010), with the eastern boundary current systems (EBCs) outlined in white. Source: Strub et al., 2013. 3
Figure 2.3 – Representation of the Benguela region bathymetry (blue hues) and topography (green to brown) with the 1 arc-minute global model ETOPO1. Red line represents the cross-section studied in this thesis. 4
Figure 2.4 – Schematic of the inter and intra-basin relationships proposed to explain Benguela Niños mechanisms. 5
Figure 2.5 – CLLJ frequency of occurrence (%) for (a) JJA and (b) DJF, with regions of interest enclosed in red. Source: Ranjha et al., 2013. 7
Figure 2.6 – Conceptual model of lower atmosphere for the coast of California during the day. Source: Beardsley et al., 1987. 8
Figure 2.7 – (a) Mean vector winds (m/s) and (b) SST (ºC) for October in southeastern Atlantic. Contours indicate speed. Values averaged for the period 1948 to 2005. Source: Nicholson, 2010. 9
Figure 2.8 – 3D perspective of the marine layer for a case study with expansion and compression of the MABL. Source: Winant et al., 1988. 10
Figure 3.1 – SST anomaly for the Niño-3.4 region during the period September 1981 to December 2010. Datasets: NOAA High Resolution Dataset (orange) and Extended Reconstructed Sea Surface Temperature version 4 (blue). 12
Figure 3.2 – Map with the region of occurrence of the Benguela Coastal Low-Level Jet (blue) and the Angola-Benguela Area (orange). 14
Figure 3.3 – SST mean anomalies for time period of 09/1981 to 12/2016 for the ABA region. Positive values shown as red and negative as blue. Dashed lines indicate ± 0.5 ºC limits. 15
Figure 3.4 – Boxplots of the SST anomalies averaged over the Niño-3.4 (left) and the ABA (right) regions. 15
Figure 4.1 – Seasonal Benguela Coastal Low-Level Jet properties: frequency of occurrence (a) and mean wind speed (b) for the Benguela region. For each group the 4 panels refer to the months of December to February (DJF), March to May (MAM), June to August (JJA), and September to November (SON), as indicated on the top of each panel. 18
Figure 4.2 – SST anomaly averaged over the ABA region for the time period between September 1981 and December 2016. Red line represents the Theil-Sen regression. 19
Figure 4.3 – As in Fig. 4.2, but for the jet wind anomaly, regarding the climatology 1980-2016. 19
Figure 4.4 – As in Fig. 4.3, but for the jet frequency of occurrence anomaly. 20
Figure 4.5 – As in Fig. 4.3, but for the surface wind anomaly. 20
Figure 4.6 – Conditional probabilities of an intense surface wind given that: the jet does occur (a); the jet does not occur (b), and the probability that: the jet does not occur (c); the jet occurs (d), given that the surface wind is intense. 21
Figure 4.7 – 2-meter temperature (top panels) and respective anomaly (bottom panels) over the ABA region, averaged for the cases of strong (left), weak (centre) and neutral (right) jet. 21
Figure 4.8 – As in Figure 4.7 but for the sea surface temperature and with black arrows on the top panels representing the jet wind speed anomaly field for each case, respectively. 22

Figure 4.9 – Surface pressure over the SE Atlantic Ocean (top), and its respective anomaly field over the Benguela (middle) and ABA regions for strong (left), weak (centre) and neutral (right) jet. 23
Figure 4.10 – As in Figure 4.7 but for the latent heat flux. 24
Figure 4.11 – Sensible heat flux anomaly field in the ABA region for cases of strong (left), weak (centre) and neutral (right) jet. 25
Figure 4.12 – As in Figure 4.11, but for the specific humidity anomaly. 25
Figure 4.13 – As in Figure 4.7, but for the momentum flux anomaly. 26
Figure 4.14 – Sea surface temperature (top panels) and respective anomaly field (bottom panels) averaged over the Benguela Niño (left), Niña (centre) and neutral (right) cases. 27
Figure 4.15 – As in Figure 4.14 (bottom panels), but for the 2-meter temperature anomaly field. 28
Figure 4.16 – As in Figure 4.14 but for the surface pressure in the Benguela region. 28
Figure 4.17 – Surface wind speed anomaly (top panels) and jet wind speed anomaly (bottom panels) averaged over the Benguela Niño (left), Niña (centre) and neutral (right) cases. The black arrows represent the wind speed anomaly field and the colours the magnitude of the anomaly. 29
Figure 4.18 – As in Figure 4.15, but for the specific humidity anomaly. 30
Figure 4.19 – As in Figure 4.15, but for the latent heat flux anomaly. 30
Figure 4.20 – As in Figure 4.15, but for the sensible heat flux anomaly over the sea (top panels) and for the whole ABA region (bottom panels). 31
Figure 4.21 – As in Figure 4.15 but for the momentum flux anomaly. 32
Figure 4.22 – Probability density functions for the anomalies of jet frequency of occurrence (top) and of jet wind intensity (bottom) for the composites of Benguela Niña (blue), Niño (orange) and neutral (yellow), and full time series (purple). 33
Figure 4.23 – Vertical distribution of the wind speed intensity (left panels) and its anomaly (right panels) for the west-east cross section at the jet northern core, averaged for the cases of strong (top), weak (middle) and neutral (bottom) jet. Grey area is the topography represented with the 1 arc-minute global model ETOPO1. 34
Figure 4.24 – As in Figure 4.23, but for the zonal wind component. 34
Figure 4.25 – As in Figure 4.23 (right panels), but for the potential temperature anomaly. 35
Figure 4.26 – As in Figure 4.23, but for the omega fields and overlaid with the jet wind speed (left panels) and anomaly (right panels) contour lines. 35
Figure 4.27 – Vertical distribution of the wind speed anomaly for the west-east cross section at the jet northern core, averaged over the Benguela Niño (top), Niña (middle) and neutral (bottom) cases. 36
Figure 4.28 – As in Figure 4.27, but for the potential temperature anomaly. 36
Figure 4.29 – As in Figure 4.26, but for the zonal wind (left panels) and its anomaly (right panels) of each SST composite. 37
Figure 4.30 – As in Figure 4.29 but for the omega field. 37
Figure 4.31 – Mean annual cycle of potential temperature from the surface up to 3 km, when jet occurs, averaged for the full period (first panel), Benguela Niño (second panel), Niña (third panel), and neutral (fourth panel). The black line indicates the jet height, respectively for each case. 38
Figure 4.32 – Distributions of jet height (left) and wind speed (right) for the full, Niño, Niña and neutral cases, respectively. The median values are indicated by the horizontal line inside each box, the first and third quartiles are indicated by the bottom and top sides of the box and the 10th and 90th percentiles by the whiskers. The small square inside each box indicates the mean value. 38

Figure 4.33 – As in Figure 4.31, but for the wind speed. Black arrow indicates an example referenced in the text. 40
Figure 4.34 – As in Figure 4.31, but for the vertical gradient of potential temperature. Black arrow and red circle indicate an example referenced in the text. 41
Figure 4.35 – The first and third panels show the mean annual cycle of potential temperature from the surface up to 3 km, when jet occurs, averaged for Benguela Niño and Niña, respectively. The second and forth panels show the mean annual cycle of sensible (blue) and latent (orange) heat fluxes, averaged for the Benguela Niño and Niña, respectively. Black arrows indicate examples referenced in the text..... 42
Figure 4.36 – As in Figure 4.35, but for wind speed on first and third panels. Black arrows indicate examples referenced in the text..... 42
Figure 4.37 – As in Figure 4.35, but for the specific humidity (q) and momentum flux (τ) on second and forth panels. 43
Figure 4.38 – As in Figure 4.37, but for the wind speed in first and third panels. 44
Figure 4.39 – As in Figure 4.37, but for vertical gradient of potential temperature in first and third panels. 44
Figure A1 – Cross-correlations between SST Niño 3.4 anomaly and: Benguela surface wind speed anomaly (left), and Benguela SST anomaly (right). 51
Figure A2 – Maximum correlation between SST Niño 3.4 anomaly and: Benguela surface wind speed anomaly (left), and Benguela SST anomaly (right). 51
Figure A3 – Vertical distribution of the wind speed intensity for the west–east cross section at the jet northern core, averaged for the cases of strong (top), weak (middle) and neutral (bottom) jet. 52

LIST OF TABLES

Table 3.1 – JRA-55 variables used in this work. 13
Table 4.1 – Values of jet height corresponding to the percentiles represented in Figure 4.32 (left). 39
Table 4.2 – Values of wind speed corresponding to the percentiles represented in Figure 4.32 (right). 39

LIST OF ACRONYMS

ABA	Angola-Benguela area
BCLLJ	Benguela coastal low-level jet
CLLJ	Coastal low-level jet
EBC	Eastern boundary current
EBUS	Eastern boundary upwelling system
LLJ	Low-level jet
MABL	Marine atmospheric boundary layer
SAA	South Atlantic Anticyclone
SST	Sea surface temperature

1. Introduction

The Benguela Coastal Low-level Jet (CLLJ) is a quasi-permanent atmospheric feature of the southeastern Atlantic, and has the second highest mean wind speeds of this jet type, after the Oman CLLJ (Lima *et al.*, 2017). As its worldwide counterparts, it has a direct impact over its coastal climate, playing an important role in the interaction between land, ocean and atmosphere. From time to time, an El Niño-like phenomenon affects the Benguela upwelling system, particularly the Angola-Benguela region. The anomalous warming of the surface waters known as Benguela Niño disrupts the local ecosystems, and consequently brings socio-economic impacts. While each of the introduced phenomena have been studied separately, although not extensively, their relationship is still unknown. This work explores how the ocean surface and the marine atmospheric boundary layer respond to one another when affected by both the Benguela Niño and the Benguela CLLJ. The relationship between these two phenomena is also investigated. Given the biological and economic importance of this coastal upwelling region, it is paramount to understand the connection between the two highly-impactful features.

This thesis is organised as follows. In order to grasp the fundamental concepts explored in the current study, Section 2 provides an overview of the global upwelling systems (2.1), a brief description of the Benguela region and its main features (2.2), the forcing mechanisms of the Benguela Niño and its known impacts (2.3), an overview of coastal low-level jets, such as their location and driving mechanisms (2.4), and in a more detailed manner, the main properties of the Benguela CLLJ (2.5).

Section 3 is devoted to the data and methodologies used in the thesis to obtain the results, which are presented in Section 4 and discussed in Section 5 along with the final conclusions.

2. Fundamental concepts: an overview

2.1 Global Upwelling Systems

The ocean surface circulation along the eastern boundary regions of the subtropical oceanic gyres is the result of strong alongshore winds associated to the presence of semi-permanent high-pressure systems at those latitudes (e.g., the Azores High and the South Atlantic Anticyclone (SAA) at the North and South Atlantic, respectively). These mainly meridional and equatorward winds advect the upper ocean water offshore, by Ekman transport. As continuity of mass requires a replenishment of the advected water, deeper, denser and colder water surfaces. This process is known as upwelling, which is associated with an outcropping of the isopycnicals towards the coast, creating, in turn, an equatorward geostrophic surface flux: the wind-driven eastern boundary currents (Talley *et al.*, 2011), as illustrated in Figure 2.1. Each of the four Eastern Boundary Upwelling Systems (EBUS) is, therefore, associated to its corresponding Eastern Boundary Current (EBC), as delimited in white in Figure 2.2. They include the California Current off the western North America coast and the Iberian/Canary Current along the western coasts of Iberian Peninsula and northern Africa, in the Northern Hemisphere. In the Southern Hemisphere, they encompass the Benguela Current off southwestern Africa and the Peru-Humboldt Current off western South America.

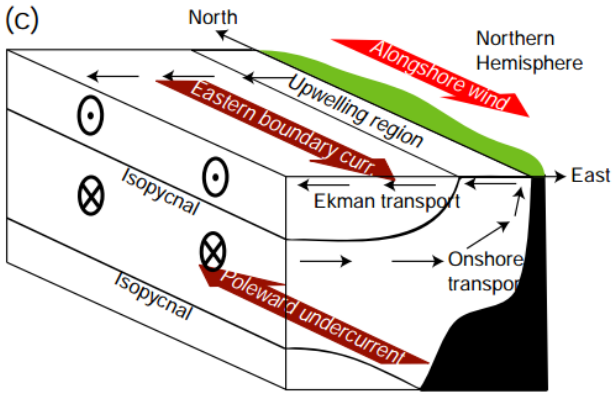

Figure 2.1 – Schematic of the coastal upwelling due to alongshore wind coupled with Ekman transport, in the Northern Hemisphere. Source: Talley et al., 2011.

The upwelling of subsurface water, colder and thus richer in nutrients than the original surface water, is a characteristic of the EBUS. Consequently, these regions are some of the most productive marine ecosystems in the Atlantic and Pacific oceans, contributing with more than 20% of the global capture fisheries, being essential habitats of marine biodiversity (Pauly and Christensen, 1995). Therefore, any change in the variability of the EBUS may have nefarious impacts on its highly vulnerable ecosystems and socio-economically, since there are about 80 million people living along the coasts near these systems (García-Reyes *et al.*, 2015). In fact, in a recent study, Bakun *et al.* (2015) stated that the EBUS may suffer both physical and biochemical modifications due to the impacts of climate change, such as ocean stratification and variations on the surface wind field distribution.

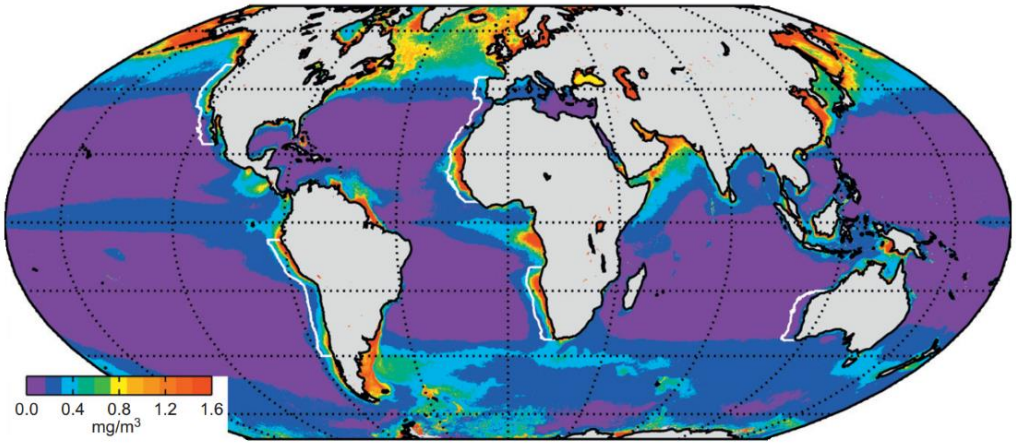

Figure 2.2 – Mean surface pigment concentrations from the SeaWiFS ocean color sensor, averaged over its full mission (September 1997–December 2010), with the eastern boundary current systems (EBCs) outlined in white. Source: Strub et al., 2013.

2.2 The Benguela region

The Benguela Current is a broad northward flow off southwestern Africa, part of the South Atlantic subtropical oceanic gyre, that develops near Cape Agulhas, at approximately 35ºS, and follows the coast towards the equator up to about 15º-16ºS, off the Angola coast (Fennel, 1999; Kämpf and Chapman, 2016). As in other eastern boundary currents, the Benguela Current is cold and driven by the eastern flank winds of the semi-permanent high-pressure system, the South Atlantic Anticyclone (SAA). However, it is most unique in the way that it is bounded by two warm currents, instead of one: the Agulhas Current to the south and the Angola Current to the north, separated from the latter by the sharp thermal Angola-Benguela Frontal Zone (Shannon *et al.*, 1987; Reason and Smart, 2015). This permanent feature suffers a southward displacement during the late summer with the intrusion of the warm Angolan water into the Benguela current (Shannon *et al.*, 1986), going as far as 17ºS, off the coast of Namibia (Shannon *et al.*, 1987; Hardman-Mounford *et al.*, 2003). As the other EBCs, the Benguela Current is accompanied by intense coastal upwelling and, therefore, high marine productivity (Kämpf and Chapman, 2016), crucial in supporting the livelihood of the people of Angola, Namibia and South Africa. In fact, it is estimated that the subsistence and commercial fisheries at the regional marine ecosystem had a direct economic impact of 517 million US dollars in 2006 (Sumaila, 2016).

The Benguela upwelling system comprises several cells along the southwestern African coast (Lutjeharms and Meeuwis, 1987). In the light of their study, and others, the Lüderitz cell, near 25ºS, is considered to be the most intense, with the lowest mean sea surface temperature (SST) of the eight wind-driven cells they identified in the southeast Atlantic, explained by the wide shelf and low eddy activity (Lachkar and Gruber, 2012). The northernmost is the Cunene cell, around 18ºS, where the Ekman drift is maximum, similarly to Lüderitz cell (Parrish *et al.*, 1983).

The Namib Desert is a narrow coastal desert, about 50 to 150 km wide. To the east, it is limited by steep topography, with coastal mountains surpassing 1000 m of elevation (Figure 2.3). To the west, it is bounded by the northward-flowing Benguela current. During summer months, as with other subtropical deserts, there is an intense surface heating due to higher solar insolation, which leads to increased outgoing longwave radiation. The air above the surface warms and expands both vertically and horizontally, which in turn reduces the air density (Ackerman and Knox, 2003). The surface pressure decreases until there is a difference of 3 to 10 mb (sometimes even greater) in comparison with the surrounding areas. Due to its nature, this mechanism is often called thermal (or heat) low (Warner, 2004).

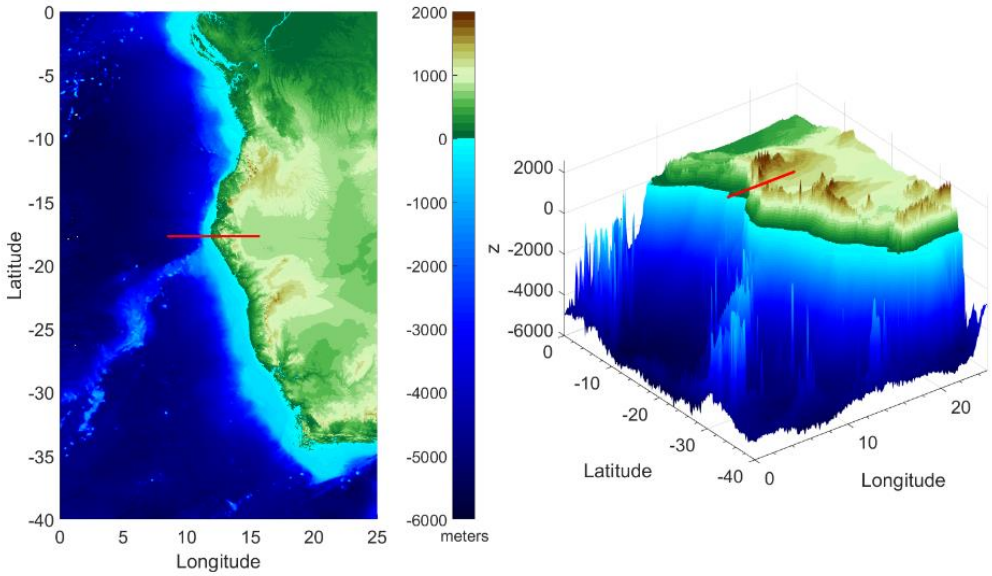

Figure 2.3 – Representation of the Benguela region bathymetry (blue hues) and topography (green to brown) with the 1 arc-minute global model ETOPO1. Red line represents the cross-section studied in this thesis.

The South Atlantic Anticyclone (SAA), particularly intense during the summer, is another atmospheric feature affecting the Benguela upwelling system, aside from the continental thermal low. This subtropical high-pressure system has a well-defined seasonality and strongly influences both the wind stress and SST fields off southwestern Africa, due to the prevailing along-shore winds that force the upwelling of the coastal waters (Risien *et al.*, 2004).

2.3 Benguela Niño: an El Niño-like phenomenon

Every few years, an anomalous warming of the ocean surface occurs over the central and eastern equatorial Pacific, persisting for many months, with several impacts over the local ecosystem and climate (see Section 2.3.2). This phenomenon is known as El Niño and has been extensively studied (e.g., Trenberth, 1997; Yeh *et al.*, 2009; Wang *et al*., 2012). In the equatorial Atlantic, there is also a similar phenomenon, termed the Atlantic Niño (e.g., García-Serrano *et al.*, 2013), which will be discussed further but is not the main subject of this study. In the last decades, several authors have drawn attention to the occurrence of El Niño-like events in the southeast Atlantic, in the upwelling region of Angola-Benguela, which disrupts the climate (Nicholson, 1997; Reason and Smart, 2015) and the local ecosystems, with impacts on the marine productivity (Binet *et al.*, 2001). In spite of being less frequent and less intense than the El Niño (Shannon *et al.*, 1986) given the similarity to its Pacific counterpart and its location, this phenomenon has been termed Benguela Niño (Shannon *et al.*, 1986). For the same reason, an anomalously cold water event is termed Benguela Niña, following the La Niña in the Pacific.

2.3.1 Forcing mechanisms

Although some Benguela Niño events have already been studied, there is still no consensus about their forcing mechanisms, of local or remote origins, or even if the Benguela Niño is a standalone phenomenon or a southward extension of the Atlantic Niño (e.g., Lübbecke *et al.*, 2010), which occurs in the equatorial region of this oceanic basin.

Several hypotheses regarding the remote mechanisms which may force the Benguela Niño events have been suggested, mostly based on the inter and intra-basin relationships between the equatorial Pacific and Atlantic, the equatorial and southeast Atlantic (i.e., the Benguela region), and the equatorial Pacific and southeast Atlantic (Figure 2.4).

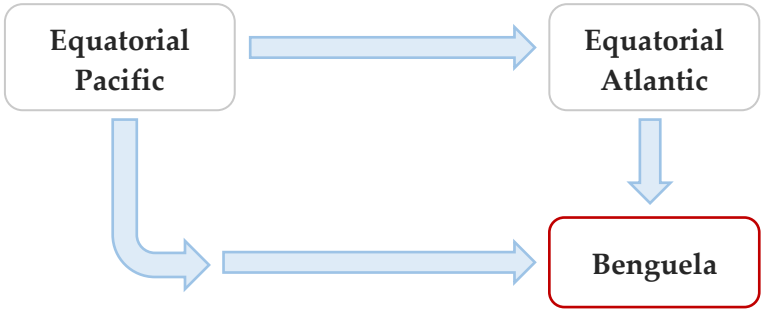

Figure 2.4 – Schematic of the inter and intra-basin relationships proposed to explain Benguela Niños mechanisms.

Through a time-space analysis of the evolution of the El Niño-Southern Oscillation (ENSO) signal in the Indic and Atlantic oceans, Nicholson (1997) suggested a connection between the Atlantic and the Pacific basins. The study shows that the equatorial Atlantic reaches its maximum cooling at the end of the year preceding the year of maximum warming on the Pacific (El Niño year). Furthermore, the maximum positive SST anomalies in the equatorial Atlantic are reached at the beginning of the year following the El Niño episode. Polo *et al.* (2014) added that an Atlantic Niño precedes a La Niña event in the Pacific, with a lag of six months between the two occurrences, assigning an order of events. On the other hand, Wang (2006) found no correlation between the Pacific and the Atlantic Niños, but states that the inter-basin SST gradient may influence tropical climate variability, instead of individual surface temperature anomalies.

A connection between the anomalous warmings of the Pacific and the Benguela coast is also a discussed topic. With NCEP reanalysis as input for the ocean model ORCA2, Colberg *et al.* (2004) showed that both the South Atlantic Ocean and its high-pressure system respond to an El Niño phase in the Pacific, with SSTs reaching their maximum at the end of the same year, and a weakening of the anticyclone throughout the year, thus changing the surface heat fluxes with a one-season lag. These results are mostly in agreement with Nicholson (1997). Nonetheless, the relationship between these events and the development of Benguela Niños is still not clear.

Using an ocean general circulation model together with satellite derived SST and sea surface height data, Florenchie *et al.* (2003) concluded that the anomalous warming which led to the Benguela Niños of 1984 and 1995 was originated near the equator, at a depth exceeding 50 m. This signal had progressed eastwards with a propagation rate consistent to the theoretical phase speed value of an equatorial Kelvin wave, until it reached the western coast of Africa, still in-depth. There, the warm anomaly started its propagation poleward, ascending to the surface at the Benguela region as a Benguela Niño event.

Lübbecke *et al.* (2010) agreed with the formation mechanism proposed by Florenchie *et al.* (2003), and added that the propagation of the Kelvin wave is caused by a modification of the trade winds intensity. These authors stated that the warm events at Benguela are preceded by a weakening of the South Atlantic Anticyclone (SAA), the dominant wind system over the basin, which comprises the midlatitude westerlies, the equatorward winds along the west coast of southern Africa and the south-easterly trade winds. A weakening of the anticyclone weakens the trade winds as well, generating

equatorial Kelvin waves, which propagate eastward (Wang, 2002), deflecting the thermocline. The equatorial Atlantic SSTs will, therefore, increase, as well as the latent heat flux to the atmosphere (Florenchie *et al.*, 2004).

Shannon *et al.* (1986) referred that changes in the alongshore local winds do not explain SST variations in the Angola-Benguela region. However, based on a coupled ocean-atmosphere model and satellite observations, Richter *et al.* (2010) argued that meridional anomalies in the local wind field are important for the development of a Benguela Niño event. These anomalies would weaken the South Atlantic high-pressure system, causing a warming at the Benguela coast 2 to 3 months later. Even though the authors do not discard the importance Kelvin waves might have on the development of warm events, they claim a variation on the local wind field has a great impact over the two regions.

2.3.2 Impacts

An abnormal increase in sea surface temperature along an upwelling region is a disturbance to the balance already established and brings important consequences to local ecosystems. As the nutrient-rich upwelled water is replaced by saline, warm waters (Shannon *et al.*, 1986), many species migrate in search of favourable conditions (Binet *et al.*, 2001; Rouault *et al.*, 2003; van der Lingen *et al.*, 2006). Gammelsrød *et al.* (1998) reported that intrusions of warm waters have been associated with mortalities of sardine, horse mackerel and kob off the coasts of Angola and northern Namibia, and rock lobsters suffer significant mortality when migrating (Cockcroft, 2001).

Many authors also reported that anomalous warm-water events in tropical southeast Atlantic were connected to increased rainfall in coastal Angola and also in northern Namibia (e.g., Rouault *et al.*, 2003; Reason and Smart, 2005; van der Lingen *et al.*, 2006).

2.4 An overview of Coastal Low-Level Jets

The marine atmospheric boundary layer (MABL) is the lowest part of the atmosphere under the direct influence of the ocean surface (Stull, 1988), where turbulent fluxes control its interactions with the atmosphere (Collaud Coen *et al.*, 2014). A low-level jet (LLJ) is a MABL mesoscale feature characterised by maximum wind speeds between 10 m/s and 20 m/s (Stull, 1988), typically found within the first 1000 m, but mostly below 500 m above sea level. Its vertical extension is in the order of hundreds of meters, while its typical horizontal extension is much larger, sometimes exceeding thousands of kilometres (Ranjha *et al.*, 2013).

The identification and location of a LLJ may be achieved using many criteria, from a simple analysis of the vertical profile of the horizontal wind, where one can determine where the maximum velocity occurs (Bonner, 1968; Stull, 1988), to more complex categorizations, based on the spatial location of the jet, its structure (both horizontal and vertical), period of occurrence, and its physical mechanism of formation (Ranjha *et al.*, 2013; Semedo *et al.*, 2016; Lima *et al.*, 2017). Several hypotheses have been proposed on what forces the LLJs, from topographic forcings to inertial oscillations on the planetary boundary layer (Stull, 1988; Stensrud, 1996). Frequently, more than one mechanism can contribute to the jet formation, discerning a specific jet type which occurs over a certain region, during a specific period of time (Stull, 1988). The coastal low-level jets (CLLJ) are a type of LLJ and will be the one of the two main foci of this work.

Most of the studies on coastal low-level jets were locally developed, being the California CLLJ the one receiving the most attention. Consequently, the proposed methodologies only applied to those specific jet areas, and were not appropriate to perform a global analysis, as it would compromise the

accurate identification of all the CLLJs or their distinction from other types of low-level jet present in the same region. The first global climatology on the CLLJs was presented by Ranjha *et al.* (2013). They used the European Centre for Medium-Range Weather Forecasts (ECMWF) ERA-interim reanalysis as the input for an algorithm based not only on the horizontal wind profile but also on the vertical absolute temperature, since the presence of a CLLJ has a distinctive signature on both. As such, the proposed algorithm applied to atmospheric vertical profiles detects a CLLJ occurrence when the following criteria are met:

1. The jet maximum is found within the lowest 2 km of the troposphere;
2. The wind speed at the maximum is at least 20% higher than at the surface;
3. The wind speed above the jet maximum decreases to below 80% of that at the surface within 5 km above the maximum;
4. The temperature at the maximum is lower than at two model levels above (inversion detection);
5. The maximum temperature does not occur at the surface, as to verify the surface-based inversion.

The use of relative values of maximum speed for the jet definition, with a decrease starting at that level, allows an identification based on the behaviour of the wind speed profile, apart from the intensity values at that level, and helps prevent the so called false positives due to peaks in the wind speed at the level of the jet. Therefore, the presented set of criteria allows an objective identification of CLLJs, and can be applied to any vertical profiles. The global CLLJ frequency of occurrence distribution obtained from this methodology is shown in Figure 2.5.

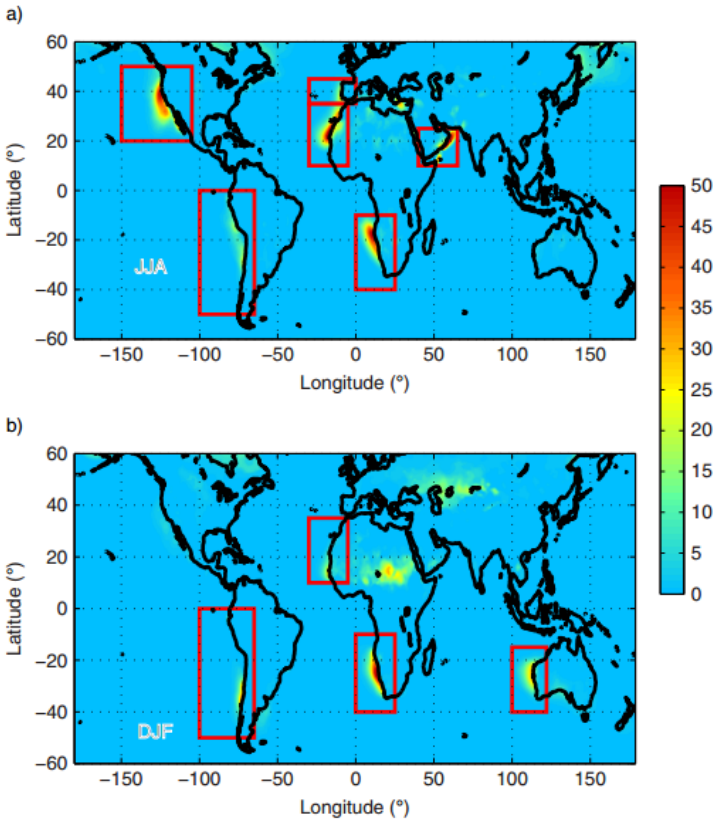

Figure 2.5 – CLLJ frequency of occurrence (%) for (a) JJA and *(b) DJF, with regions of interest enclosed in red. Source: Ranjha et al., 2013.*

Coastal low-level jets typically occur along the eastern flank of subtropical semi-permanent high-pressure systems, at mid latitudes (e.g., Ranjha *et al.* 2013; Lima *et al.*, 2017), along cold eastern boundary equatorward ocean currents. The presence of a thermal low over land, caused by intense heating of the surface mainly during summer months, and the high-pressure systems over the ocean are the main forcing mechanisms of along coast parallel winds, where the CLLJ occur (Lima *et al.*, 2017). As such, these regions should be consistent with the location of each EBUS (Figure 2.2), and the respective wind-driven surface current. In fact, as show in Figure 2.5, CLLJs occur over well-known regions of coastal upwelling. In the Northern Hemisphere the areas of CLLJ occurrence can be found along the California current (California CLLJ; Winant *et al.*, 1988; Parish, 2000) and the Canaries current (Iberian Peninsula and North Africa CLLJs, respectively; Soares *et al.*, 2014). In the Southern Hemisphere, CLLJs can be found along the Humboldt current (Peru-Chile CLLJ; Garreaud and Munõz, 2005; Munõz and Garreaud, 2005), the Benguela current (Benguela CLLJ; Nicholson, 2010) and the western Australia (Western Australia CLLJ); Stensrud, 1996). The only CLLJ not located over an EBUS is the Oman CLLJ, at the Arabian Sea (Ranjha *et al.*, 2013; Ranjha *et al.*, 2015). Moreover, while the other CLLJs are equatorward, the Oman CLLJ propagates away from the equator. This difference lies in its being under the influence of the boreal summer Indian Monsoon system, which forces a parallel flux along the Arabian Peninsula south-eastern coast, and the Somali non-coastal low-level jet (Findlater, 1969; Ranjha *et al.*, 2013).

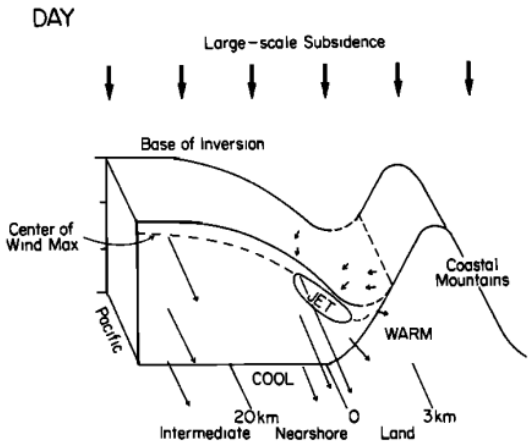

Figure 2.6 – Conceptual model of lower atmosphere for the coast of California during the day. Source: Beardsley et al., 1987.

Throughout the summer months, parallel along-shore winds cause the upwelling of deeper, colder waters near the coast. This will enhance cross-shore temperature and pressure gradients, as the thermally-induced low pressure system is present over land, leading to a local increase of wind speed and further lowering the sea surface temperature (Winant *et al.*, 1988; Semedo *et al.*, 2016). The latter generates a decrease of evaporation (or latent heat flux) and, consequently, water vapour content of the atmosphere over the ocean surface in these regions, in a positive feedback cycle. The warm, dry air of the subtropical high-pressure system of the basin subsides, establishing sharp temperature and humidity inversions when in contact with the cold well-mixed layer, thus capping the marine atmospheric boundary layer (Beardsley *et al.*, 1987; Burk and Thompson, 1996), as shown in Figure 2.6. Since the coastal upwelled waters have lower temperatures, the air at the base of the inversion will be coldest nearshore and warmer both inland and offshore, tilting it towards the coast. The inversion will thus be shallower nearshore, occasionally at lower heights than the coastal mountain range (blocking the cross-shore wind component), allowing the development of a thermal wind. The local wind flow will therefore

be enhanced, reaching its maximum right below the base of the inversion, decreasing its intensity both offshore, where the MABL is thicker, and towards the surface, due to friction (Beardsley *et al.*, 1987; Winant *et al.*, 1988; Burk and Thompson, 1996; Semedo *et al.*, 2016). This developing mechanism explains why coastal low-level jets are parallel to the coast, limited to the MABL and are generally located over coastal upwelling/eastern boundary cold current regions, as well as why they occur mostly during the summer, when the ocean-land temperature horizontal gradient is stronger.

On the other hand, the strong parallel winds restrict the advection of moist marine air inland. As a consequence, and even though this particular type of jet develops over the ocean, it is common to find dry, barren deserts in the neighbouring land. Such is the case of the Atacama and Peruvian deserts of South America and the Namib Desert of southwestern Africa, to name a few (Warner, 2004). Under these conditions, the occurrence of a coastal low-level jet may enhance the aridity of the nearby deserts already conditioned by the lack of evaporation due to the cold bordering currents.

2.5 Benguela Coastal Low-level Jet

Even though coastal low-level jets have been studied throughout the last decades, the Benguela CLLJ was only introduced and studied by Nicholson (2010). Since then, little has been published about this particular coastal wind structure, which occurs along the southwestern African coast.

2.5.1 Jet Structure

Nicholson (2010) analysed the wind field in the Benguela region using data from the NCEP-NCAR reanalysis, which has a spatial resolution of 1º latitude x 1º longitude, together with SST data from the NOAA Extended Reconstructed Sea Surface Temperature dataset. The author revealed some characteristics of the Benguela jet, referring that its core is best developed in October, at 1000 hPa, where mean wind speeds exceed 10 m/s. The jet winds are mainly southeasterly, parallel to the coast of Namibia, thus covering the strong upwelling region, and extend over a large area of the South Atlantic (Figure 2.7).

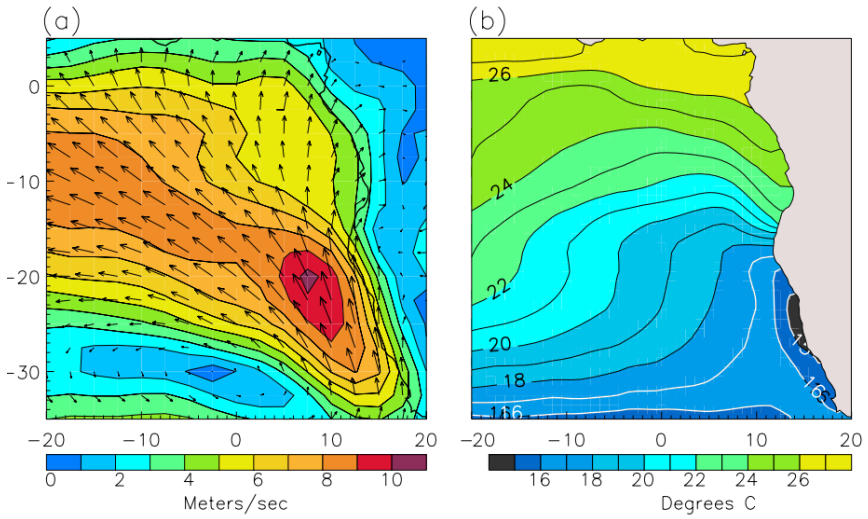

Figure 2.7 – (a) Mean vector winds (m/s) and (b) SST (ºC) for October in southeastern Atlantic. Contours indicate speed. Values averaged for the period 1948 to 2005. Source: Nicholson, 2010.

In a detailed analysis of the Benguela CLLJ based on observations, reanalyses and atmospheric model simulations, Patricola and Chang (2016) showed that the representation of the Benguela jet is highly dependent on the product chosen. Whereas products with horizontal resolution finer than ~2º identify two near-shore wind speed maxima, the ones with coarser resolution, such as the NCEP used by Nicholson (2010), do not represent this characteristic which is unique to the Benguela jet. To identify the reason behind the existence of two cores, the authors compared two Weather Research and Forecasting (WRF) simulations at 27 km: one in which the "real" coastline was represented, and the other with an exclusively meridionally oriented coastline at 17.5ºS. They found that in the latter case the northern jet maximum (at 17.5ºS) is not present.

Chao (1985) showed that when winds interact with either the coastal topography or changes in its orientation, such as the presence of a convex coastline (e.g., capes), their intensity and direction may alter. If the coast turns away from the alongshore low-level flow, the latter will respond by changing its direction and expanding horizontally. In doing so, the thickness of the MABL will decrease, accelerating the flow to supercritical speeds, in what is called in hydraulic theory the expansion fan (Figure 2.8). If, however, the coast curves outwards, the flow will be compressed and weakens as the MABL height increases, becoming subcritical. This mechanism is known as hydraulic jump (Winant *et al.*, 1988; Rogerson, 1999).

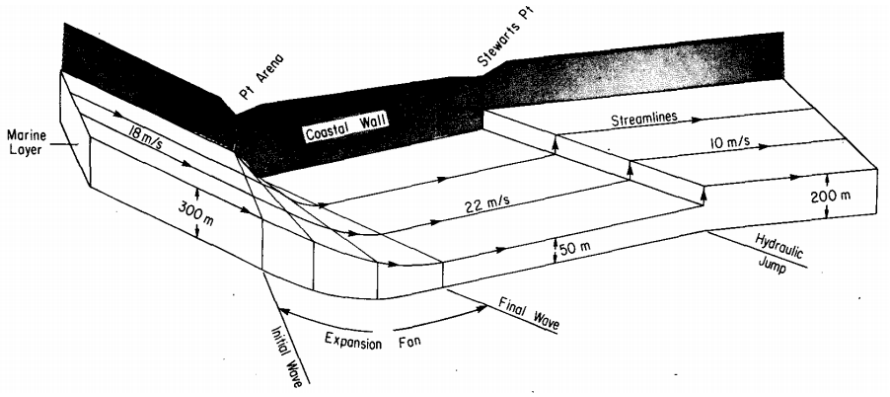

Figure 2.8 – 3D perspective of the marine layer for a case study with expansion and compression of the MABL. Source: Winant et al., 1988.

When Patricola and Chang (2016) modified the originally convex coastline, the wind speed reduced at 17.5ºS, which is consistent with the absence of the hydraulic expansion fan, and enhanced both up and downstream of the modified coastline, indicating the absence of the hydraulic jump. Since the topography remains steep in both simulations and in the light of the theory described above, the authors conclude that the modification in the Benguela CLLJ structure arises from the non-convex geometry.

A recent study showed that the Benguela CLLJ is the second most intense coastal jet (after the Oman CLLJ), with 17 m/s mean wind speed (Lima *et al.*, 2017). During the austral winter it is a relatively shallow jet, occurring frequently between 400 and 500 m above sea level. In the summer months, it is placed between 400 and 900 m. Overall, it extends about 300 km offshore, as indicated by the Rossby radius (Ranjha *et al.*, 2013). Regarding its vertical structure, Patricola and Chang (2016) considered a vertical cross section at the grid point nearest to the northern jet core (17.5ºS), as it is quasi-permanent throughout the year. The higher resolution reanalyses place the wind speed maximum (indicative of the jet core) at 975 hPa, near the coast, instead of the offshore 1000 hPa core identified by the NCEP reanalyses (Nicholson, 2010).

2.5.2 Variability

The Benguela CLLJ (BCLLJ) presents a pronounced seasonal variability in both wind speed and location. According to the output meridional wind at 10 m from the SCOW climatology (1999-2009) used by Patricola and Chang (2016), the northern jet core is located at 17.5ºS near the coast and coincides with Cunene upwelling cell and the Angola-Benguela front. It persists throughout most of the year, but is more intense during the austral transition seasons. The southern maximum is located some degrees offshore at 25º-30ºS and coincides with the Lüderitz upwelling cell. It is stronger during the austral spring and summer. Both cores have maximum wind speeds greater than 8 m/s. In the summer and winter months, the jet is essentially southeasterly (Ranjha *et al.*, 2013). The Benguela CLLJ is weaker in austral winter and the southern core is not present.

3. Data and methods

3.1 Data

3.1.1 NOAA OI SST V2 High Resolution Dataset

There are several sea surface temperature datasets available and updated to the present day, such as the Centennial In Situ Observation-Based Estimates of the Variability of SST and Marine Meteorological Variables v2 (COBE-SST2, Hirahara *et al.*, 2014) and the NOAA Extended Reconstructed SST V4 (ERSST v4, Huang *et al.*, 2015). The NOAA Optimum Interpolation Sea Surface Temperature V2 High Resolution Dataset (NOAA OI SST V2, Reynolds *et al.*, 2007) was selected since it provides a finer spatial resolution of 0.25º x 0.25º and one of the objects of this study is a SST anomaly-based phenomenon in a relatively confined region. This dataset is based on ocean temperature satellite observations from the infrared Advanced Very High Resolution Radiometer (AVHRR) and *in situ* platforms and it spans the period from September 1981 to the present.

To monitor the El Niño, the NOAA Climate Prediction Center uses the ERSST v4 dataset to compute the Oceanic Niño Index, an SST based index averaged over an area over the east-central Pacific (the Niño 3.4). For comparison reasons, the NOAA OI SST V2 and the ERSST v4 were averaged over the Niño 3.4 region and the result of the SST anomalies is depicted in Figure 3.1.

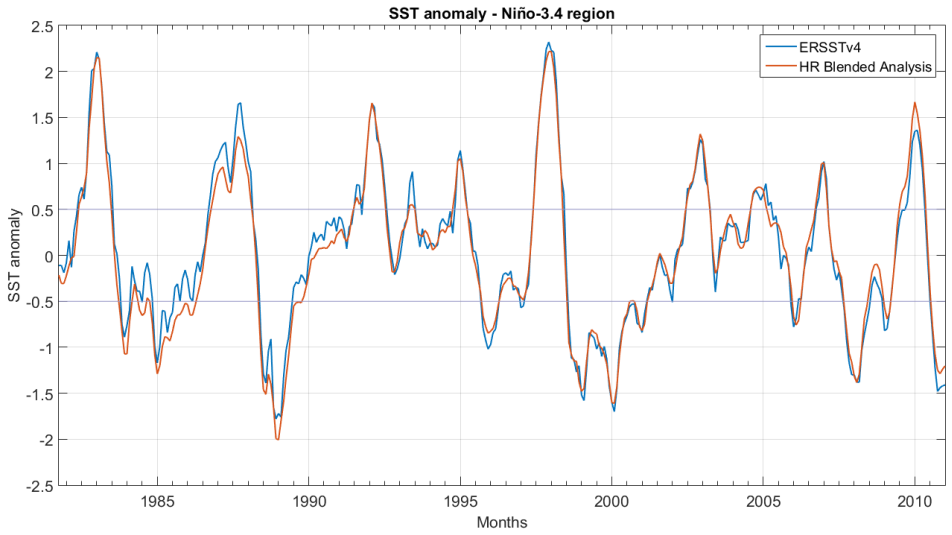

Figure 3.1 – SST anomaly for the Niño-3.4 region during the period September 1981 to December 2010. Datasets: NOAA High Resolution Dataset (orange) and Extended Reconstructed Sea Surface Temperature version 4 (blue).

The selected dataset (NOAA OI SST v2) has an overall good description of the main characteristics in the ERSSTv4. The few discrepancies between the two datasets may be attributed to the coarser 2º x 2º grid resolution of the ERSSTv4.

3.1.2 JRA-55 Reanalysis

Reanalyses have been widely used for researching the mechanisms of the earth's climate system, the study of predictability, and climate monitoring (Kobayashi *et al.* 2015). Some known global reanalyses available include the National Centers for Environmental Prediction (NCEP) Climate Forecast System Reanalysis (CFSR; Saha *et al.* 2010), the ERA-Interim (Dee *et al.*, 2011) produced by the ECMWF, and

the Japanese 55-year Reanalysis (JRA-55, Kobayashi *et al.*, 2015) carried by the Japanese Meteorological Agency (JMA). Out of the three, the JRA-55 covers the longest period (1958 to the present) and has a high resolution (TL319, ~55 km). It also represents the surface winds in an improved manner, being the most similar to the high-resolution satellite-based Scatterometer Climatology of Ocean Winds (SCOW, Risien and Chelton, 2008), as shown by Patricola and Chang (2016). Therefore, this study uses the JRA-55 to analyse the MABL structure in general, and when influenced by the Benguela Niño and the BCLLJ. The JRA-55 was produced with the higher resolution version of the JMA Global Spectral Model in reduced gaussian grid with 60 vertical levels up to 0.1 hPa, and provides atmospheric analysis based on incremental 4D-Var assimilation scheme (Courtier *et al.* 1994) every 6 hours (Kobayashi *et al.* 2015). The surface and model level variables used are presented in Table 3.1.

Table 3.1 – JRA-55 variables used in this work.

Variable	Surface	Model level
2-meter specific humidity	X	
2-meter temperature	X	
10-meter u-component of wind	X	
10-meter v-component of wind	X	
Geopotential height		X
Latent heat flux	X	
Momentum flux	X	
Potential temperature		X
Pressure	X	X
Sensible heat flux	X	
u-component of wind		X
v-component of wind		X
Vertical velocity		X

3.2 Methodology

This thesis is focused on the properties of the MABL and how they are conditioned by the Benguela Niño and the BCCLJ. As such, a methodology capable of conveying the changes in the MABL during Niño and Niña events, and under the influence of different jet intensities is presented in this subsection.

3.2.1 Jet detection algorithm

When studying the global CLLJ climatology, Ranjha *et al.* (2013) proposed a jet detection method, already presented in Section 2.4, based on the analysis of the wind speed and temperature vertical profiles derived from the ERA-Interim Reanalysis. Although several studies (e.g., Soares *et al.*, 2014; Ranjha *et al.*, 2015) have successfully detected the occurrences of coastal low-level jets using this method, it reveals some limitations. As Patricola and Chang (2016) showed, the reanalysis used by Ranjha *et al.* (2013) under-forecasts the wind speeds, and the CLLJs strength may have been underestimated. Furthermore, false detections could have been obtained in regions where CLLJs should

not be present, such as continental areas. In a recent study, Lima *et al.* (2017) revised the algorithm presented by Ranjha *et al.* (2013), which forced the temperature at the jet maximum to be lower than that at two model levels above (inversion detection). These authors argued that forcing the temperature at the jet maximum to be lower than that at two model levels above (inversion detection) discard a jet if it occurs at the top of MABL or at the level below the top, where in fact a jet may occur (e.g., Burk and Thompson, 1996; Garreaud and Muñoz, 2005; Parish, 2000). Lima *et al.* (2017) redefined that criterion of the Ranjha *et al.* (2013) algorithm to "The jet maximum is within or at the top of the MABL temperature inversion", which brought a slight increase in the detection of each coastal jet in all areas.

Lima *et al.* (2017) also used the JRA-55 reanalysis, among others, as input to the revised algorithm, of which results: the frequency of occurrence, its intensity and height, as well as the model level data when the jet occurred. In the current thesis, the Benguela CLLJ results produced by Lima *et al.* (2017) is used as base for the analysis of the jet properties and its relation with the Benguela Niño.

3.2.2 Regions of interest

In order to study if and how the Benguela Niño impacts the structure and variability of the BCLLJ, and vice-versa, an area comprising both the influence of the jet and SSTs was required. The Angola-Benguela Area (ABA; Figure 3.2 – orange box), widely used in different studies (e.g., Florenchie *et al.*, 2003; Richter *et al.*, 2010) fits this purpose best, as it harbours both the Benguela Niño events and the northern core of the CLLJ throughout the year. Other extended areas, both southward and eastwardly, were tested (not shown) but the signal of the phenomena was not as clear.

A larger area which resulted from the jet detection algorithm, described in the previous section, was also considered in this study, henceforth called Benguela Area (Figure 3.2 – blue box).

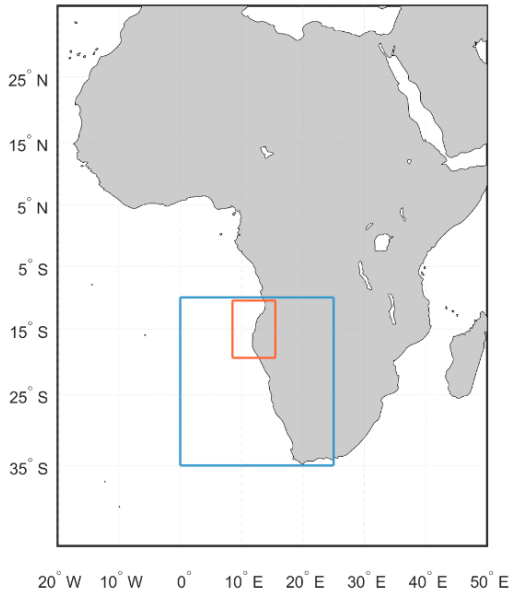

Figure 3.2 – Map with the region of occurrence of the Benguela Coastal Low-Level Jet (blue) and the Angola-Benguela Area (orange).

3.2.3 Building the Niños catalogue and SST composites

As the Benguela Niño is a phenomenon characterised by SST anomalies in the ABA region, these were calculated in each grid point of that area, relative to the monthly mean series between September 1981 and December 2016. After determining the mean spatial SST anomaly (Figure 3.3), the Niños catalogue was developed in similarity to the Oceanic Niño Index (ONI, NOAA Climate Prediction Center) methodology. Since the SST anomalies for the Niño-3.4 (over which the ONI is computed) and ABA regions have very similar statistical behaviours (Figure 3.4), it was decided to use the same approach. Therefore, a Benguela Niño (Niña) episode was defined as the period of at least 5 consecutive months with SST anomalies greater than + 0.5ºC (lesser than – 0.5ºC), on a 3-month running mean of the anomalies, previously calculated in the ABA region. The remaining months, i.e., the months not part of a Niño or Niña event, were considered as "neutral". In total, there were identified 6 Benguela Niño, 9 Niña, and 16 neutral events.

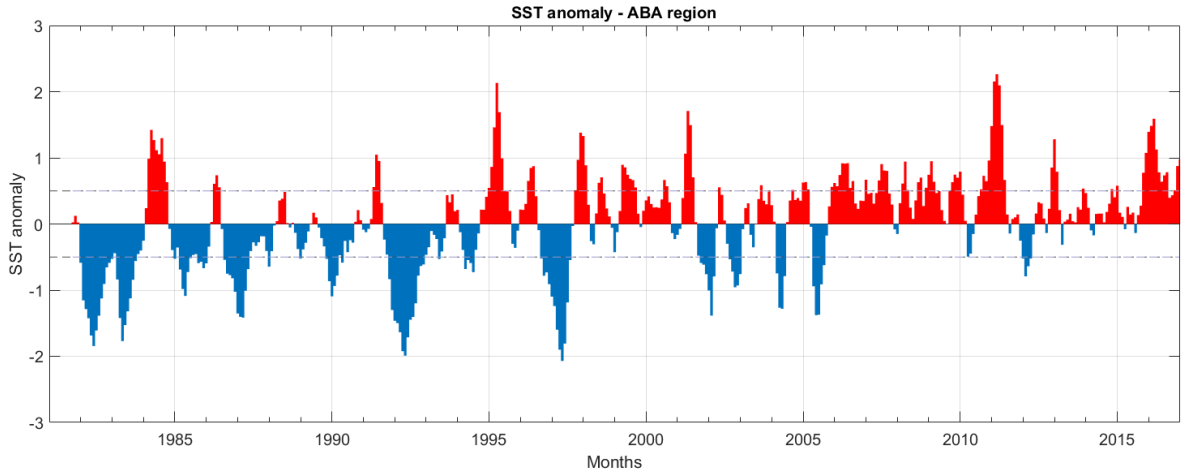

Figure 3.3 – SST mean anomalies for time period of 09/1981 to 12/2016 for the ABA region. Positive values shown as red and negative as blue. Dashed lines indicate ± 0.5 ºC limits.

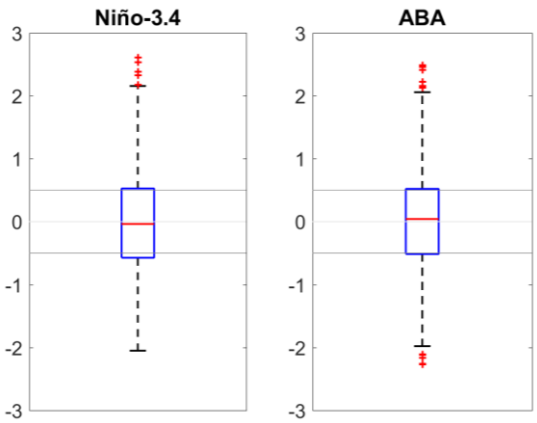

Figure 3.4 – Boxplots of the SST anomalies averaged over the Niño-3.4 (left) and the ABA (right) regions.

In order to assess how the MABL responds to the Benguela Niño and Niña, SST composites were computed based on the obtained catalogue. For the SST anomalies in the ABA grid, the months

corresponding to Niño events were aggregated and averaged. The same was performed with Niña and neutral months, forming three composites in total.

3.2.4 Building the CLLJ catalogue and jet wind composites

To define the jet catalogue, some calculations were performed beforehand. Firstly, because the JRA-55 variables hold a value for each synoptic hour, and the outputs from the jet detection algorithm maintain this temporal resolution, the daily mean for the jet wind speed was computed. Secondly, the anomalies of the obtained series were calculated for each grid point in the ABA region for the period between 1980 and 2016. Finally, these values were spatially averaged when needed. The ABA jet is then classified as "strong" ("weak") when the daily jet anomaly exceeds (is below) the 90th (10th) percentile.

The jet wind composites were obtained similarly to the SST composites. All days falling in the "strong" or "weak" category were grouped and averaged. The remaining days were considered "neutral".

3.2.5 MABL properties: temporal and spatial analysis

In an initial survey of the jet wind properties (its intensity and frequency of occurrence) and their relationship with the SST, the previously assembled time series of the respective anomalies (averaged over the ABA region) were evaluated. The tendency of each time series was determined by the Theil-Sen linear regression estimator, following the procedure proposed by Gilbert (1987). This methodology estimates the true slope (i.e., the change per unit time) of a linear trend while ignoring the gross errors and outliers present in the data. To compute the Theil-Sen estimator, it is necessary to determine the slope estimates, Q, for each station, defined in Equation 3.1 as:

$$Q = \frac{x_{i\prime} - x_i}{i' - i} \tag{3.1}$$

where $x_{i\prime}$ and $x_i$are data values at times i' and i, respectively, and where $i' > i$. The Theil-Sen estimator is then defined as the median of Q. These tendencies, however, should be analysed with caution, as the reanalyses have been proven to be somewhat biased under long-term trend monitoring (Bengtsson et al., 2004).

To better understand the local connection between the surface wind and the jet wind, four conditional probabilities were computed. The first two are the probabilities of an intense surface wind (A), which is defined as greater than its 75th percentile for each grid point, conditioned on the following events: 1) the jet does occur (B_1) and 2) the jet does not occur (B_2). The remaining two are 3) the probability that the jet does occur given that the surface wind is intense $P(B_1|A)$, and 4) the probability that the jet does not occur given that the surface wind is intense, $P(B_2|A)$.

These quantities can be computed for each point in the region by the following ratios:

$$\begin{cases} P(A|B_i) = \dfrac{P(A \cap B_i)}{P(B_i)}, \text{for cases 1) and 2)} \\ P(B_i|A) = \dfrac{P(B_i \cap A)}{P(A)}, \text{for cases 3) and 4)} \end{cases} \tag{3.2}$$

where i = 1, 2 depending on the case and assuming $P(B_1) \neq 0$ and $P(B_2) \neq 0$ on cases 1) and 2) and assuming $P(A) \neq 0$ on cases 3) and 4), since the probability is not defined if the denominator vanishes.

In order to investigate the Benguela Niño (and Nina) signal on the jet properties, the probability density function was calculated for the frequency of occurrence and jet wind speed anomalies for each SST composite, averaged over the ABA box. Since the input data consist of anomalies and not their original values, the Gaussian (or normal) distribution is the best fit, instead of the Weibull distribution, typically used when analysing wind speed data (Harris and Cook, 2014). The probability density function (PDF) of a normal distribution is given by:

$$\mathcal{N}(x|\mu,\sigma^2) = \frac{1}{\sigma\sqrt{2\pi}} e^{\frac{-(x-\mu)^2}{2\sigma^2}} \tag{3.3}$$

where σ^2 and μ are, respectively, the variance and the mean of the input series x (Evans *et al.*, 1993).

Because the MABL is under the direct influence of the ocean surface, any anomalous changes of the latter, for example, the occurrence of an Benguela Niño event, may perturb the physical properties of the MABL, such as the Benguela CLLJ, and vice-versa.

To understand how the surface and its fluxes are affected by the CLLJ, the properties of interest were applied to the jet wind composites. For this purpose, the SST, 2-meter temperature and specific humidity, surface pressure, surface momentum flux, and latent and sensible heat fluxes time series were averaged over each group of composites. For the JRA-55 variables, their respective anomalies were calculated regarding the period 1980 to 2016. Both the original SST values and their anomalies were conditioned to the jet wind composite. The same methodology was followed for the SST composites, this time to study the surface properties response to the Benguela Niño and Niña.

As the jet is a low-level feature, a surface analysis is insufficient to fully comprehend how it may be connected to the El Niño-like events in Benguela. Moreover, for a further understanding of the interaction between the surface and the low troposphere under the influence of such features, a vertical view is required. To this end, considering that the MABL structure is described by the model levels variables, each of these properties (Table 3.1) was computed for the jet wind composites. Since the northern jet wind maximum is the one that overlaps the area of occurrence of the Benguela Niño, the grid point closest to this core (17.5ºS) was chosen to study the ABA west-east cross-sections (Figure 2.3) for the composite-averaged variables. In addition, for this specific analysis and the next, the SST composites were redefined. Instead of the presented in Section 3.2.3, the composites were computed regarding the months of Niño, Niña and neutral, coincident with the jet occurrence. They were then gathered and temporally averaged, as the original methodology.

Finally, following the same input as the aforementioned analysis, the annual climatology of the SST and jet wind composites were computed for the full MABL. With this approach it is possible to observe the evolution of the different MABL properties throughout the year in the three SST composites, when the Benguela CLLJ occurs. As a proxy to the MABL inversion height, the vertical gradient of the potential temperature was obtained, and the jet height was studied in its context. To complete, the surface variables momentum, sensible and latent heat fluxes and specific humidity were also calculated for the annual climatology of each SST composite. This final analysis allows a simple yet insightful onlook of the ocean-atmosphere interaction when both the Benguela Niño and the BCLLJ occur.

4. Results

The original purpose of this work was to establish a relationship between the Benguela CLLJ and Benguela Niño, as well as between the Humboldt CLLJ and the El Niño, and possibly the connection between El Niño events and the Benguela CLLJ, as suggested by Nicholson (2010). There was effectively work done regarding El Niño and the BCLLJ, and Humboldt, but the results were weak and overall not satisfactory. Cross-correlations between the area-averaged Niño-3.4 SST and the Benguela surface wind series (and their respective anomalies) were calculated, in order to understand if there was some evidence of the referred influence of the El Niño over the wind (surface and low-level) in Benguela, albeit through simple methods. The maximum correlation values resulting from the cross-correlation analysis were always inferior to absolute 0.5 (Figure A1), and the correlation obtained for the whole series was inferior to absolute 0.1 for all the combinations made with the variables. The maximum correlation value corresponded to a monthly-based lag between the two input series. For this specific lag, the Niño-3.4 averaged SST was correlated to each grid point of the Benguela region, for the SST and surface wind speed (Figure A2). Again, the results were weak and this study was not pursued further. Because the dynamics involved in the Humboldt and Benguela regions are different, it was decided that the study should be focused in only one area. This way, the ocean-atmosphere dynamics during a Niño and CLLJ occurrences would be conducted more thoroughly. Due to its much-discussed importance and lack of understanding on this particular region, this work settles on the Benguela area and the interaction between Benguela Niño events and the CLLJ.

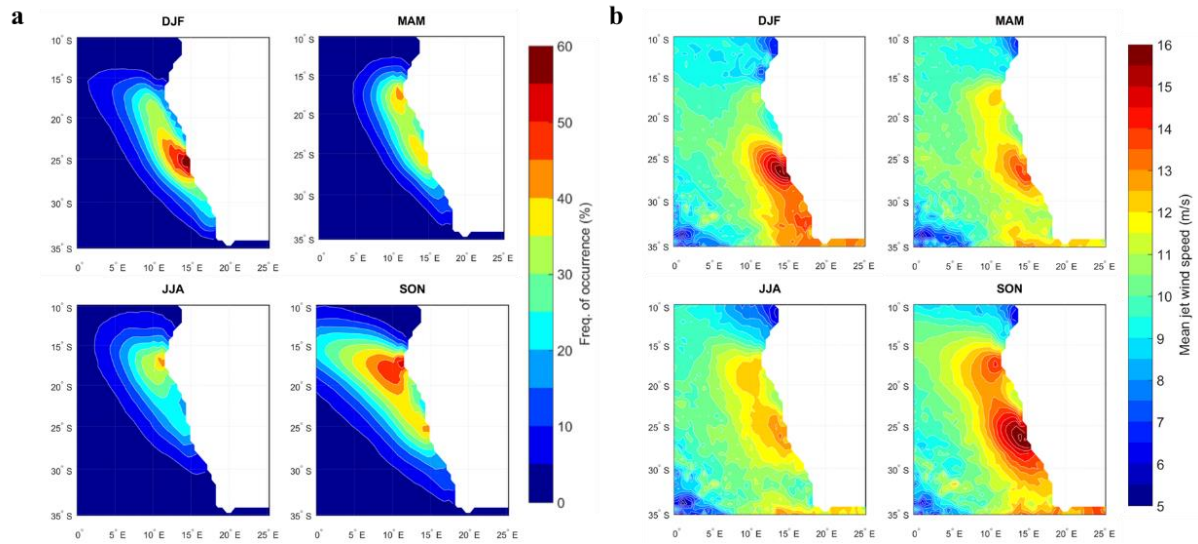

Figure 4.1 – Seasonal Benguela Coastal Low-Level Jet properties: frequency of occurrence (a) and mean wind speed (b) for the Benguela region. For each group the 4 panels refer to the months of December to February (DJF), March to May (MAM), June to August (JJA), and September to November (SON), as indicated on the top of each panel.

4.1 Benguela Coastal Low-Level Jet

The Benguela CLLJ, as aforementioned, is a quasi-permanent feature in the region. Figure 4.1 illustrates the seasonality of both the frequency of occurrence and the mean wind speed of the Benguela CLLJ. The presence of two wind speed maxima with distinct characteristics is clear. The maximum frequency of occurrence on the southern core takes place during the austral summer months, with frequency values exceeding 60%, whereas the northern core presents a maximum exceeding 50% but during the austral spring months. As for the wind speed, the southern core has stronger winds in general, with a mean exceeding 15 m/s on the austral summer and spring. However, it is less prominent on the

austral winter, although still stronger than the northern core, which has its peak on the austral spring, with a mean exceeding 13 m/s. Nevertheless, there is no doubt that the jet as a whole feature is present throughout most of the year, essentially due to its northern core, as shown by Patricola and Chang (2016).

4.2 Surface wind, low-level jet wind and the surface temperature

Investigating how the main properties of this work (SST and wind speed in ABA) have evolved over the years is crucial as a first step to understand the relationship of the Niño and the CLLJ in a global warming scenario. The Theil-Sen estimator for the SST anomaly shows an increase of 0.3ºC each decade, for the study period (Figure 4.2). Regarding the jet wind speed and frequency of occurrence anomalies, both time series have a negative tendency, of -0.4 m/s per decade (Figure 4.3) and -0.6% per decade (Figure 4.4), respectively. On the other hand, the surface wind speed anomaly time series (Figure 4.5) displays an increase (0.2 m/s per decade), showing an appearingly conflicting result.

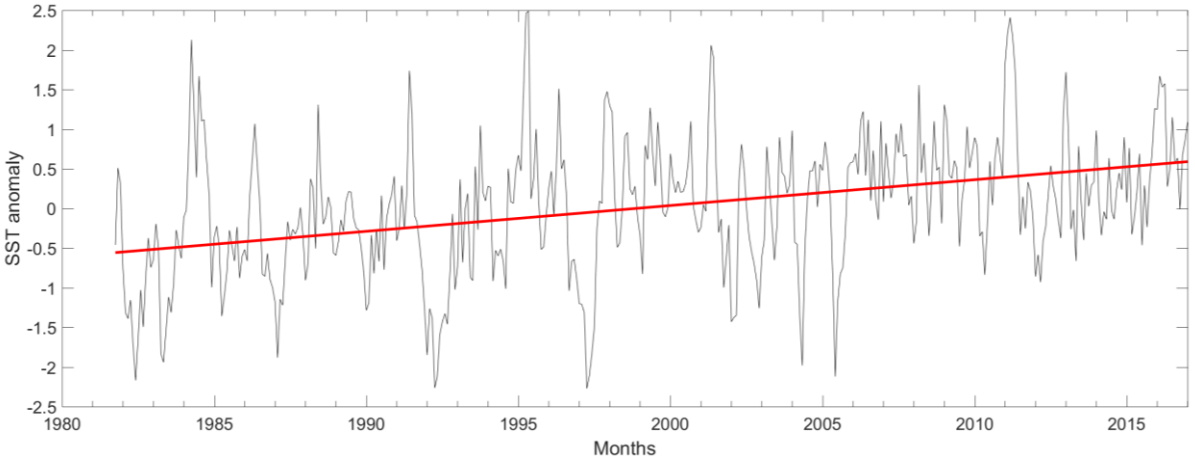

Figure 4.2 – SST anomaly averaged over the ABA region for the time period between September 1981 and December 2016. Red line represents the Theil-Sen regression.

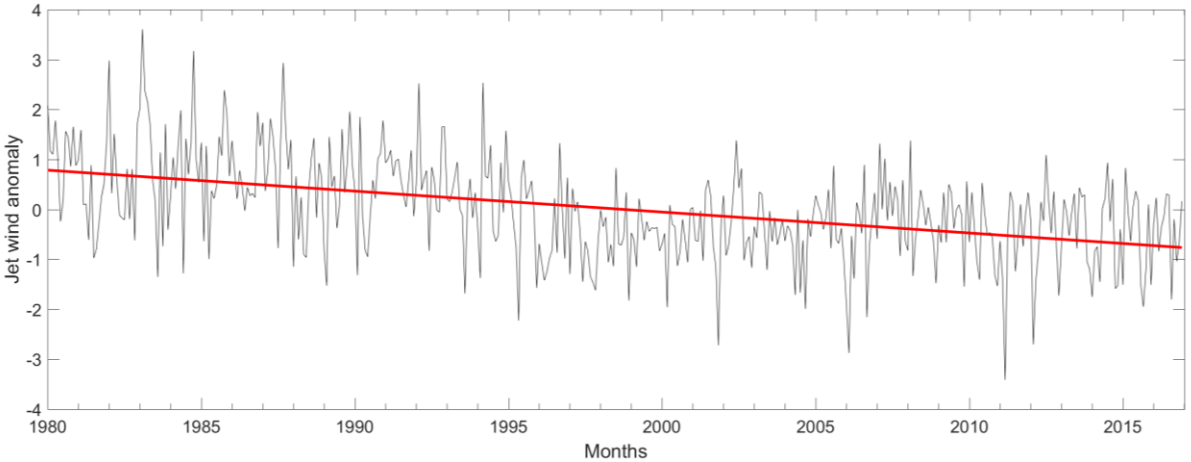

Figure 4.3 – As in Fig. 4.2, but for the jet wind anomaly, regarding the climatology 1980-2016.

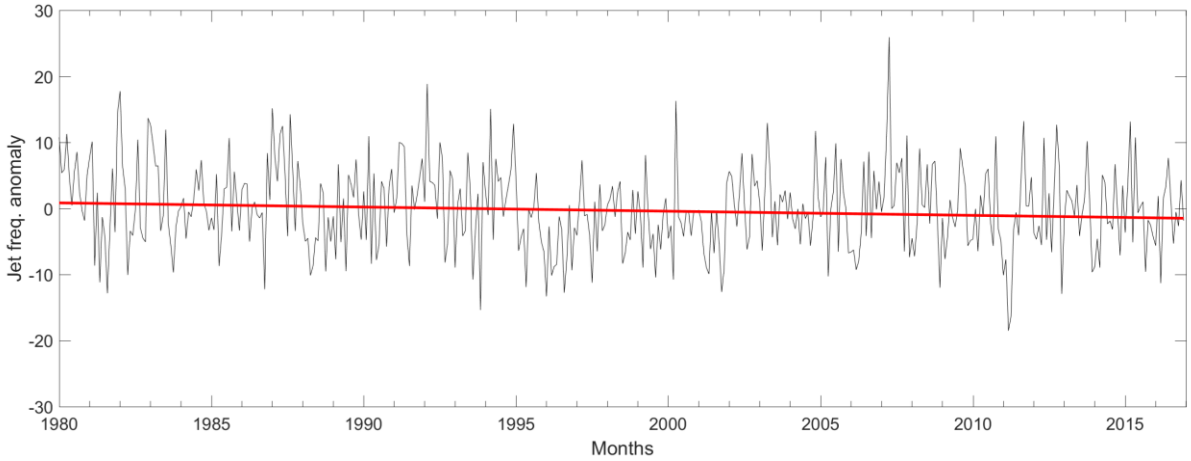

Figure 4.4 – As in Fig. 4.3, but for the jet frequency of occurrence anomaly.

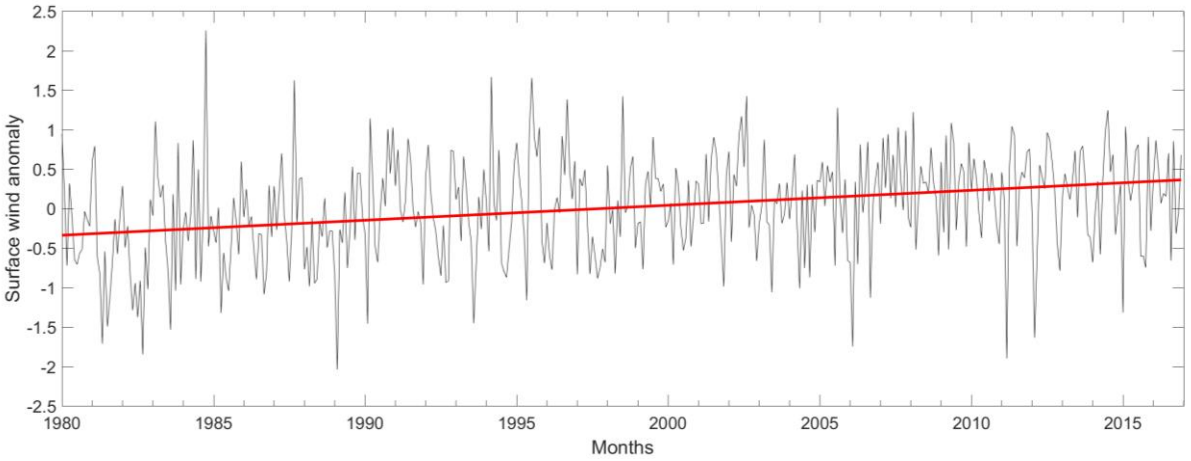

Figure 4.5 – As in Fig. 4.3, but for the surface wind anomaly.

In order to explore this apparent contradiction, some conditional probabilities considering both variables were computed and are presented in Figure 4.6. The probability that the local surface wind is strong given that the jet occurs (Figure 4.6a) is not only low, but its maximum values do not agree with the mean position of the jet cores. On the other hand, the probability that the surface wind will be intense when the jet does not occur (Figure 4.6b) is lower than 20% in the core regions. It was expected that the two probabilities would be complementary. Seeing this is not the case, it appears that the jet is a necessary, but not sufficient, condition for a local strengthening of the surface wind field. As such, there should be other factors influencing its intensity. It is possible that the surface wind anomaly increase over time is explained by the positive tendency of the SST anomaly time series, and a consequent increase of surface heat fluxes.

The probability of occurrence (or not) of the jet given that the surface wind is strong, was also computed (figures 4.6d and 4.6c, respectively). If the surface wind is intense, the probability that the jet will not occur is less than 15% on the location of the jet maxima. The opposite is shown for an occurrence of the jet: if the surface wind is strong, the probability that the jet will occur is very high (greater than 85%). These results reveal that the jet is heavily dependent on the local surface wind field, whereas the latter is subject to other factors aside from low-level winds.

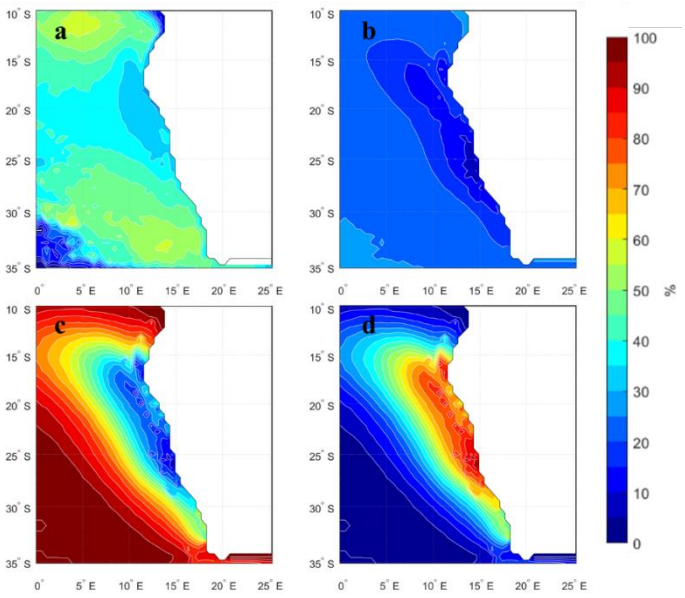

Figure 4.6 – Conditional probabilities of an intense surface wind given that: the jet does occur (a); the jet does not occur (b), and the probability that: the jet does not occur (c); the jet occurs (d), given that the surface wind is intense.

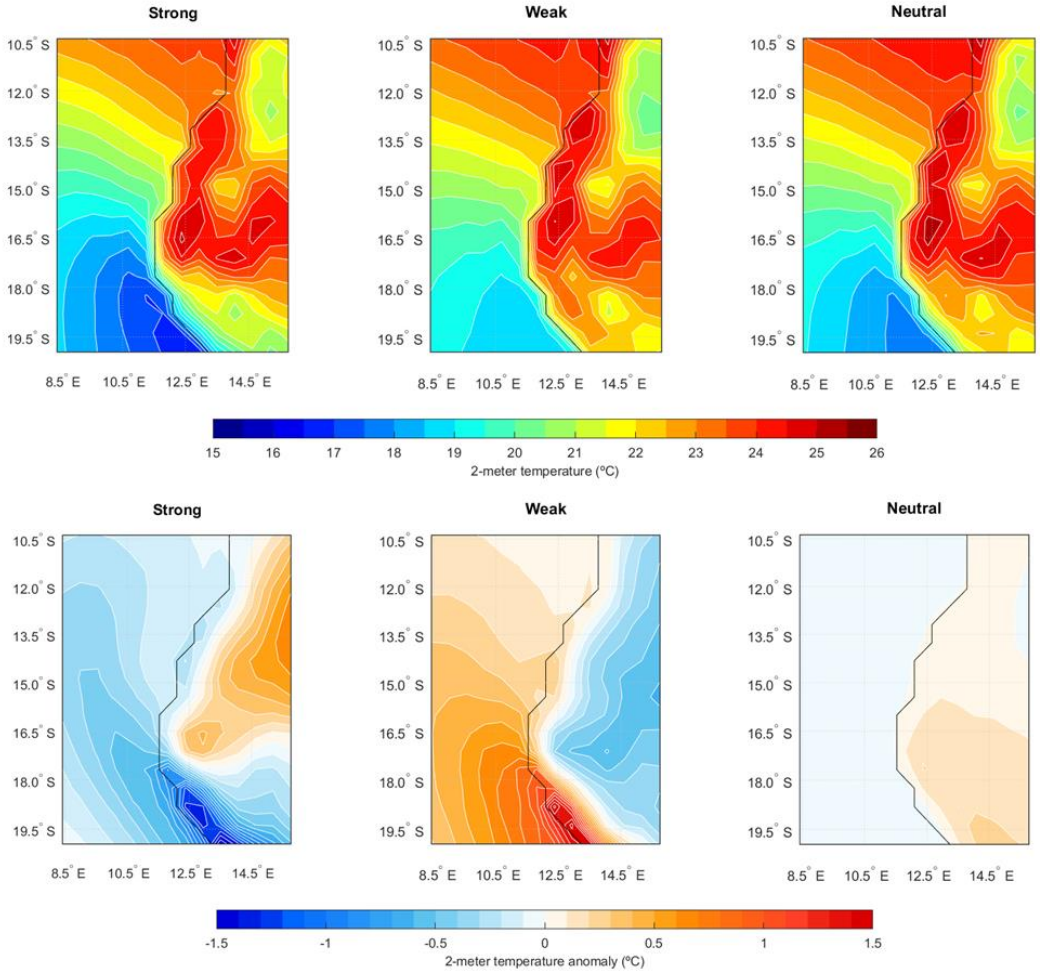

Figure 4.7 – 2-meter temperature (top panels) and respective anomaly (bottom panels) over the ABA region, averaged for the cases of strong (left), weak (centre) and neutral (right) jet.

Both the Benguela Niño (and Niña) and the jet have a signature on the ocean surface. Before establishing a relationship between the two features, it is important to understand how the surface changes under their influence. Here, it is shown how a strong and weak jet influences the surface properties. A case in which there is no jet occurrence is not presented, as the comparison between a jet and no jet scenario is not relevant for this work. Instead, a composite of when the jet is neither strong nor weak (termed here as neutral) is more appropriate. From here onwards, in this subsection, the analysis refers to mean values obtained for each composite.

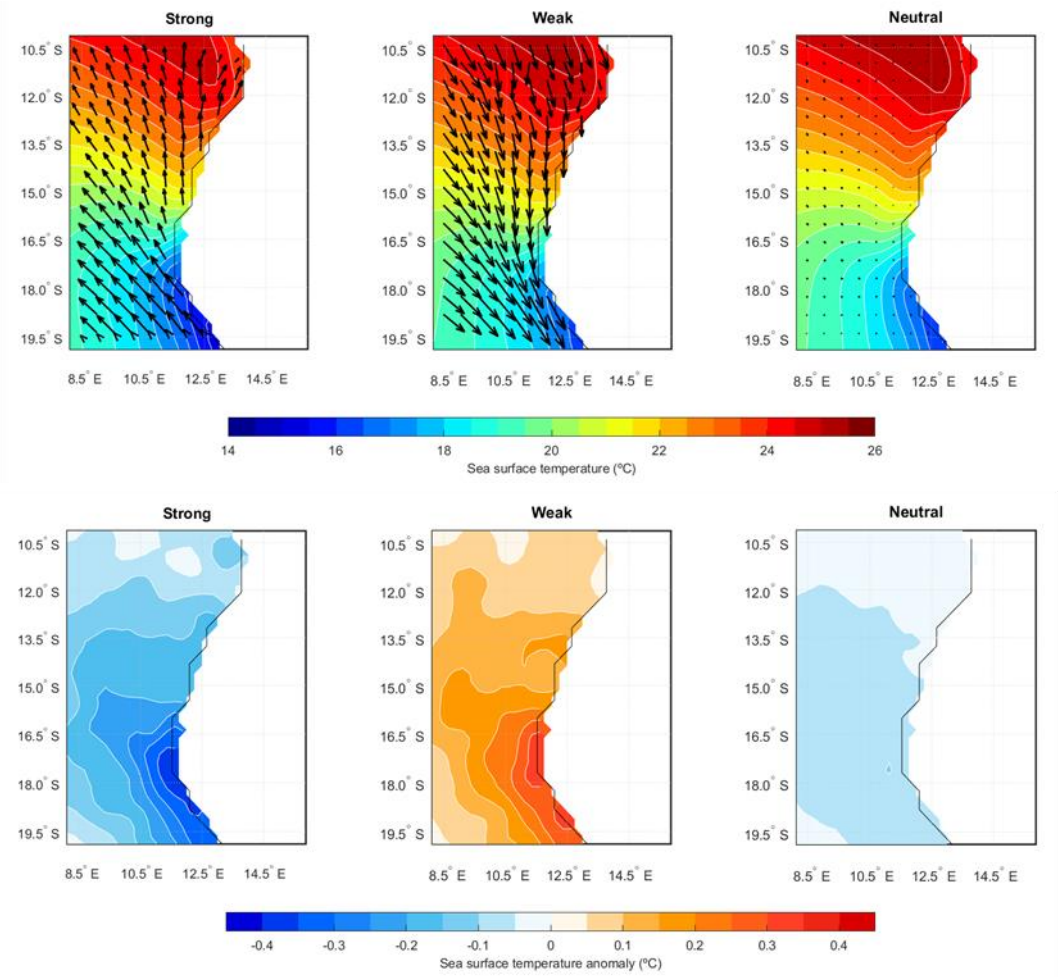

Figure 4.8 – As in Figure 4.7 but for the sea surface temperature and with black arrows on the top panels representing the jet wind speed anomaly field for each case, respectively.

When the Benguela CLLJ is more intense, the ocean-land thermal gradient is stronger if compared to the weak and neutral cases, as supported by the 2-meter temperature fields (Figure 4.7, top). This is consistent with the physical forcing of this type of jet. For the jet wind speed, the opposite ocean-land temperature gradients between the strong and weak composites are consistent with the positive and negative signals in the jet wind anomaly fields, respectively, shown by the black arrows overlaying the SST fields in Figure 4.8 (top). This figure shows, as expected, that the ocean surface is colder under the influence of a stronger jet, with the lowest SST anomalies (Figure 4.8, bottom) underlying the northern jet wind speed maximum, by the coastline. For a weak jet, the opposite is observed. Furthermore, the 2-meter temperature anomalies (Figure 4.7, bottom) show a strong gradient near 19ºS, near the coastal inlands, especially when the jet is less intense. Since the land is warmer (colder) than the ocean when

the jet is strong (weak), this gradient may be connected to the strengthening (weakening) of the thermal low, or to its phase of development. In fact, the strong 2-meter temperature anomaly gradient overlaps an also intense surface pressure anomaly gradient, with positive (negative) anomalies mainly over the ocean and negative (positive) over land for the strong (weak) jet composite (Figure 4.9, bottom).

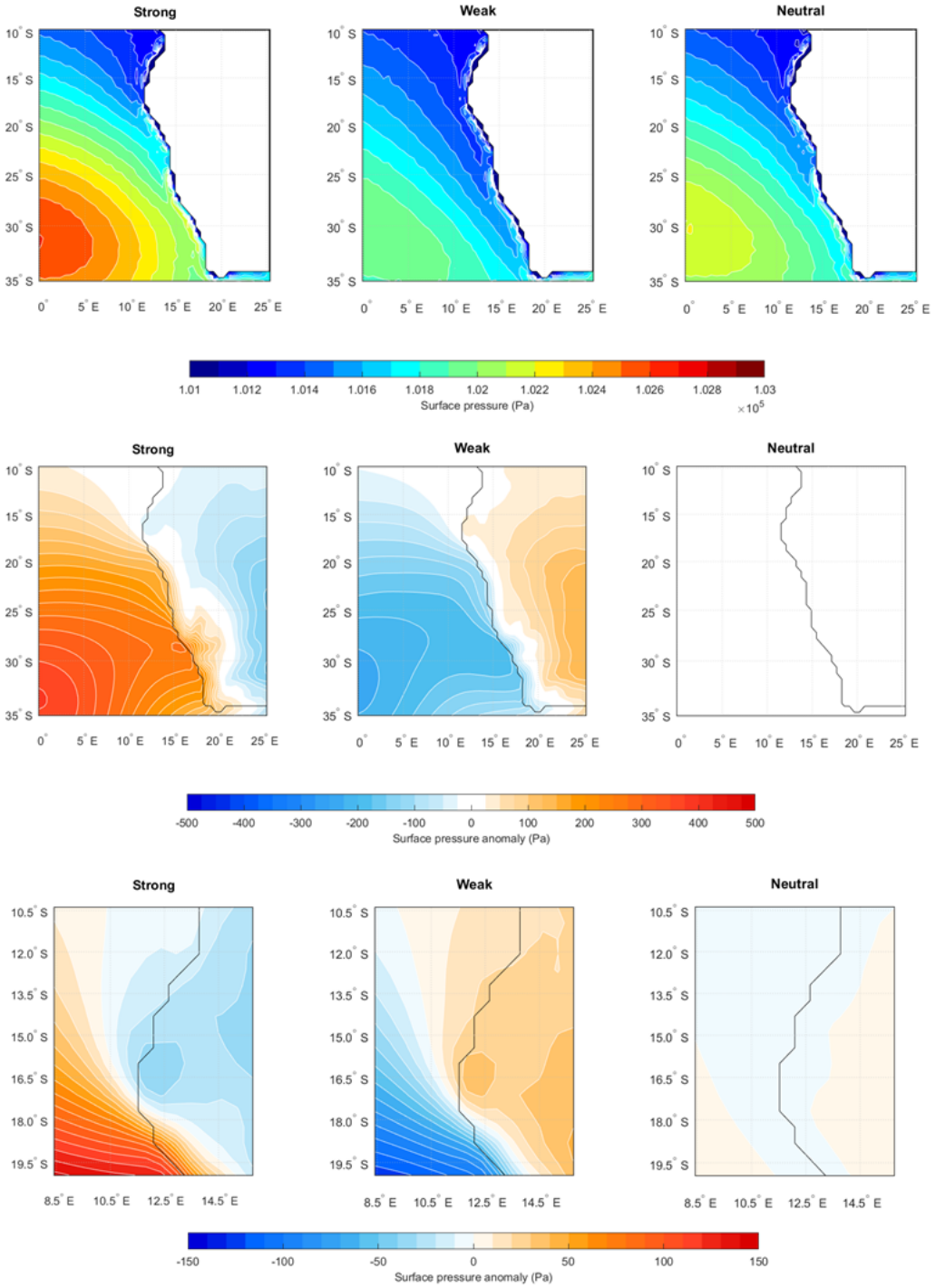

Figure 4.9 – Surface pressure over the SE Atlantic Ocean (top), and its respective anomaly field over the Benguela (middle) and ABA regions for strong (left), weak (centre) and neutral (right) jet.

The thermal low contributes to the development of the jet in addition to the SAA, that has been shown to influence the surface winds (e.g., Lübbecke *et al.*, 2010; Richter *et al.*, 2010). As Figure 4.9 (middle) shows, higher jet wind speeds are associated to positive surface pressure anomalies over the ocean, and thus, to an intensification of the SAA (Figure 4.9, top). This result is in agreement with the studies previously mentioned. When the jet is weak there is an inversion of the surface pressure anomaly field, with negative anomalies over the ocean and positive over land (Figure 4.9, middle). It has also been suggested that a weakening of the SAA impacts, either by remote (Lübbecke *et al.*, 2010) or local (Richter *et al.*, 2010) forcings, the development of Benguela Niños. The fact that a relaxation of the jet winds is connected to both higher SSTs and negative surface pressure anomalies is a good indication of the possible relationship between the Benguela Niño episodes and the intensification of the coastal jet.

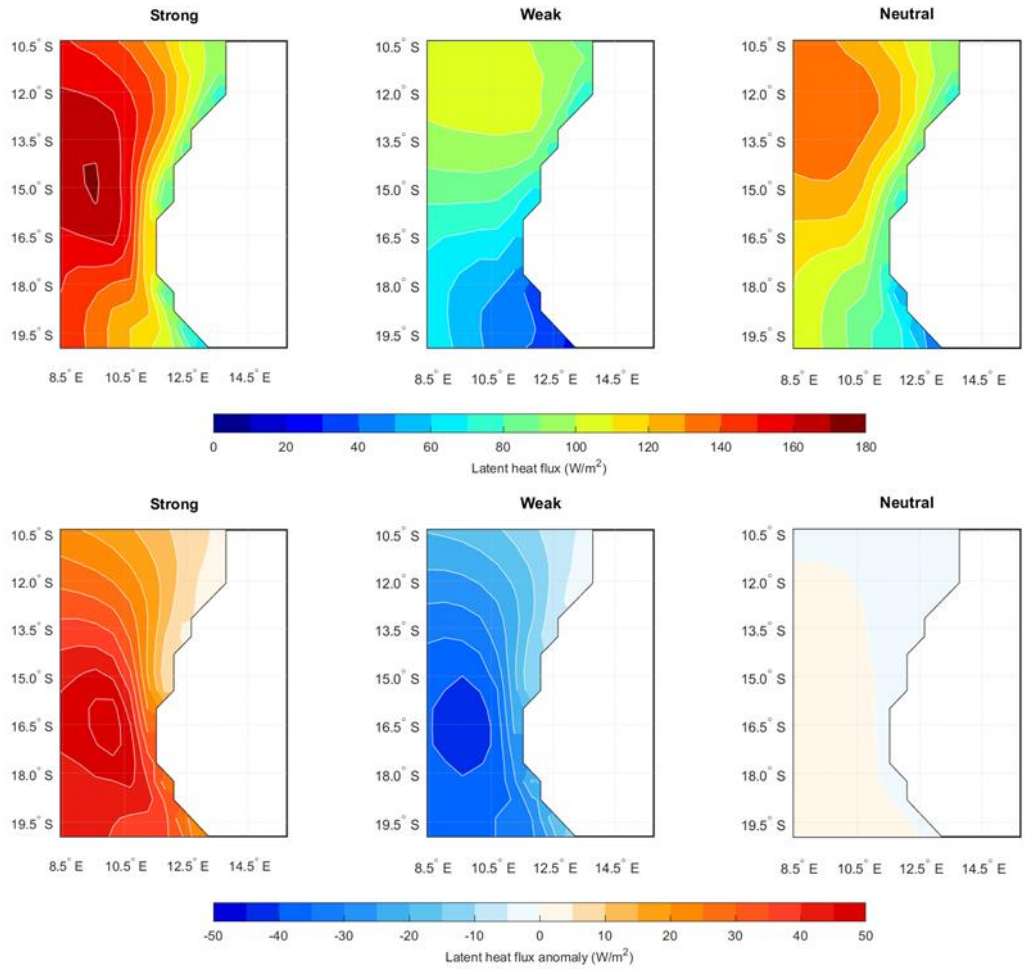

Figure 4.10 – As in Figure 4.7 but for the latent heat flux.

To understand the physical setting that differentiates a strong from a weak coastal-level jet, the mean latent and sensible heat fluxes were also computed for each jet composite. During a strong jet occurrence, latent heat flux over the ocean can reach values up to 180 W/m^2, while a weak jet is accompanied by maximum heat flux values of 110 W/m^2. The position of these maxima deserves attention: while for weak and neutral jet cases the highest latent heat flux value is observable in the northwest corner of the ABA box, in the strong composite the maximum is located some kilometres south, near 15ºS (Figure 4.10, top). The highest absolute anomaly values, however, are located near 16.5ºS for both strong and weak composites (Figure 4.10, bottom). As with the latent heat flux, the

sensible heat flux anomalies are overall positive (negative) over the ocean and land when the jet is strong (weak), as shown in Figure 4.11. Since the latent heat and the sensible heat fluxes are influenced by the specific humidity (Figure 4.12) and surface temperature gradients, respectively, and both these properties appear to decrease (increase) during strong (weak) jet events, the results appear contradictory. On the other hand, both heat fluxes are influenced by the surface wind. As discussed earlier in this section, the jet is heavily dependent on the local surface wind. On this account, if the jet is present, the surface wind is also intensified. Therefore, an intense surface wind is most likely behind this negative (positive) heat flux anomaly field over the ocean for strong (weak) jet winds.

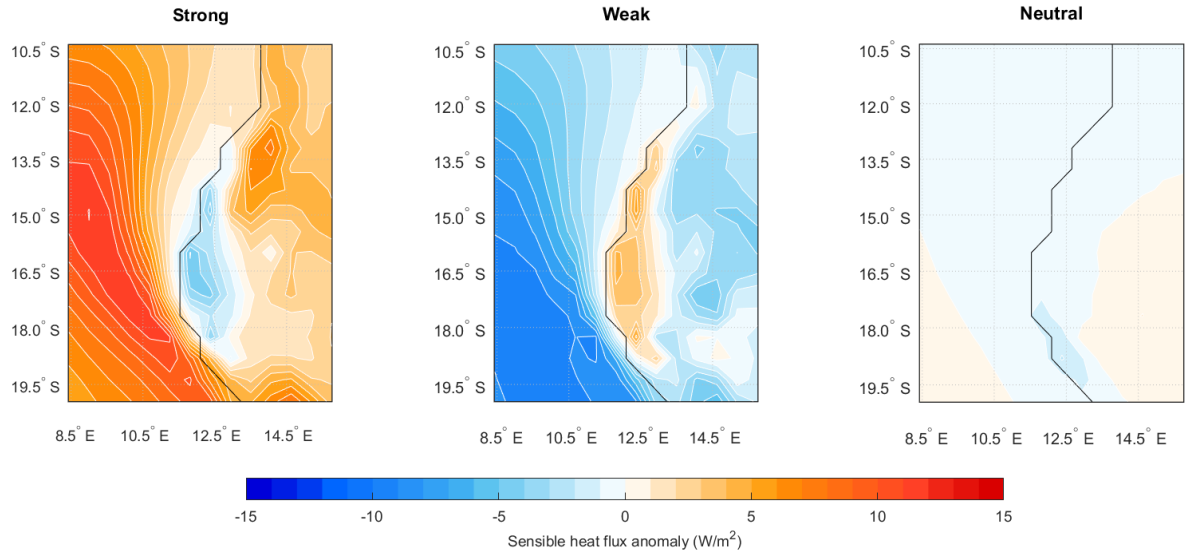

Figure 4.11 – Sensible heat flux anomaly field in the ABA region for cases of strong (left), weak (centre) and neutral (right) jet.

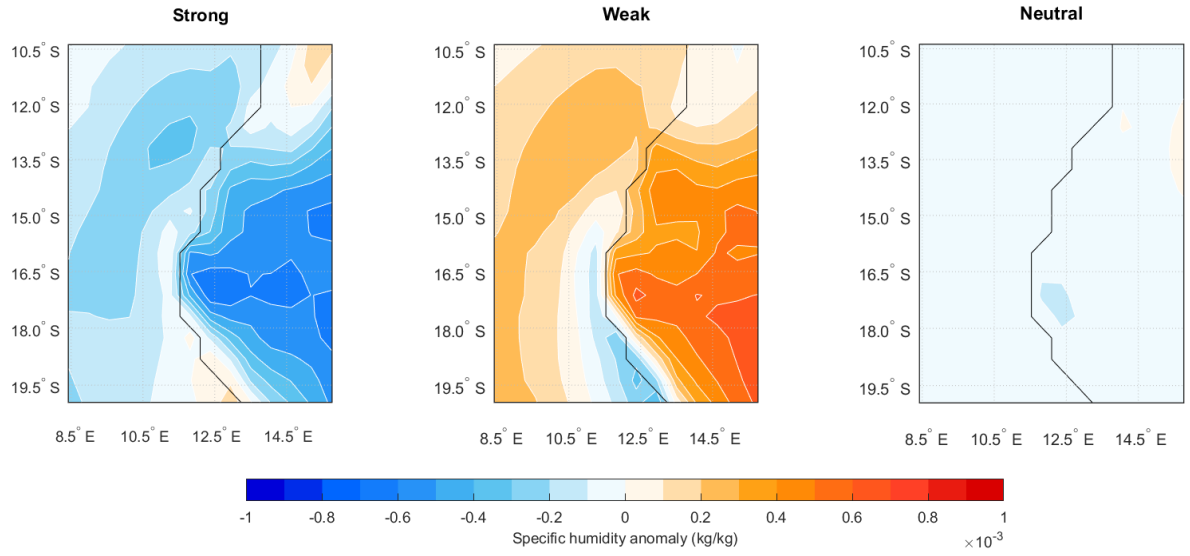

Figure 4.12 – As in Figure 4.11, but for the specific humidity anomaly.

The last physical property explored in this context was the momentum flux (Figure 4.13). While this variable has a strong meridional variability and a maximum at the northern core of the jet in the strong composite, the weak jet composite shows no specific signature (Figure 4.13, top). Taking the neutral composite in account, as well as the momentum flux anomalies (Figure 4.13, bottom), it is clear that any changes in this variable arise from changes in the jet northern maximum. As the jet intensifies, it is able to strengthen the momentum transport, thus increasing its flux. By the same reasoning, a relaxation of the jet winds is associated with a decrease in the transfer of momentum from the surface to the atmosphere.

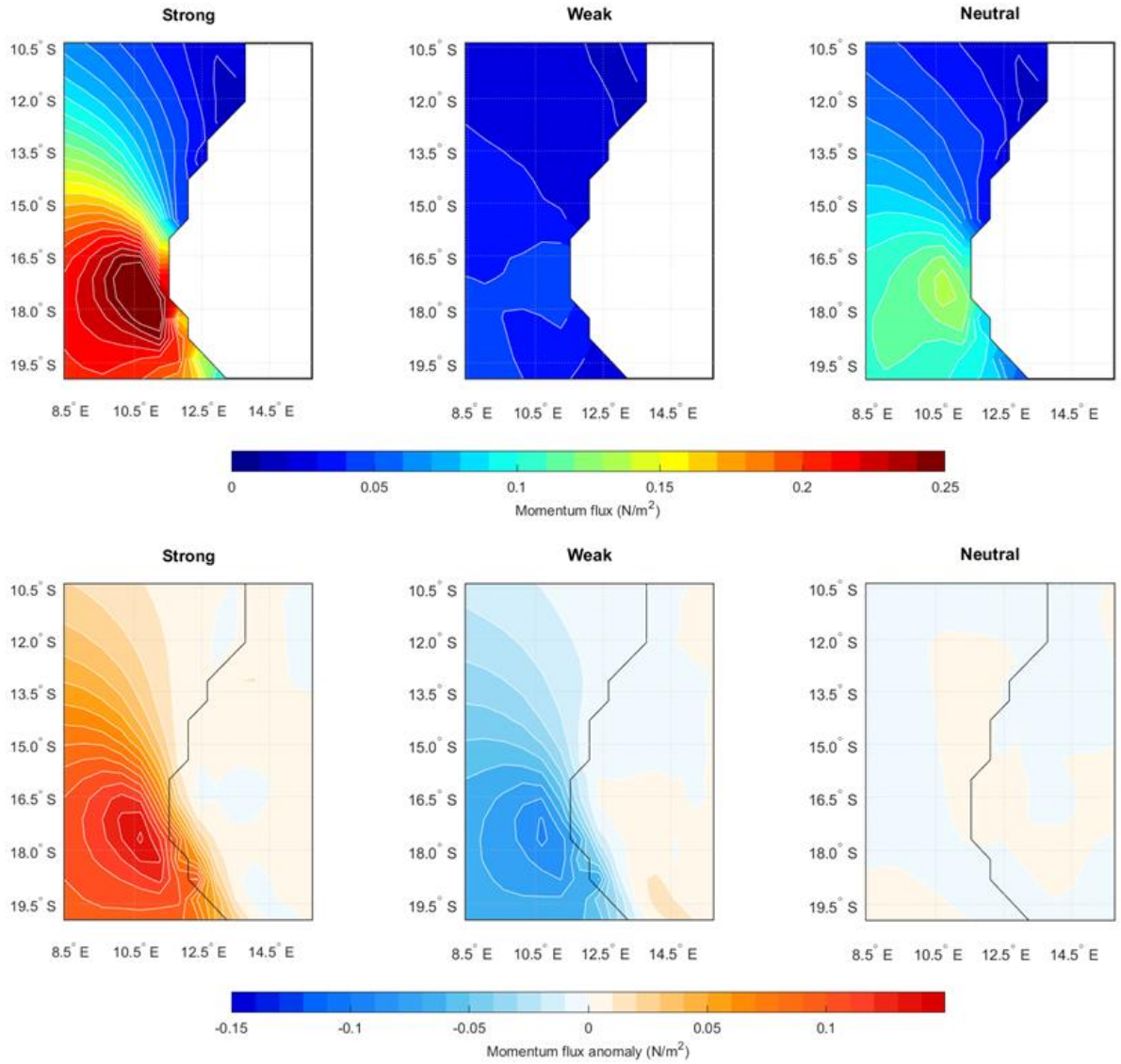

Figure 4.13 – As in Figure 4.7, but for the momentum flux anomaly.

To improve the understanding on how the ocean surface and its fluxes are connected with Benguela Niño and Niña events, it was followed the same methodology as with the jet composites.

In the occurrence of Benguela Niños, the maximum SST is greater than 26ºC, and has a minimum of about 18ºC. On the other hand, a Benguela Niña is characterised by lower than normal SSTs, with a minimum value of 14ºC, compared to 16ºC reached in the neutral composite (Figure 4.14, top). The events intensity, however, does not disclose the location where the events manifest. The maximum absolute SST anomalies are a suitable proxy, and Figure 4.14 (bottom) reveals that during both Niño and Niña they manifest some kilometres north of the jet core, at about 16.5ºS, with maximum absolute anomalies of 1.5ºC. The 2-meter temperature intensity and anomaly fields have a very similar pattern to the SST fields, the second adding only that the land surface is slightly colder during Benguela Niño and Niña events (Figure 4.15).

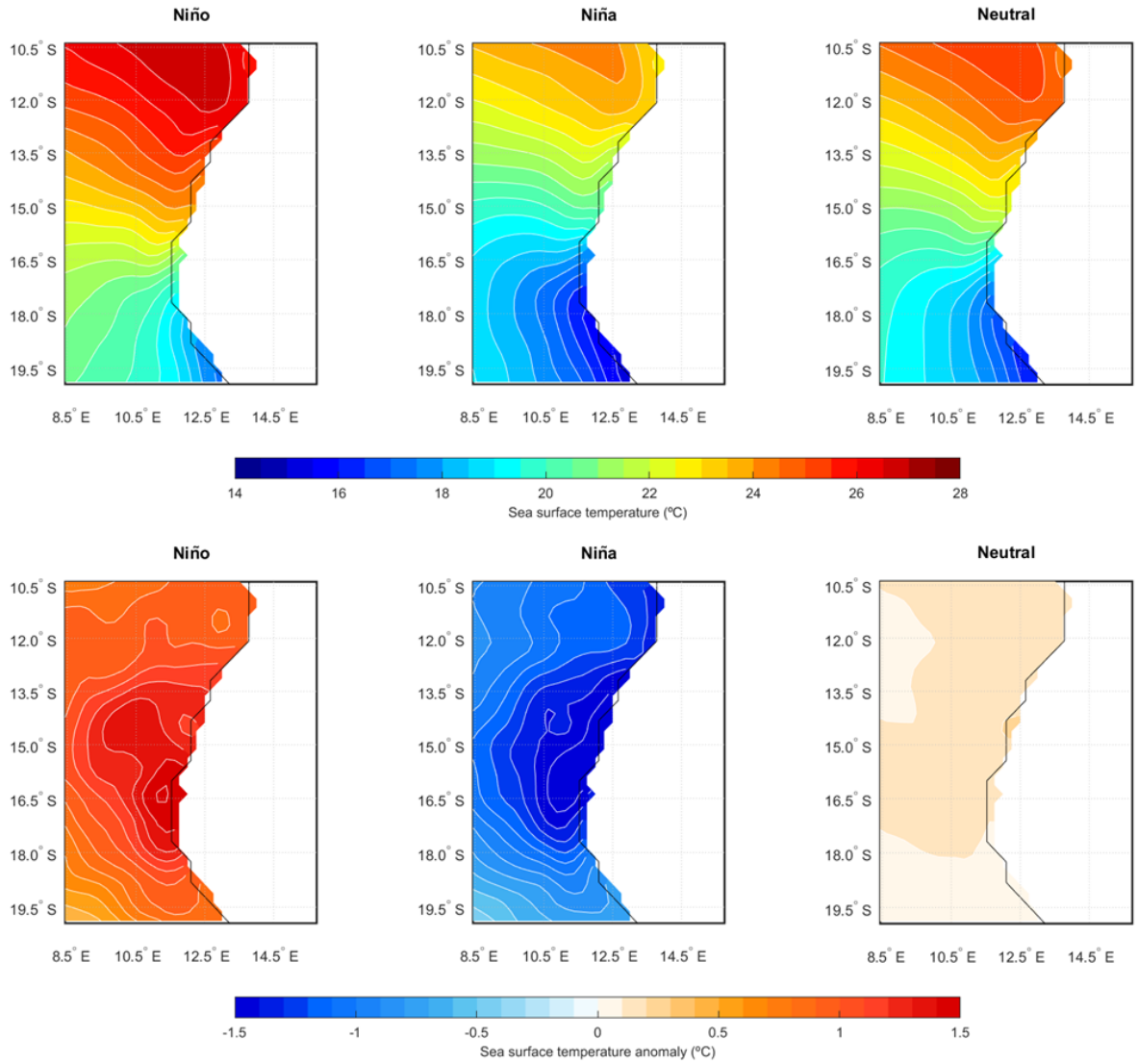

Figure 4.14 – Sea surface temperature (top panels) and respective anomaly field (bottom panels) averaged over the Benguela Niño (left), Niña (centre) and neutral (right) cases.

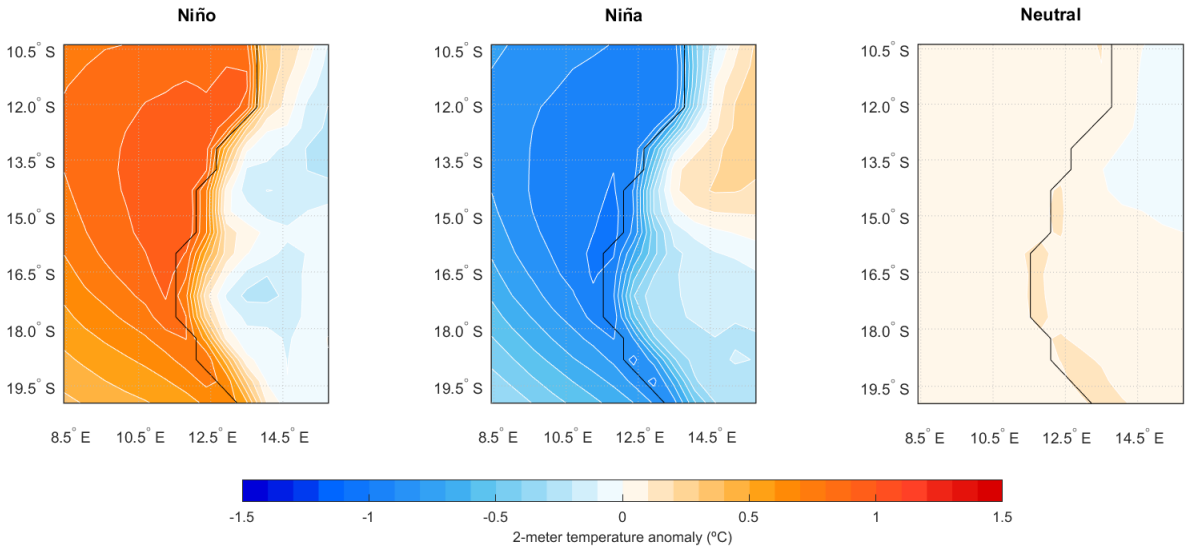

Figure 4.15 – As in Figure 4.14 (bottom panels), but for the 2-meter temperature anomaly field.

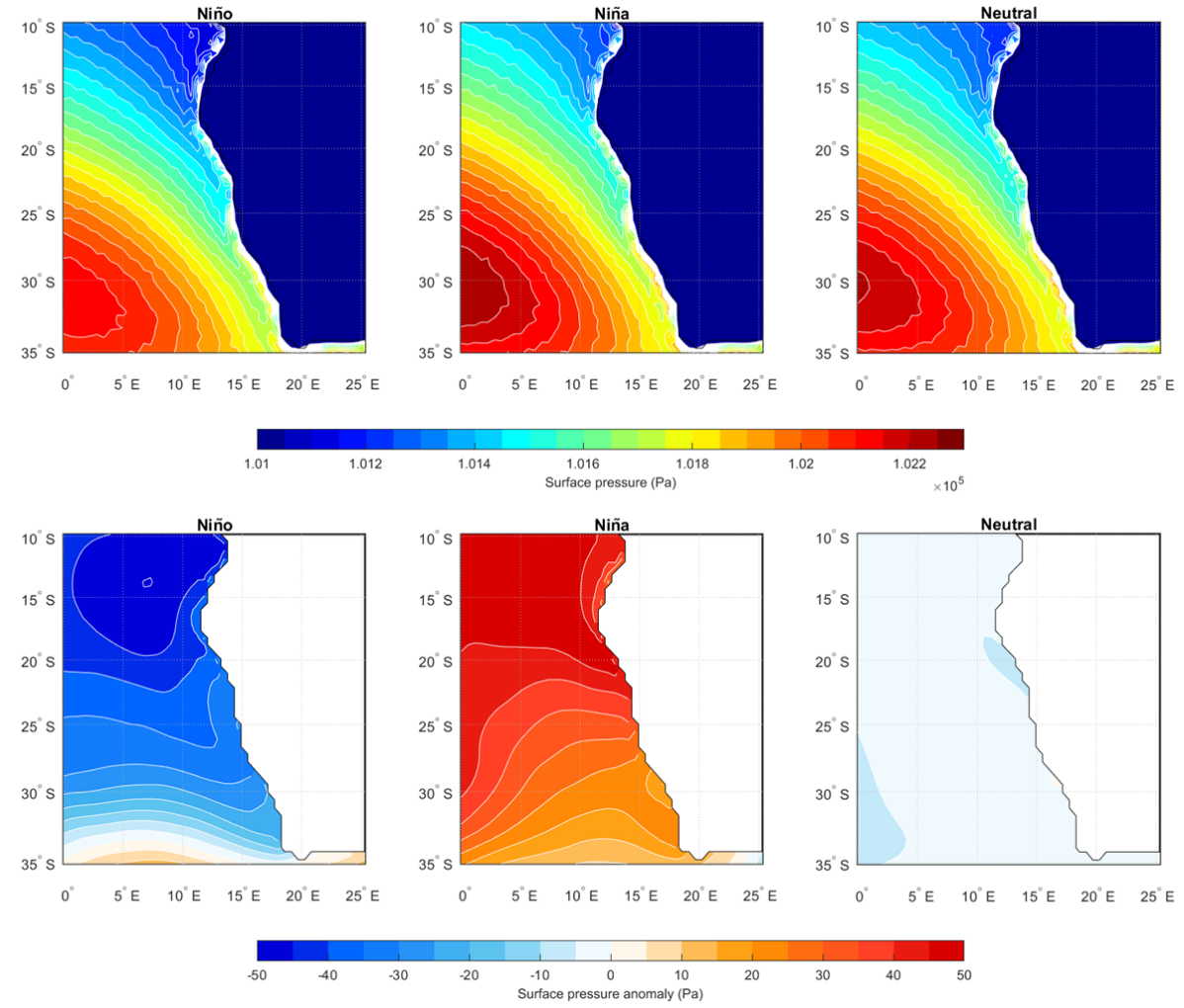

Figure 4.16 – As in Figure 4.14 but for the surface pressure in the Benguela region.

The analysis of the surface pressure field over the Benguela region shows that Benguela Niño events are connected to a weakening of the SAA (Figure 4.16, top), which is consistent with the literature (e.g., Florenchie *et al.*, 2004; Lübbecke *et al.*, 2010). The Niñas, on the other hand, are associated with a strengthening of the anticyclone. The respective anomaly fields show that the maximum anomaly is located not over the mean SAA position, but near 13ºS (Figure 4.16, bottom) for the Niño and Niña composites. The surface wind anomaly fields over the ABA region (Figure 4.17, top) do not seem to explain the spatial behaviour of the former variable. During the Niño events the surface wind anomaly field is unexpectedly positive, showing an intensification of this variable, while strong low-level winds are associated with colder SSTs. An analysis of the jet wind speed anomaly field (Figure 4.17, bottom) reveals that during Benguela Niño events, the jet maximum is weakened (yet, to its north the anomalies are still positive), while the Niña composite shows an overall intensification of the jet, in agreement with previous results. Again, the surface wind appears to be somewhat disconnected from the low-level jet.

During the Benguela Niño, as the ocean surface waters are anomalously warm, the temperature of the overlying air will also be higher than usual, and will, therefore, be able to hold a higher content in water vapour than the colder surface air typical of the Benguela Niña. This is clear in the positive anomalies of specific humidity of the Niño composite, and its negative values during Niñas (Figure 4.18). The highest absolute anomalies observed extend from the ocean to the coast. This advection is most likely caused by the local mainly zonal surface and jet wind anomalies, portrayed by the surface and low-level wind speed anomaly vectors (Figure 4.17 top and bottom, respectively).

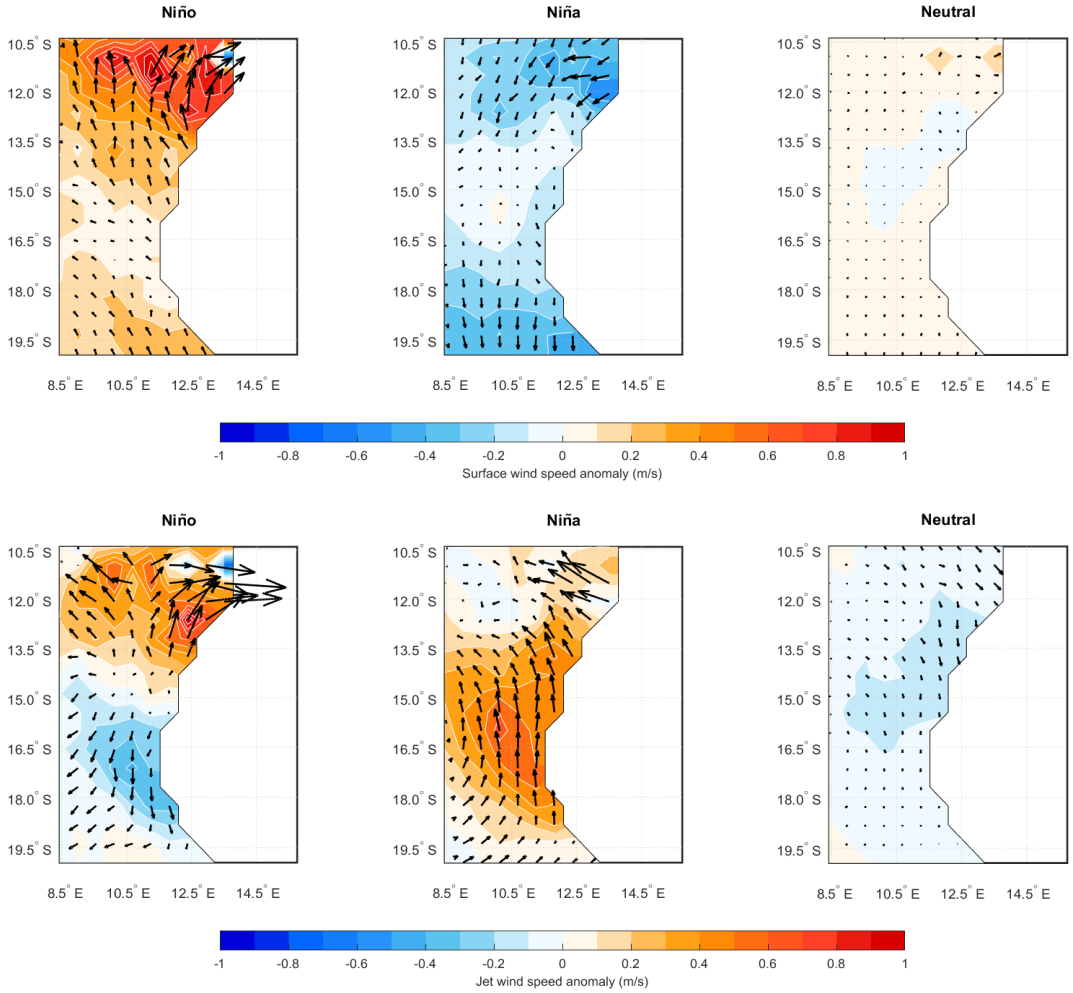

Figure 4.17 – Surface wind speed anomaly (top panels) and jet wind speed anomaly (bottom panels) averaged over the Benguela Niño (left), Niña (centre) and neutral (right) cases. The black arrows represent the wind speed anomaly field and the colours the magnitude of the anomaly.

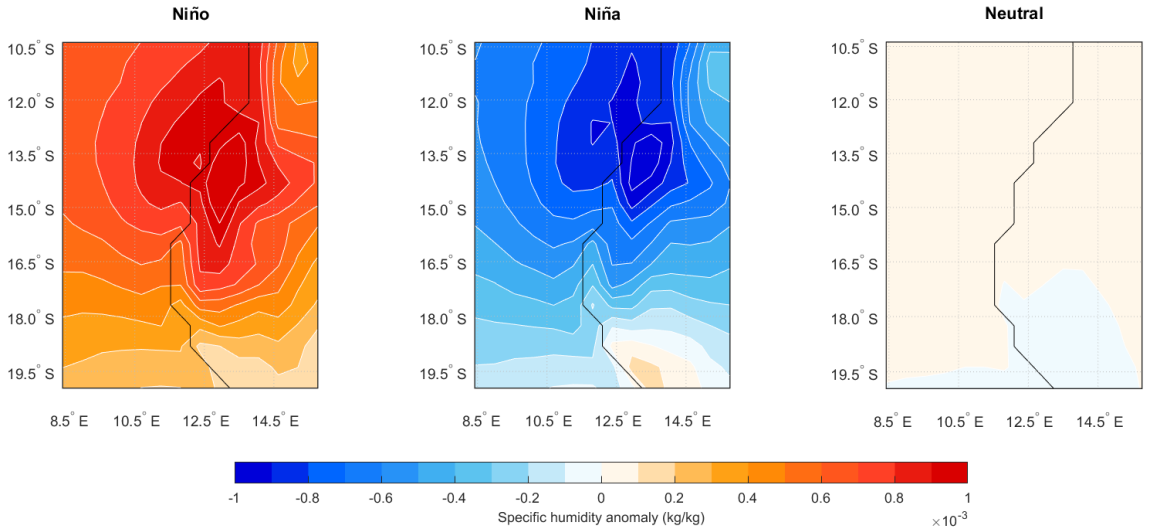

Figure 4.18 – As in Figure 4.15, but for the specific humidity anomaly.

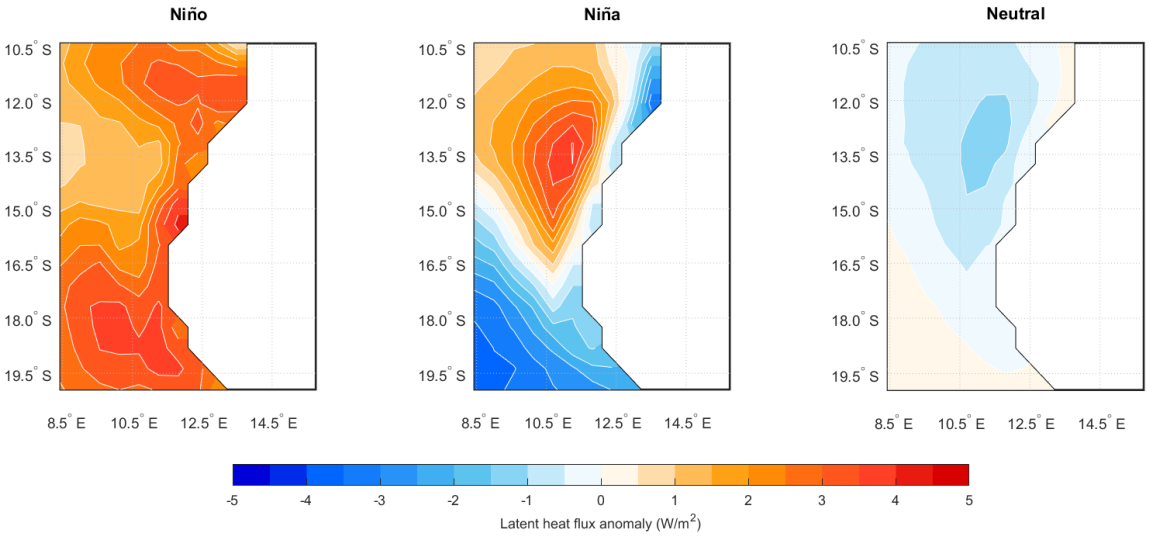

Figure 4.19 – As in Figure 4.15, but for the latent heat flux anomaly.

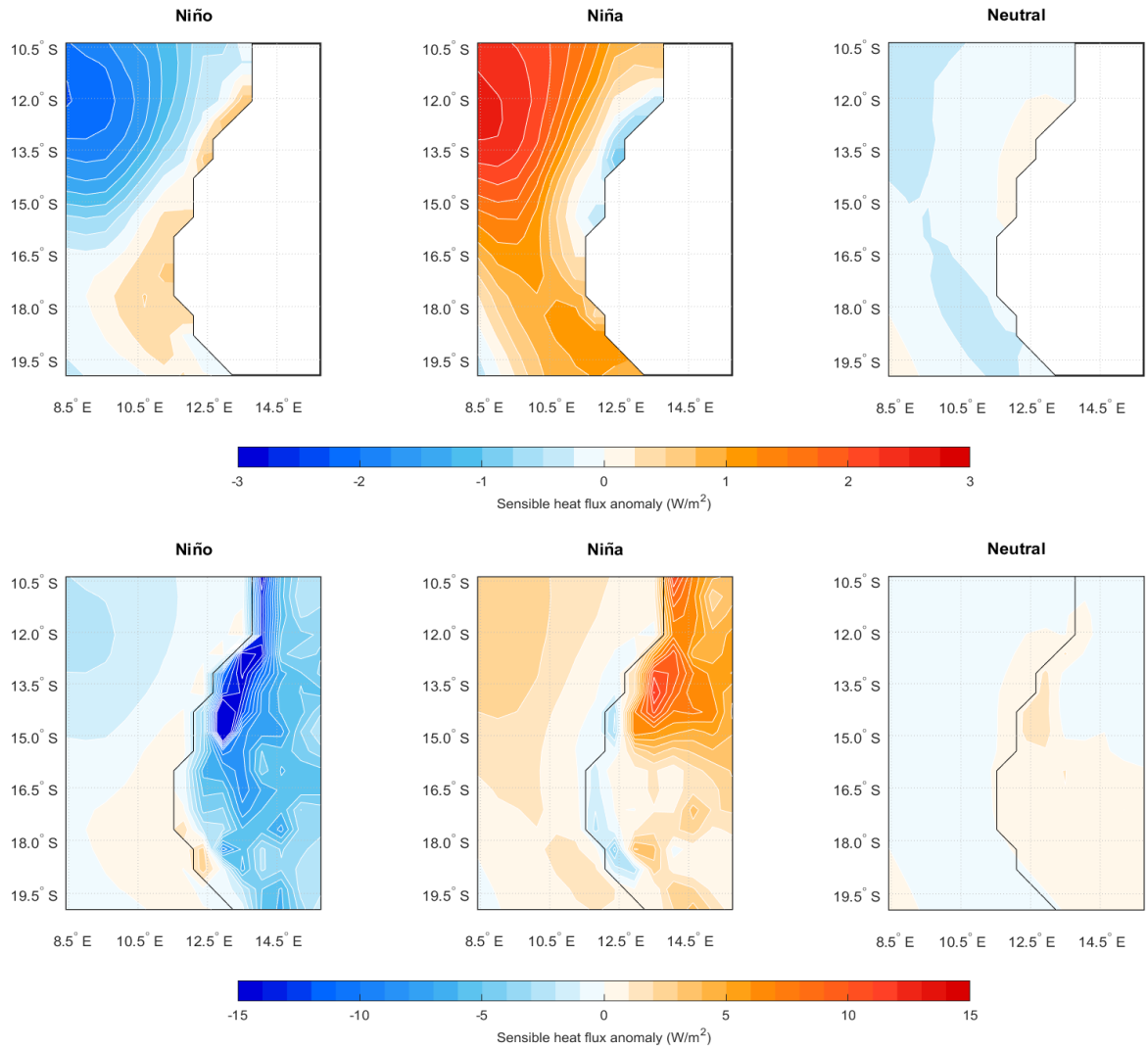

Figure 4.20 – As in Figure 4.15, but for the sensible heat flux anomaly over the sea (top panels) and for the whole ABA region (bottom panels).

The latent heat flux is related to the specific humidity; if the latter increases, the former should also show positive anomalies. Such is the case for the Benguela Niño composite (Figure 4.19). For the same reasoning, the opposite should be evident for Benguela Niña events. Yet, in the Niña composite, the latent heat flux anomaly has dipole-like field, with a positive maximum at about 13.5ºS and a negative core at about 19.5ºS.

The sensible heat flux anomaly fields are shown in Figure 4.20. Over the ocean (top), the Niño composite is marked by a decrease in the northwestern region of the ABA box, which is consistent with the location of the maximum enhancement of the flux (~12ºS), extending southeastward, shown during Niña events. Over land, the sensible heat anomalies are stronger, the location of their highest absolute values coherent with that of the momentum flux anomalies over land (Figure 4.21). Additionally, its maximum positive (negative) anomaly is located over the lowest (highest) specific humidity values, in the continent (Figure 4.18).

Most of the surface conditions observed for a strong (weak) jet are consistent with those for a Benguela Niña (Niño), suggesting a connection between the phenomena. A more detailed analysis is pursued in the next section.

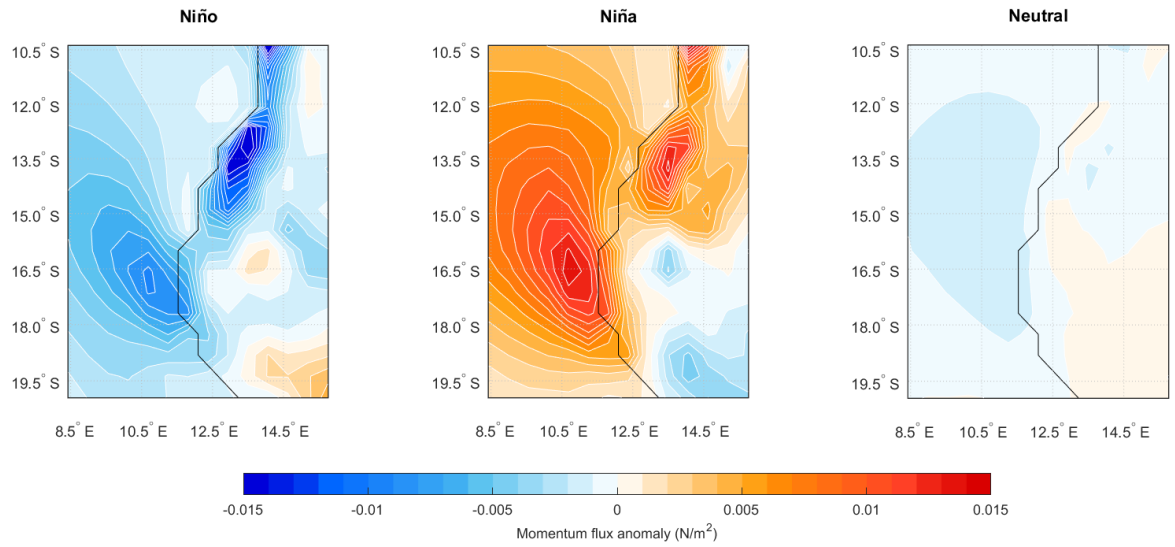

Figure 4.21 – As in Figure 4.15 but for the momentum flux anomaly.

4.3 Relationship between BCLLJ and Benguela Niño

The first obtained evidence that the BCLLJ might be influenced by the Benguela Niño is presented in Figure 4.22. Here, it is shown that the PDFs of both the frequency of occurrence and the intensity anomalies of the jet (Figure 4.22, top and bottom, respectively) have different behaviours during events of Benguela Niño (orange), Niña (blue) and neutral (yellow). The curves corresponding to the two variables (frequency of occurrence and intensity) have a similar behaviour in all the SST composites. The neutral distribution curve (purple), which represents the average of the neutral cases, has a mean value close to the full time series, although with a slightly lower variance, since the former does not include the SST anomalous events. Regarding the Benguela Niño and Niña curves, the distributions suffer a shift in opposite directions, accordingly with the expectations. During Benguela Niño events, the jet is less frequent and weaker, with lower values of both frequency and wind speed. The opposite is observed for the frequency of occurrence anomaly during Benguela Niñas, as for the jet wind anomaly. The jet frequency PDF also shows a higher standard deviation for these cases than for the Niños (7.25% and 6.67%, respectively). During Niñas, the jet is, in average, stronger and occurs more frequently than the neutral and Benguela Niño events. These results are consistent with what is expected from the theory; when the ocean-land thermal contrast is more intense (as happens during Benguela Niña events), the jet is also more intense. The opposite is observed for the Niño composite, when the SSTs are anomalously higher than normal.

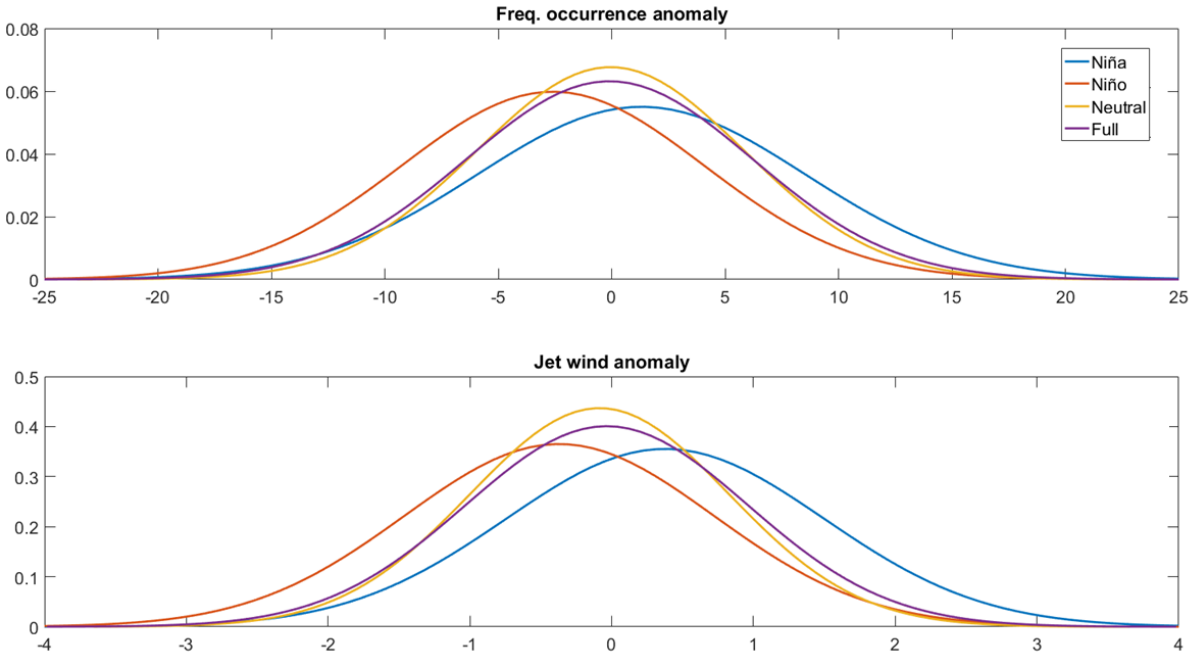

Figure 4.22 – Probability density functions for the anomalies of jet frequency of occurrence (top) and of jet wind intensity (bottom) for the composites of Benguela Niña (blue), Niño (orange) and neutral (yellow), and full time series (purple).

For each jet wind composite (strong, weak and neutral), west-east cross-sections at its northern core were computed for the model level properties. This allows an improved understanding of the structures linked to the different jet composites.

The vertical distributions of the wind speed intensity and its anomaly is illustrated in Figure 4.23, left and right, respectively. In all its composites, the jet wind speed is maximum at 400-500 m, near the coast. Its intensity decreases rapidly with height, from nearly 17 m/s on strong events, and has an offshore tilt. Because of the intensity of the jet, the wind speed anomaly fields has a more pronounced signature aloft, at approximately 1000 m above sea level. Both components of the wind speed were also investigated. The meridional component shows a very similar distribution to the module (not shown). As for the zonal wind component (Figure 4.24), some characteristics should be discussed. Firstly, the wind tends to veer west (as this component is mostly negative), especially during strong jet events at 1000 m of altitude. Secondly, there is an intense vertical gradient from the jet level to the surface and upwards, particularly so in the strong and neutral composites. Lastly, there is a noteworthy positive zonal wind speed tongue that is present in the upper levels of the cross-section, that tilts towards the coast. There is also the ocean-land contrast shown by the the anomaly fields: while the zonal wind component has negative (positive) anomalies some meters above the ocean during strong (weak) jet events, the opposite ensues over land. Put simply, a stronger jet is associated to a more negative u-component wind.

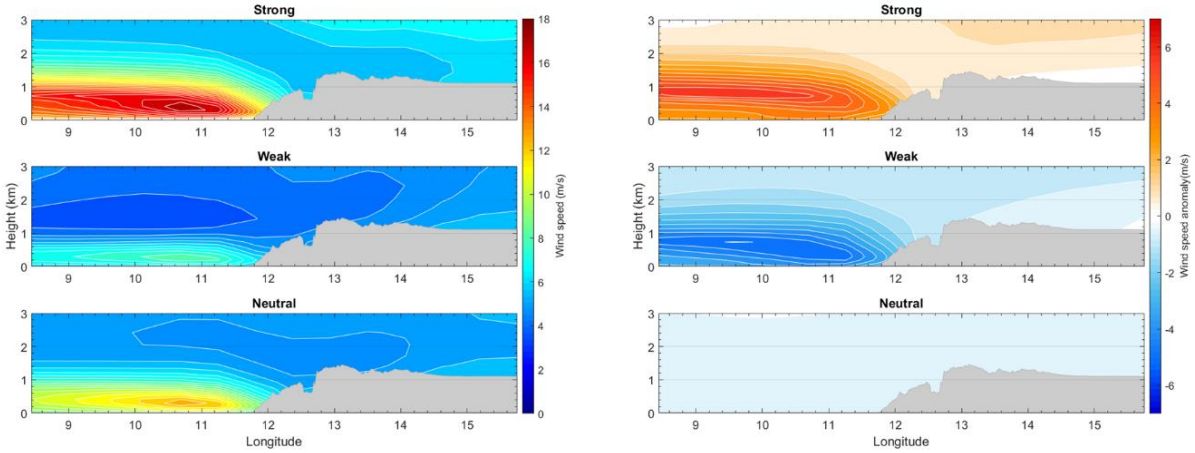

Figure 4.23 – Vertical distribution of the wind speed intensity (left panels) and its anomaly (right panels) for the west-east cross section at the jet northern core, averaged for the cases of strong (top), weak (middle) and neutral (bottom) jet. Grey area is the topography represented with the 1 arc-minute global model ETOPO1.

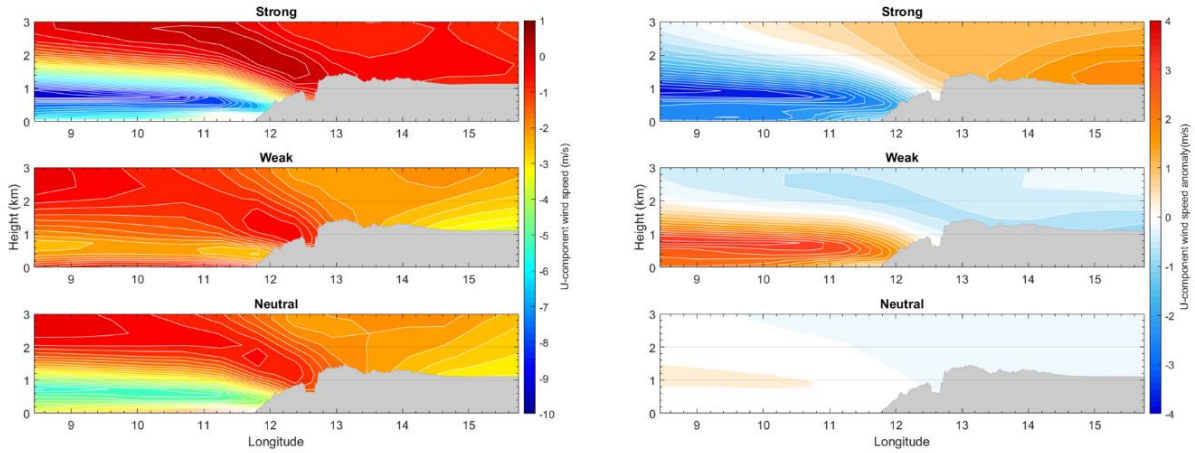

Figure 4.24 – As in Figure 4.23, but for the zonal wind component.

The potential temperature anomaly field is displayed in Figure 4.25. This result corroborates the surface analysis: during strong jet occurrences there is a cooling of the surface and the MABL, with the lowest values consistent with the jet level; the weak jet composite reveals positive anomaly of the potential temperature over the ocean. Furthermore, this property has contrasting anomaly values between land and the ocean, with more intense values over the latter.

Figure 4.26 displays the omega intensity and anomaly fields for each jet composite, overlayed with the jet wind speed and respective anomaly contour lines. During strong jet occurrences, the lower atmosphere is characterised by enhanced subsidence over the steep coast, near 12ºE. Overall, in the strong jet composite, there is an increase of omega, diminishing along and offshore. On the other hand, a weak jet is acompanied by a much weaker subsidence at the same region. Over land, particularly at 13ºE, where the coast is higher, there is a strong ascending motion, consistent with the diurnal heating and the presence of a thermal low known to be one of the forcings of the BCLLJ.

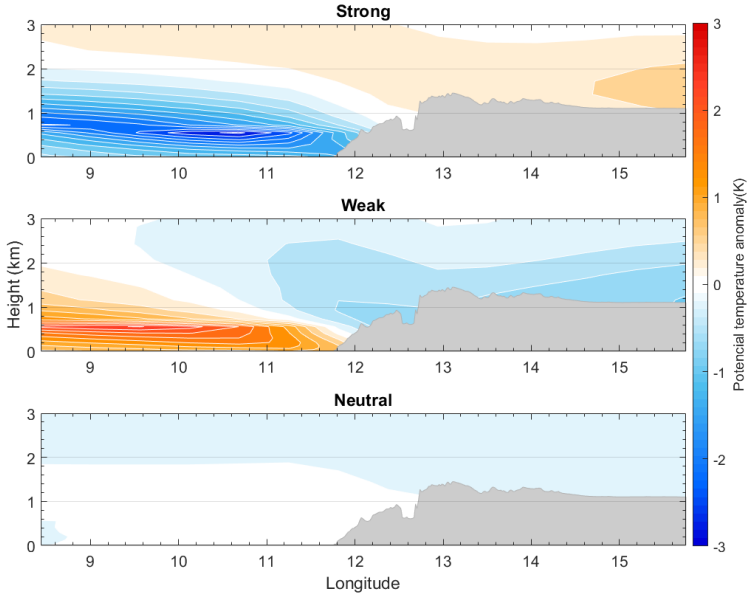

Figure 4.25 – As in Figure 4.23 (right panels), but for the potential temperature anomaly.

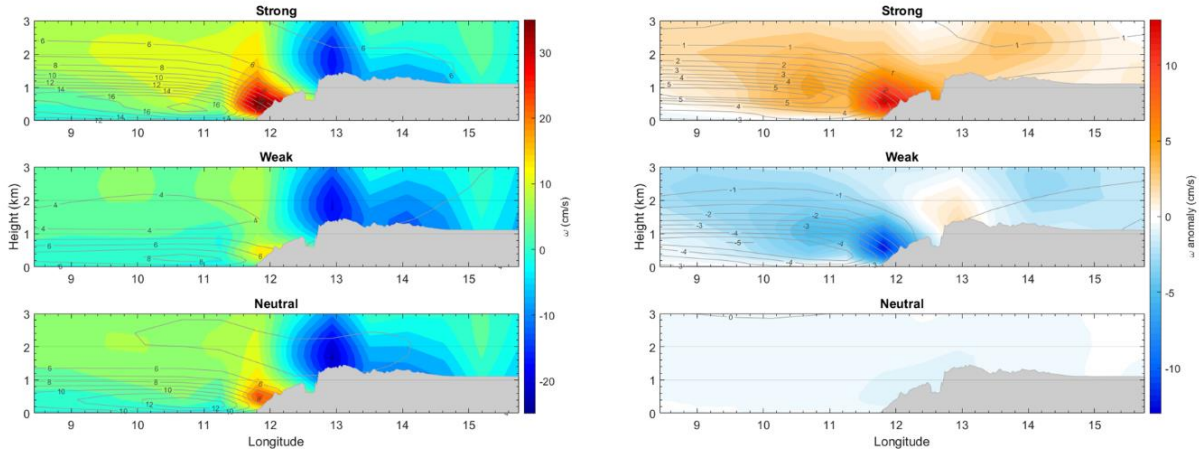

Figure 4.26 – As in Figure 4.23, but for the omega fields and overlaid with the jet wind speed (left panels) and anomaly (right panels) contour lines.

In order to characterise the vertical structure of the MABL under the influence of Benguela Niños and the jet, the west-east cross-sections were computed for the SST composites given the occurrence of the low-level jet.

Whereas the wind speed field (Figure A3) shows no significant signal of the influence of the Niños (or Niñas), its anomaly field (Figure 4.27) allows a clearer view of the changes in the MABL. The Niño composite shows an overall weakening of the wind speeds, particularly at and above the jet level, over the ocean, confirming what has been shown in previous analyses. There are, however, some minor enhancements at 2000 m and over land. During Niñas, when the ocean surface is colder (Figure 4.28) the wind speeds are strengthened, as expected.

While the Benguela Niño (Niña) phenomenon manifests on the ocean surface, an anomalous positive (negative) temperature is propagated throughout the vertical extent of the MABL (Figure 4.28). The higher absolute potential temperature anomalies are observed at about the jet level and close to the coast.

Similarly to the jet wind composites, the El Niño-like phenomenon in Benguela also shows a tilting U-component wind tongue towards the coast, although its signature is less pronounced (Figure 4.29). All the SST composites show that the wind veers mainly west. Regarding its anomaly fields, the surface wind has a slightly stronger zonal component during Niños, and a very weak signal over the ocean surface during Niñas. The wind tongue observed in altitude is represented by the negative anomalies above the jet level for the Niño composite, and positive for the Niña.

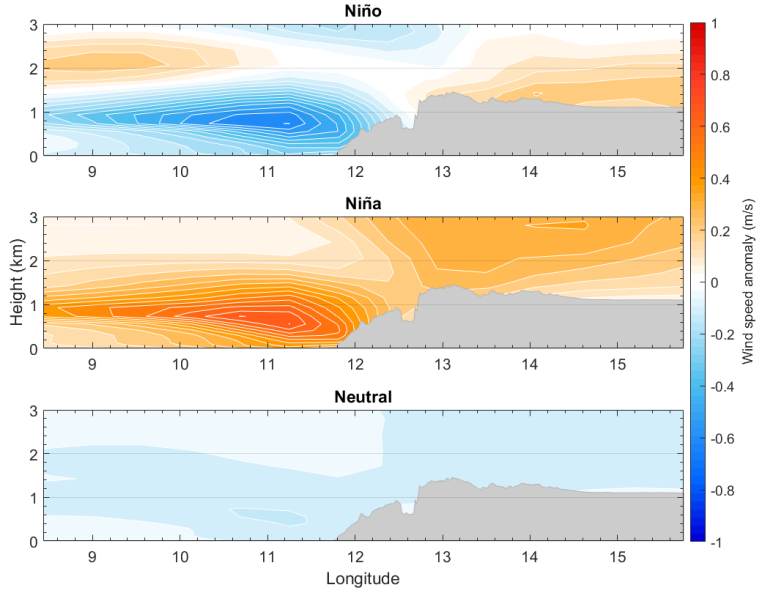

Figure 4.27 – Vertical distribution of the wind speed anomaly for the west-east cross section at the jet northern core, averaged over the Benguela Niño (top), Niña (middle) and neutral (bottom) cases.

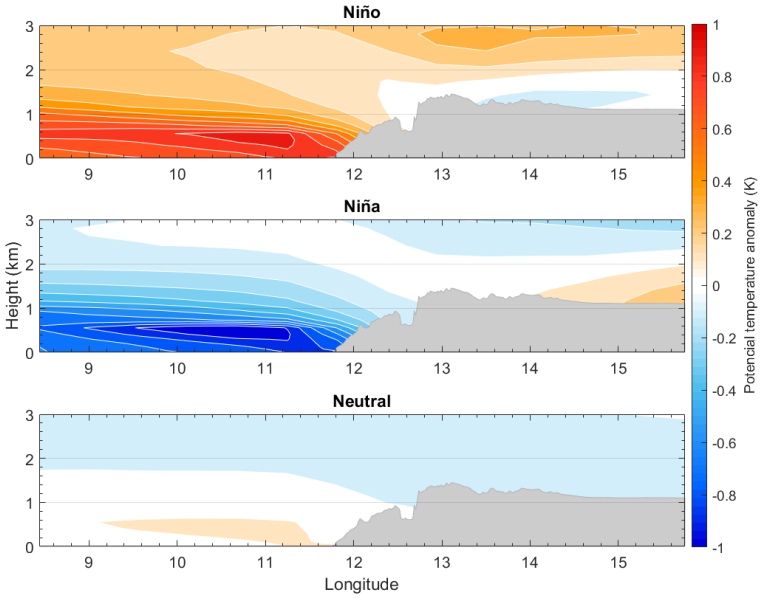

Figure 4.28 – As in Figure 4.27, but for the potential temperature anomaly.

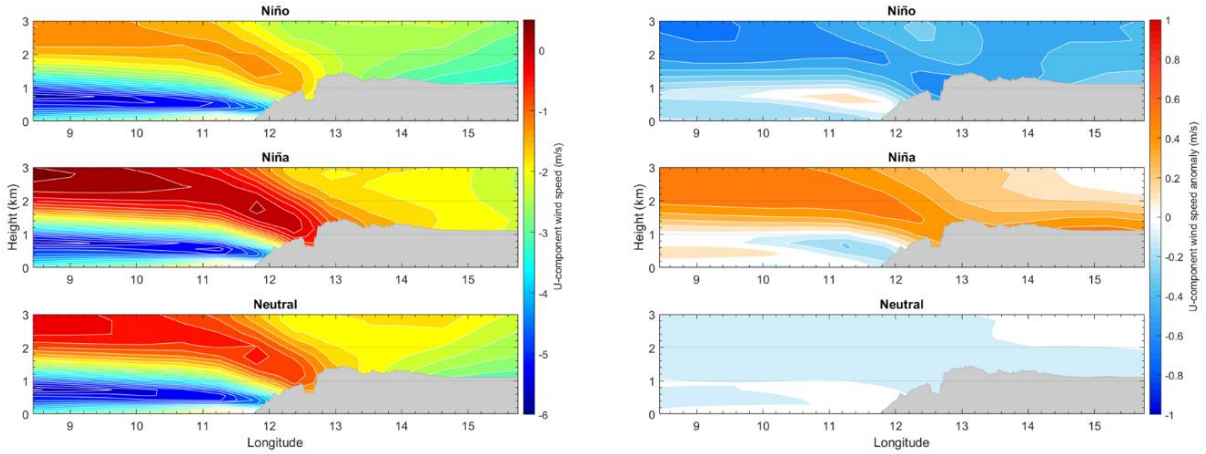

Figure 4.29 – As in Figure 4.26, but for the zonal wind (left panels) and its anomaly (right panels) of each SST composite.

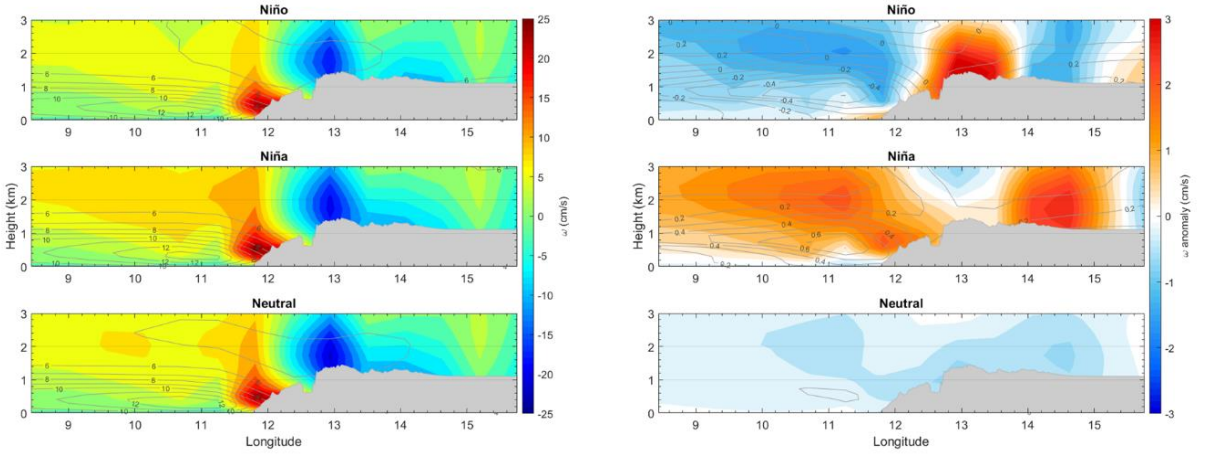

Figure 4.30 – As in Figure 4.29 but for the omega field.

Regarding the omega fields (Figure 4.30), it appears there is little difference between the SST composites, with maximum absolute anomalies inferior to 3 cm/s. In spite of that, the positive anomaly field observed during the Benguela Niña composite is consistent with enhanced jet events. The Niño omega anomalies show overall negative values, i.e., less subsidence. Inland, there is a weakening of the thermal advection, evidenced by the positive omega anomalies.

The following and final set of results show the annual climatology of the variables of interest for each SST composite. Seeing as the jet doesn't always manifest and may not coincide with a Benguela Niño or Niña, the present blank spaces will indicate that in all of the events, that day has no occurrence.

The potential temperature has a clear seasonal cycle, as shown by the full and neutral composites (Figure 4.31), with a well-mixed MABL during the austral spring months, and less during the autumn. During Benguela Niños, the MABL is weakly mixed till the spring months, and the Niña composite shows a cooler mixed layer.

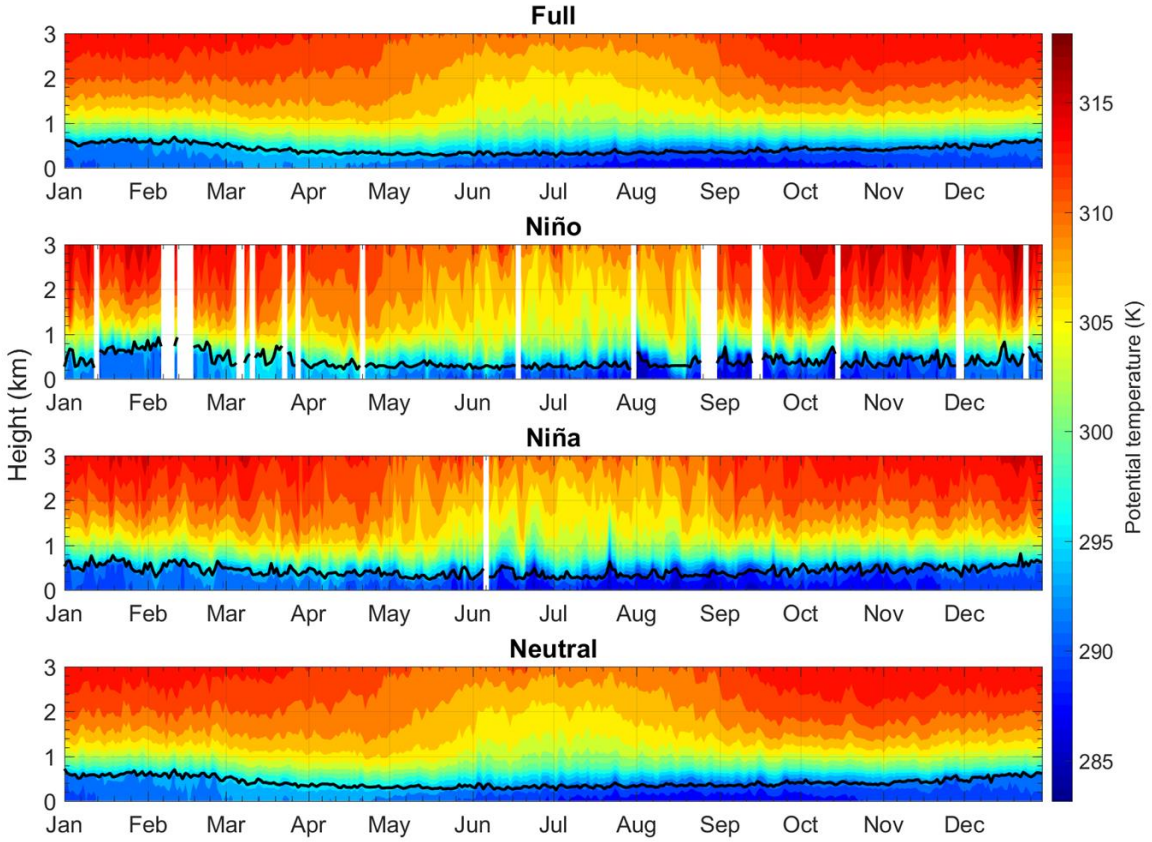

Figure 4.31 – Mean annual cycle of potential temperature from the surface up to 3 km, when jet occurs, averaged for the full period (first panel), Benguela Niño (second panel), Niña (third panel), and neutral (fourth panel). The black line indicates the jet height, respectively for each case.

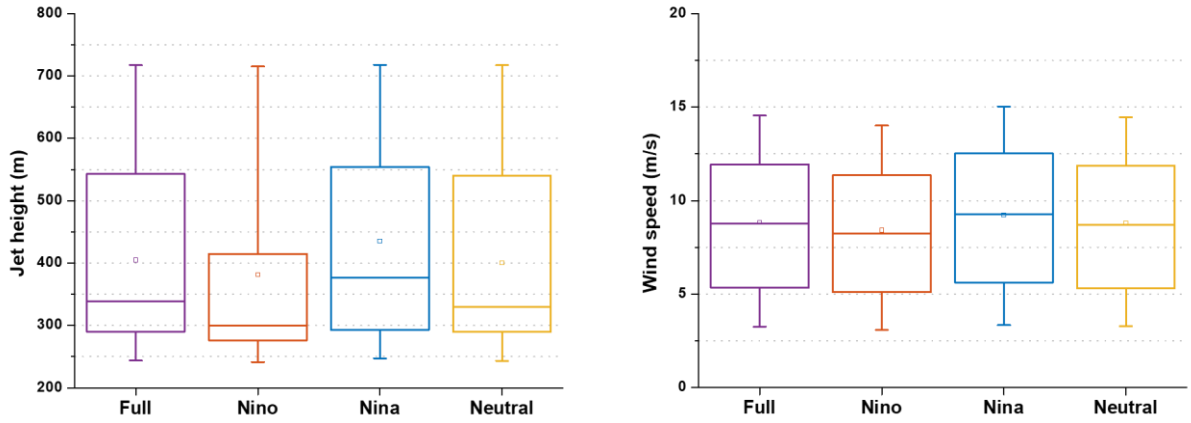

Figure 4.32 – Distributions of jet height (left) and wind speed (right) for the full, Niño, Niña and neutral cases, respectively. The median values are indicated by the horizontal line inside each box, the first and third quartiles are indicated by the bottom and top sides of the box and the 10th and 90th percentiles by the whiskers. The small square inside each box indicates the mean value.

Also evident from the full and neutral composites is the northern jet core height. At the beginning and end of the year cycle the jet is placed higher, and is also influenced by the Benguela Niño and Niña, as shown by figures 4.31 and 4.32 (right). While the full and neutral composites have a similar distribution, with the jet often positioned below the 400-meter height mark, there are greater differences between Niños and Niñas. Whereas the jet height median for the Niño composite is about 300 m (Table

4.1), it reaches more than 375 m during Benguela Niña. When compared with the other composites, the jet height has less variability during Niños, with 50% of the values between 275 m and 400 m. Between February and March, the jet is placed at a height of nearly 1000 m in the Niño composite (Figure 4.31, for example).

Table 4.1 – Values of jet height corresponding to the percentiles represented in Figure 4.32 (left).

	Jet height (m)			
Percentile	**Full**	**Niño**	**Niña**	**Neutral**
10th	243,75	241,42	247,14	243,51
25th	290,02	276,31	292,83	289,65
50th	338,33	300,16	376,47	329,90
75th	542,94	414,60	554,09	540,06
90th	717,30	714,90	717,89	717,27

The wind speed evolution when jet occurs throughout the year is shown in Figure 4.33. The full and neutral series easily corroborate the known jet wind cycle: higher intensities during the austral spring months, with a lesser peak in the autumn. It is also clear that the occurrence of Benguela Niña events enhances the jet wind speeds, especially in the first half of the year. Yet, it is surprising to see that, contrary to what has been perceived, the stronger jet occurrences appear to manifest in the Niño composite. The statistical information regarding the wind speed for each SST composite (before computing the annual climatologies) presented in Figure 4.32 (left) and Table 4.2 show that the visual analysis may be misleading. Overall, the median, the third quartile and the 90th percentile of wind speed are lower during Niños than Niñas, with about 1 m/s difference between the two composites. Furthermore, the jet seems more frequent during the Niña annual cycle, with several strong wind maxima throughout the whole year (Figure 4.33).

Table 4.2 – Values of wind speed corresponding to the percentiles represented in Figure 4.32 (right).

	Wind speed (m/s)			
Percentile	**Full**	**Niño**	**Niña**	**Neutral**
10th	3,27	3,09	3,34	3,28
25th	5,35	5,11	5,63	5,32
50th	8,76	8,24	9,28	8,70
75th	11,94	11,37	12,52	11,86
90th	14,54	14,02	15,03	14,46

An interesting feature revealed by this analysis is the vertical extension of the northern core of the Benguela CLLJ. A higher jet wind speed does not imply the feature is thicker, nor is placed higher. All the composites show that while the jet is more intense during the austral spring, its core lays higher in the atmosphere during the first and last months of the year, while its vertical extension is not linear to either height or wind speed.

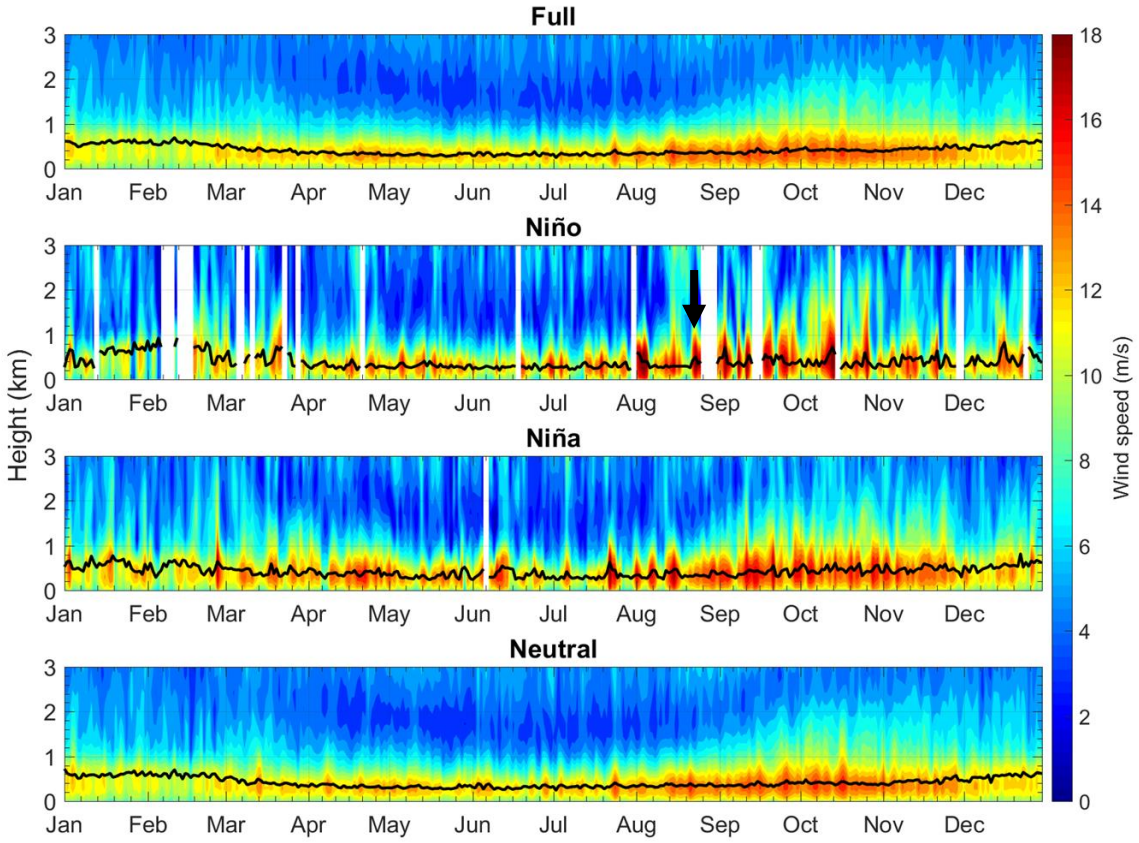

Figure 4.33 – As in Figure 4.31, but for the wind speed. Black arrow indicates an example referenced in the text.

Given that the present work analyses the ocean-atmosphere interactions, the MABL height should also be considered. Several methods may be used to determine this property (e.g., Melgarejo and Deardorff, 1974; White and Wolfe, 1991; Collaud Coen *et al.*, 2014), one of which using the vertical potential temperature profile. A maximum potential temperature gradient indicates a temperature inversion, and is a widely used proxy for the boundary layer height (Stull, 1988). Figure 4.34 displays the vertical potential temperature gradient. In general, the jet is placed below the MABL height, which is evidenced here as the strongest vertical temperature gradient values (yellow to brown colours), i.e., the temperature inversions. As with the jet wind speed, although these gradients are more frequent during the Benguela Niña annual cycle, they appear stronger during the Niños. Even so, a stronger inversion does not necessarily imply a stronger jet nor a higher height. Taking, for instance, the last maximum wind speed (Figure 4.33) value in August for the Niño composite (black arrow): though it is greater than 16 m/s, the corresponding $\frac{d\theta}{dz}$ (Figure 4.34, see black arrow) does not reveal a strong inversion. Furthermore, its height is lower than the February value identified in the figure (red circle), when the potential temperature gradient is still weaker than that of the first example given.

During Benguela Niño events the ocean surface is anomalously warm. Aside from the surface and cross-section analyses, the potential temperature vertical annual cycle shows that the air in the first kilometre is mostly warmer than the neutral case. As the surface warms, the latent heat flux, i.e., evaporation, also intensifies. Compared to the Niña composite, the Niño annual cycle shows a higher variability in the latent and also sensible heat fluxes, especially towards the second half of the year (Figure 4.35). This is also true for the momentum flux (Figure 4.36). It would be expected that as the surface is warmer, the content in water vapour would also increase (see Figure 4.18). However, the specific humidity has no significant signature over neither the potential temperature, its vertical gradient,

nor the jet wind speed and height, for the Niño and Niña composites (figures 4.37 to 4.39). Because these are conditioned by the occurrence of the BCLLJ, once the jet is characterised by high wind speeds, there is more low-level transport, which is the reason behind the lack of variability in the specific humidity series.

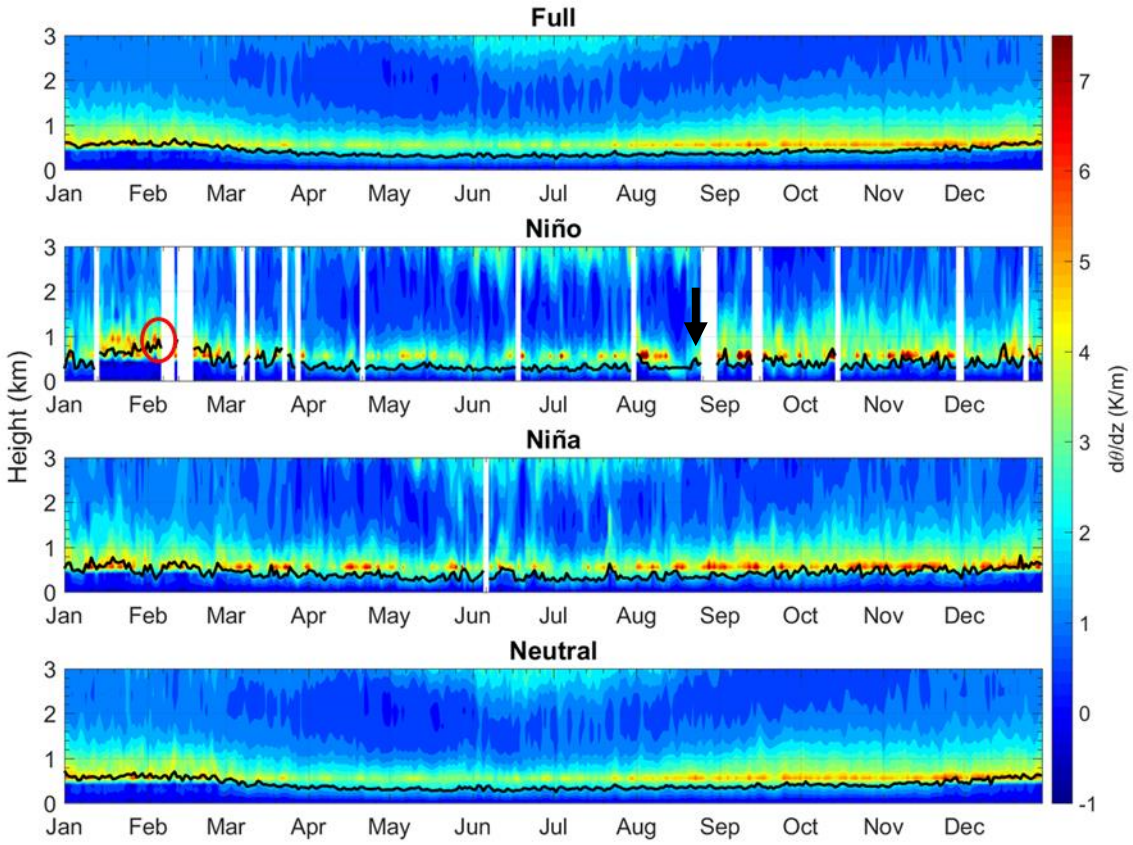

Figure 4.34 – As in Figure 4.31, but for the vertical gradient of potential temperature. Black arrow and red circle indicate an example referenced in the text.

There is a link between the surface heat fluxes and the jet height (Figure 4.35). A peak (both maximum and minimum) in the fluxes is often in accordance with the position of the jet core, especially in the Benguela Niña composite, in the austral winter. The black arrows show an example of a local minimum and maximum of the heat fluxes series coincident with a local minimum and maximum of the jet height, respectively. These changes in the heat fluxes, however, follow the modifications of the jet height only to a certain extent; an intensification on the latent or sensible heat fluxes does not necessarily imply a linear increase on the jet height. Additionally, the heat fluxes peaks are also somewhat consistent with the jet wind speeds, as depicted by the black arrows in Figure 4.36. Again, these fluctuations are not linear to the jet intensity, but are important nonetheless, for they give an insight of the physical setting that governs the Benguela CLLJ during Niño and Niña events. The momentum flux also contributes to the development of a stronger jet (Figure 4.38). As the surface heat fluxes promote turbulence in the MABL, it is not surprising that the variability of the momentum flux is similar to that of the latent and sensible heat fluxes. As such, it is also related to the jet wind speed. The momentum flux annual cycle for the Benguela Niña composite describes the jet intensity particularly well.

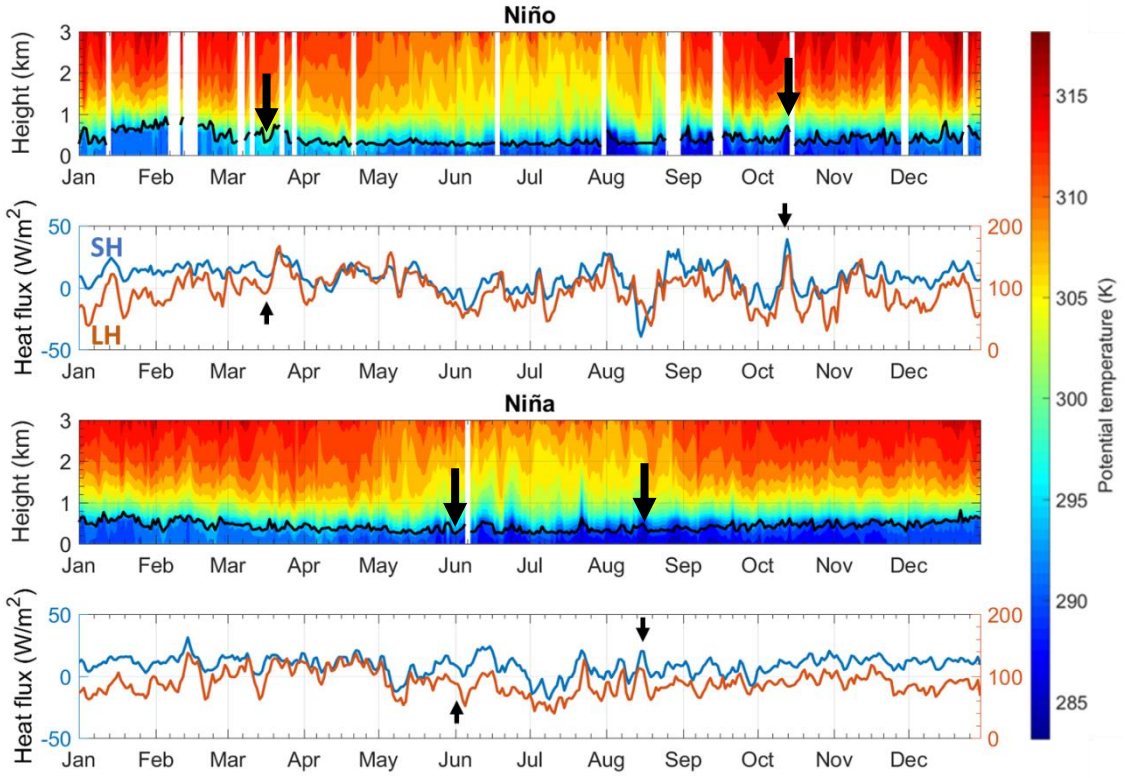

Figure 4.35 – The first and third panels show the mean annual cycle of potential temperature from the surface up to 3 km, when jet occurs, averaged for Benguela Niño and Niña, respectively. The second and forth panels show the mean annual cycle of sensible (blue) and latent (orange) heat fluxes, averaged for the Benguela Niño and Niña, respectively. Black arrows indicate examples referenced in the text.

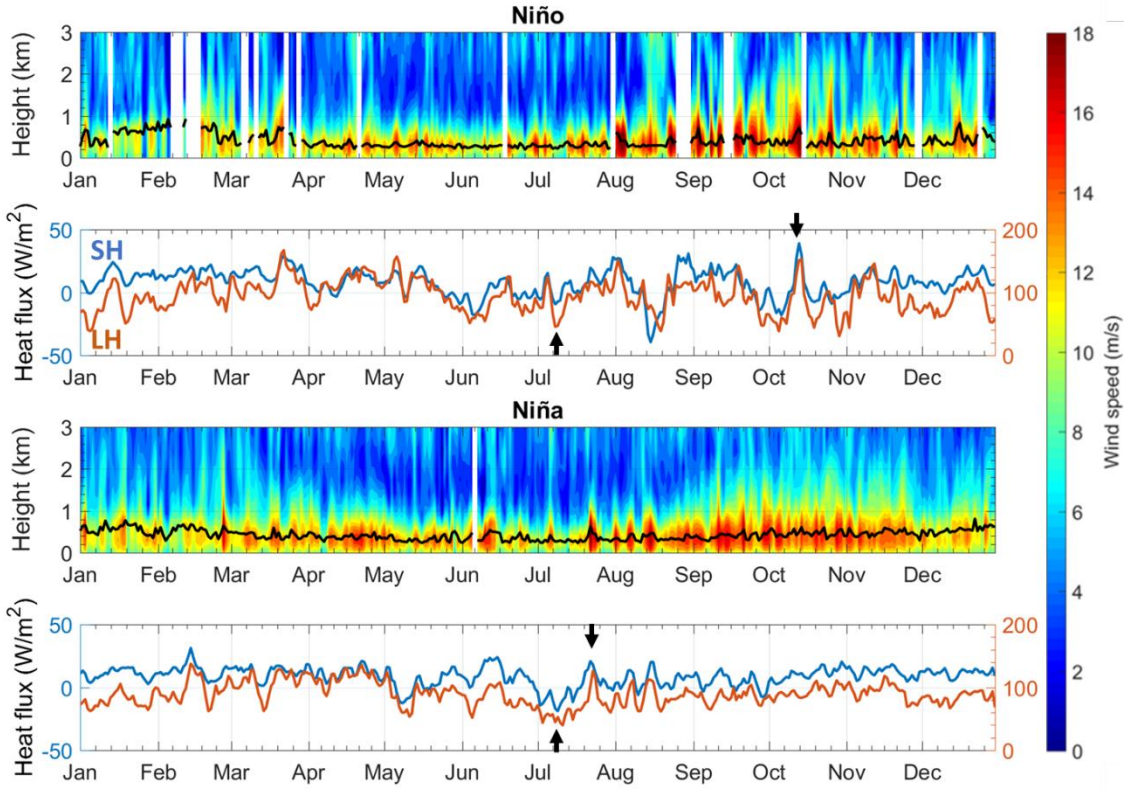

Figure 4.36 – As in Figure 4.35, but for wind speed on first and third panels. Black arrows indicate examples referenced in the text.

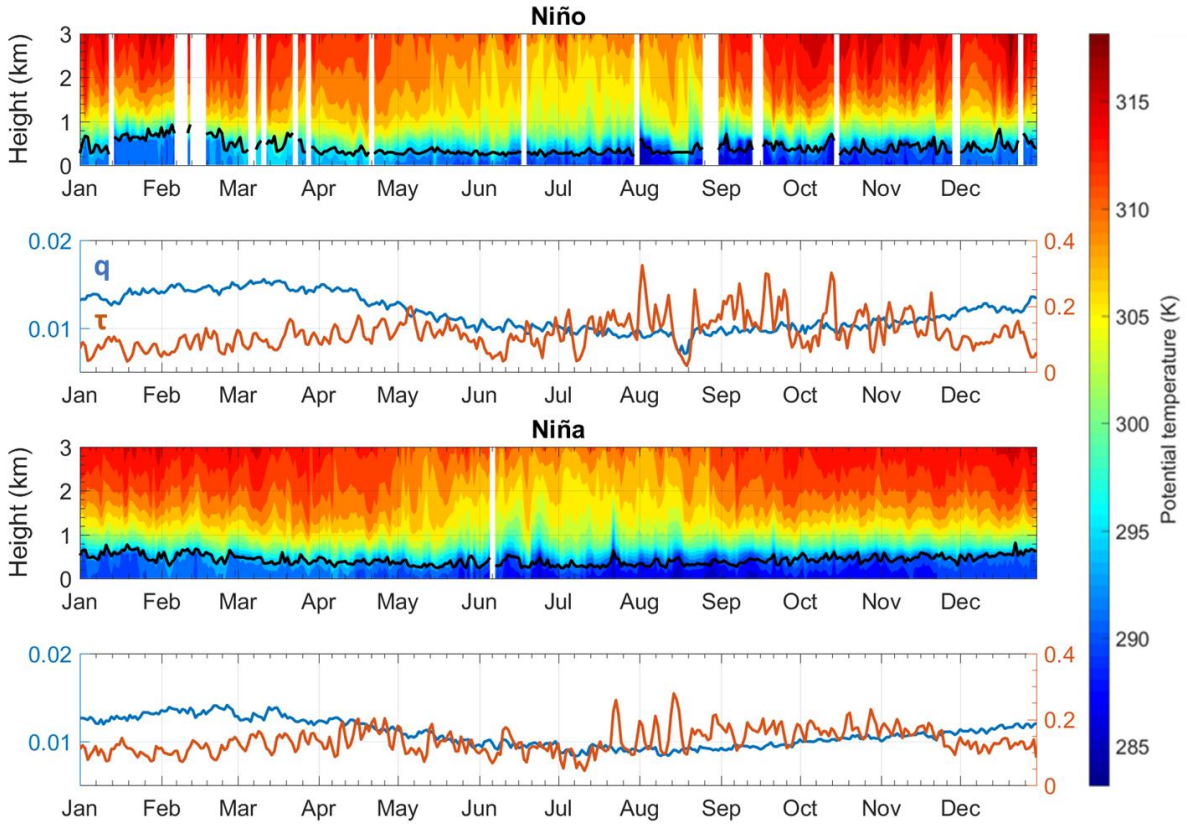

Figure 4.37 – As in Figure 4.35, but for the specific humidity (q) and momentum flux (τ) on second and forth panels.

Altogether, the three fluxes explain the jet intensity to some extent. However, there are instances in which the jet occurs but this reasoning is not applicable. For example, there is a jet core speed greater than 14 m/s in mid-August in the Niño composite. Still the heat and the momentum fluxes almost reach a local minimum. As such, the core does not appear to be associated to the fluxes, as the other Niño-cores. The MABL is not well-mixed either, with an almost non-existent temperature inversion (Figure 4.39). It also has higher potential temperature values than, for example, the beginning of August (when the most intense jet core is found in this composite). This fact alone shows how the interaction between the atmosphere and the ocean surface is highly complex, especially during Benguela Niño events. In future studies, a deeper analysis on the physical variables and/or a different approach than the one used here should be considered in order to further comprehend what drives the CLLJ during the Benguela Niño.

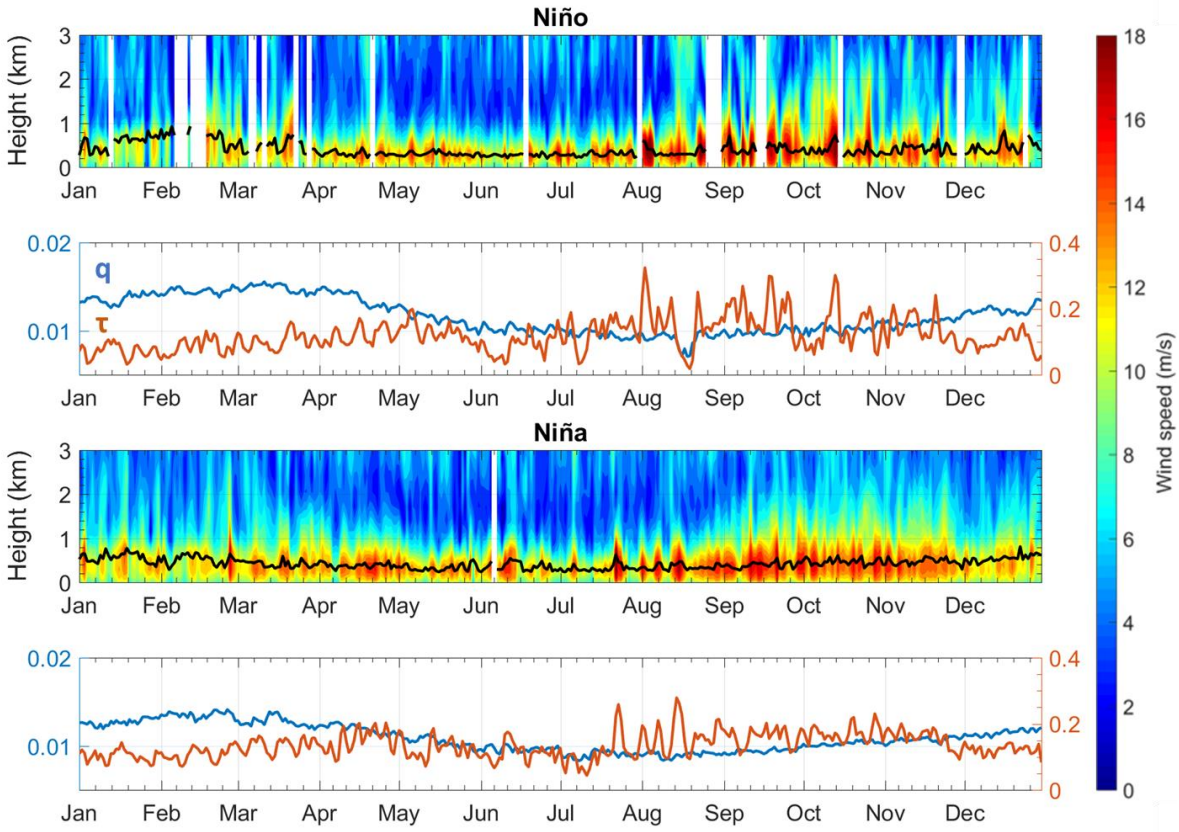

Figure 4.38 – As in Figure 4.37, but for the wind speed in first and third panels.

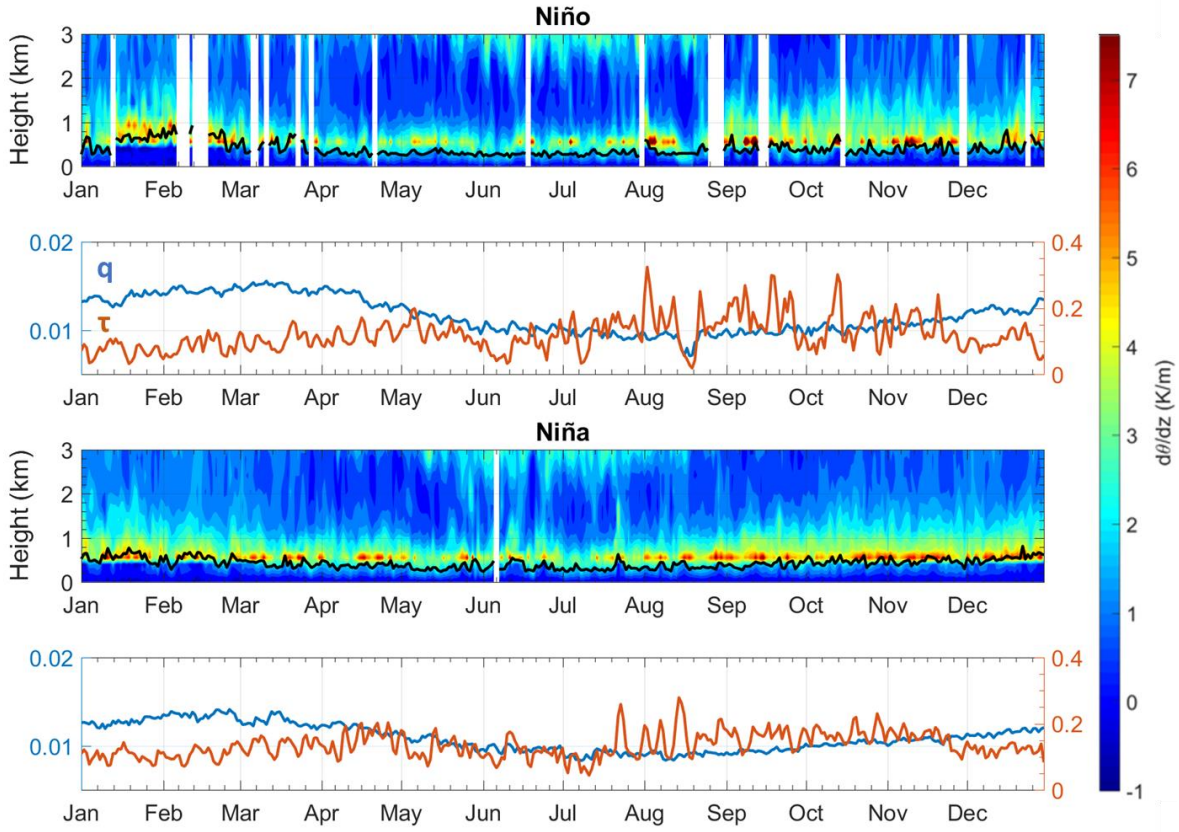

Figure 4.39 – As in Figure 4.37, but for vertical gradient of potential temperature in first and third panels.

5. Summary and conclusions

For the first time, it is presented an analysis of the vertical structure of the marine atmospheric boundary layer when both the Benguela Niño and the northern core of the BCLLJ manifest, establishing a connection between the two phenomena. The present work provides an analysis on the physical settings associated with the Benguela Niño (and Niña) events when the coastal low-level jet occurs in the Angola-Benguela Area. For this purpose, two groups of three composites each were computed, for the period between 1980 and 2016. The first comprises a time average for the cases in which the Benguela CLLJ is strong (series values above the 90th percentile), weak (values below the 10th percentile) and neutral. The second follows a similar methodology based on SST anomalies and includes a time average for the Benguela Niño, Niña and neutral events. Several physical variables were averaged over each setting, such as temperature and wind speed fields, and heat and momentum fluxes, in order to understand the background of each composite. However, it should be mentioned the limited time period studied, and hence the few episode sampling for each computed SST composite.

Through a set of conditions, it was demonstrated that the jet is heavily influenced by the local surface wind. The occurrence of the former, however, is not a necessary and sufficient condition for the intensification of the latter, suggesting that other factors influence the surface wind. As such, in order to assess the Benguela coastal low-level jet, the wind speed at the jet height should be analysed instead of the surface wind field, as some authors suggest. This contradiction is also somewhat supported by the opposite slope trends of the ABA averaged time series for the jet and surface wind speeds. It was shown here that whereas the surface wind is intensifying, the jet intensity has been weakening and been less frequent during the period 1980-2016.

There is also evidence that the physical background that sustains strong (weak) occurrences of the Benguela CLLJ is analogous to that of the Benguela Niña (Niño). During Benguela Niña (Niño) events, the CLLJ is shown to be stronger (weaker) and more (less) frequent than the neutral cases. This work shows that the Benguela Niño and Niña are connected to the coastal low-level jet, as the analysed physical properties suffer changes inherent to the SST-anomalous events.

The annual cycle of the averaged SST composites given the occurrence of the jet was computed for the first three km of the troposphere. Essentially two interesting features are found from this methodology. The surface analysis shows that the jet is weaker during Niños and enhanced with Niñas, which is corroborated by the wind speed distribution analysis computed for the SST composites. However, the vertical analysis shows an apparent intensification of the jet during the Niño, compared to the Niña composite, during the austral spring months. It is also shown that the jet is mostly placed higher in the MABL during Niñas, and has less variability during Niños. In one case, the jet was placed at almost 1000 m above sea level. Overall, the jet is localised below the MABL inversion height and influences the MABL for many hundreds of meters.

The latent and sensible heat fluxes, as well as the momentum flux have impact on the jet. On the other hand, the specific humidity has no clear influence over the feature. A maximum or minimum peak in the fluxes series often corresponds to an intensification or weakening of the jet, though not linearly. There are also situations in which the jet wind speed is intense but none of the explored variables can explain that occurrence. This proves that the Angola-Benguela region harbours many complex interactions. Therefore, the relationship between the Niños and the jet is not fully understood by only these variables and/or methodology alone. The vertical structure of the jet itself also appears to be forced by other, or a combination of, factors not explored in this work.

Furthermore, the present study demonstrates how the horizontal spatial analysis of the surface wind field is insufficient to study the development of the low-level jet, whether by itself or in conjugation

with other physical phenomena, such as the Benguela Niño. The relationship between such two features is much more complex than what the surface analysis transpires, and it affects the whole vertical extension of the MABL.

Last but not least, this work set some paths for future research. In particular, a longer analysis period should be considered for a larger sampling of Benguela Niño events and more statistically significant results. Regarding the Benguela CLLJ, it is still not clear what influences its vertical extension. For this and for an overall understanding of the complex ocean-atmosphere interactions governing the Benguela region, other sets or combination of physical properties should be assessed, in particular using ocean-atmosphere coupled simulations.

REFERENCES

Ackerman, S., Knox, J., 2003: Understanding the atmosphere. *Thomson learning*. Canada.

Bakun, A., Black, B.A., Bograd, S. J., García-Reyes, M., Miller, A.J., Rykaczewski, R. R., Sydeman, W. J., 2015: Anticipated Effects of Climate Change on Coastal Upwelling Ecosystems. *Curr. Clim. Change Rep*., 1: 85.

Beardsley, R. C., Dorman, C.E., Friehe, C.A., Rosenfield, L.K., Winant, C.D., 1987: Local atmospheric forcing during the Coastal Ocean Dynamics Experiment I: a description of the marine boundary layer and atmospheric conditions over a northern California upwelling region. *J. Geophys. Res*. 92:1467–1488.

Bengtsson, L., Hagemann, S., Hodges, K. I., 2004: Can climate trends be calculated from reanalysis data?. *Journal of Geophysical Research: Atmospheres*, 109(D11).

Binet, D., Gobert, B., Maloueki, L., 2001: El Niño-like warm events in the eastern Atlantic (6°N, 20°S) and fish availability from Congo to Angola (1964–1999). *Aquat. Living Resour.* 14, 99–113.

Bonner, W. D., 1968: Climatology of the low level jet. *Mon. Wea. Rev*., 96, 833-850.

Burk, S. D., Thompson, W. T., 1996: The summertime low-level jet and marine boundary layer structure along the California coast. *Monthly Weather Review*, 124(4), 668-686.

Chao, S., 1985: Coastal jets in the lower atmosphere. *J. Phys. Oceanogr*., 15, 361-371.

Cockcroft, A.C., 2001: Jasus lalandii "walkouts" or mass strandings in South Africa during the 1990s: An overview. *Mar. Freshwat. Res*. 52:1085-1094.

Colberg, F., 2004: South Atlantic response to El Niño–Southern Oscillation induced climate variability in an ocean general circulation model. *Journal of Geophysical Research*, 109(C12).

Collaud Coen, M., Praz, C., Haefele, A., Ruffieux, D., Kaufmann, P., Calpini, B., 2014: Determination and climatology of the planetary boundary layer height above the Swiss plateau by in situ and remote sensing measurements as well as by the COSMO-2 model. *Atmospheric Chemistry and Physics*, 14(23), 13205-13221.

Courtier, P., Thépaut, J. N., Hollingsworth, A., 1994: A strategy for operational implementation of 4D-Var, using an incremental approach. *Quarterly Journal of the Royal Meteorological Society*, 120(519), 1367-1387.

Dee, D. P., and Co-authors, 2011: The ERA-Interim reanalysis: configuration and performance of the data assimilation system. *Q. J. Roy. Meteorol. Soc.*, 137, 553-597.

Evans, M., Hastings, N., Peacock, B., 1993: Statistical Distributions. *Wiley*. New York.

Fennel, W., 1999: Theory of the Benguela upwelling system. *Journal of Physical Oceanography*, 29(2), 177-190.

Findlater, J., 1969: A major low-level air current near the Indian Ocean during the northern summer. *Q. J. Roy. Meteorol. Soc*., 95, 274 – 289.

Florenchie, P., Lutjeharms, J. R. E., Reason, C. J. C., Masson, S., Rouault, M., 2003: The source of Benguela Niños in the South Atlantic Ocean. *Geophysical Research Letters*, 30(10).

Florenchie, P., Reason, C. J. C., Lutjeharms, J. R. E., Rouault, M., Roy, C., Masson, S., 2004: Evolution of Interannual Warm and Cold Events in the Southeast Atlantic Ocean. *Journal of Climate*, 17(12), 2318–2334.

Gammelsrød, T., Bartholomae, C. H., Boyer, D. C., Filipe, V. L. L., O'toole, M. J., 1998: Intrusion of warm surface water along the Angolan Namibian Coast in February–March 1995: the 1995 Benguela niño. *African Journal of Marine Science*, 19.

García-Reyes, M., Sydeman, W. J., Schoeman, D. S., Rykaczewski, R. R., Black, B.A., Smit, A. J., Bograd, S. J., 2015: Under Pressure: Climate Change, Upwelling, and Eastern Boundary Upwelling Ecosystems. *Front. Mar. Sci*. 2:109.

García-Serrano, J., Polo, I., Doblas-Reyes, F. J., Haarsma, R. J., 2013: Multi-year prediction of the Atlantic Niño: A first approach from ENSEMBLES. *Física de la Tierra*, 25, 57.

Garreaud, R. D., Muñoz, R. C., 2005: The low-level jet off the west coast of subtropical South America: structure and variability. *Mon. Wea. Rev*., 133, 2246 – 2261.

Gilbert, R. O., 1987: Statistical methods for environmental pollution monitoring. *John Wiley & Sons*.

Hardman-Mountford, N. J., Richardson, A. J., Agenbag, J. J., Hagen, E., Nykjaer, L., Shillington, F. A., Villacastin, C., 2003: Ocean climate of the South East Atlantic observed from satellite data and wind models. *Progress in Oceanography*, 59(2), 181-221.

Harris, R. I., Cook, N. J., 2014: The parent wind speed distribution: Why Weibull?. *Journal of Wind Engineering and Industrial Aerodynamics*, 131, 72-87.

Hirahara, S., Ishii, M., and Y. Fukuda, 2014: Centennial-scale sea surface temperature analysis and its uncertainty. *J of Climate*, 27, 57-75.

Huang, B., Banzon, V. F., Freeman, E., Lawrimore, J., Liu, W., Peterson, T. C., Smith, T. M., Thorne, P. W., Woodruff, S. D., Zhang, H. M., 2015: Extended reconstructed sea surface temperature version 4 (ERSST. v4). Part I: upgrades and intercomparisons. *Journal of climate*, 28(3), 911-930.

Kämpf, J., Chapman, P., 2016: Upwelling Systems of the World. *Springer International Publishing.*

Kobayashi, S., Ota, Y., Harada, Y., Ebita, A., Moriya, M., Onoda, H., Onogi, K., Kamahori, H., Kobayashi, C., Endo, H., Miyaoka, K., Takahashi, K., 2015: The JRA-55 reanalysis: General specifications and basic characteristics. *Journal of the Meteorological Society of Japan*. Ser. II, 93(1), 5-48.

Lachkar, Z., Gruber, N., 2012: A comparative study of biological production in eastern boundary upwelling systems using an artificial neural network. *Biogeosciences*, 9(1), 293-308.

Lima, D. C. A., Soares, P. M. M., Semedo, A., Cardoso, R. M., 2017: A Global View of Coastal Low-Level Wind Jets using an Ensemble of Reanalysis. Submitted to the *Journal of Climate*.

Lübbecke, J. F., Böning, C. W., Keenlyside, N. S., Xie, S.-P., 2010: On the connection between Benguela and equatorial Atlantic Niños and the role of the South Atlantic Anticyclone. *Journal of Geophysical Research*, 115(C9).

Lutjeharms, J. R. E., Meeuwis, J. M., 1987: The extent and variability of South-East Atlantic upwelling. In: Payne AIL, Gulland JA, Brink KH (Eds) The Benguela and Comparable Ecosystem. *Afr J Mar Sci* 5:51–62.

Melgarejo, J. W., Deardorff, J. W., 1974: Stability functions for the boundary-layer resistance laws based upon observed boundary-layer heights. *Journal of the Atmospheric Sciences*, 31(5), 1324-1333.

Muñoz, R. C., Garreaud, R. D., 2005: Dynamics of the Low-Level Jet off the West Coast of Subtropical South America. *Mon. Wea. Rev*., 133, 3661-3677.

Nicholson, S. E., Kim, J., 1997: The Relationship of the El Niño–Southern Oscillation To African Rainfall. *International Journal of Climatology*, 17(2), 117–135.

Nicholson, S. E., 2010: A Low-Level J*et al*ong the Benguela Coast, an Integral Part of the Benguela Current Ecosystem. *Climate Change*, 99, 613-624.

Parish, T. R., 2000: Forcing of the summertime low-level jet along the California coast. *J. Appl. Meteorol*., 39, 2421 – 2433.

Parrish, R. H., Bakun, A., Husby, D. M., Nelson, C. S., 1983: Comparative climatology of selected environmental processes in relation to eastern boundary current pelagic fish reproduction. In: G. D. Sharp & J. Csirke, Proceedings of the Expert Consultation to Examine Changes in Abundance and Species Composition of Neritic Fish Resources, San Jose, Costa Rica, April, 1982. F.A.O. Fisheries Reports, 291, 731–777.

Patricola, C. M., Chang, P., 2016: Structure and dynamics of the Benguela low-level coastal jet. *Clim. Dyn*.

Pauly, D., Christensen, V., 1995: Primary production required to sustain global fisheries. *Nature*, 374, 255–257.

Polo, I., Martin-Rey, M., Rodriguez-Fonseca, B., Kucharski, F., Mechoso, C. R., 2014: Processes in the Pacific La Niña onset triggered by the Atlantic Niño. *Clim Dyn*, 44:115-131.

Ranjha, R., Svensson, G., Tjernström, M., Semedo, A., 2013. Global distribution and seasonal variability of coastal low-level jets derived from ERA-interim reanalysis. *Tellus* A, 65, 20412.

Ranjha, R., Tjernström, M., Semedo, A., Svensson, G., Cardoso, R. M., 2015: Structure and variability of the Oman coastal low-level jet. Tellus A: *Dynamic Meteorology and Oceanography*, 67(1), 25285.

Reason, C. J. C., Smart, S, 2015: Tropical south east Atlantic warm events and associated rainfall anomalies over southern Africa. *Frontiers in Environmental Science*, 3.

Reynolds, R. W., Smith, T. M., Liu, C., Chelton, D. B., Casey, K. S., Schlax, M. G., 2007: Daily High-Resolution-Blended Analyses for Sea Surface Temperature. *Journal of Climate*, 20(22), 5473–5496.

Richter, I., Behera, S. K., Masumoto, Y., Taguchi, B., Komori, N., Yamagata, T., 2010: On the triggering of Benguela Niños: Remote equatorial versus local influences. *Geophysical Research Letters*, 37, l20604.

Risien, C. M., Chelton, D. B., 2008: A global climatology of surface wind and wind stress fields from eight years of QuikSCAT scatterometer data. *Journal of Physical Oceanography*, 38(11), 2379-2413.

Risien, C. M., Reason, C. J. C., Shillington, F. A., Chelton, D. B., 2004: Variability in satellite winds over the Benguela upwelling system during 1999–2000. *Journal of Geophysical Research: Oceans*, 109(C3).

Rogerson, A. M., 1999: Transcritical flows in the coastal marine atmospheric boundary layer. *Journal of the atmospheric sciences*, 56(16), 2761-2779.

Rouault, M., Florenchie, P., Fauchereau, N., Reason, C. J., 2003: South East tropical Atlantic warm events and southern African rainfall. *Geophysical Research Letters*, 30(5).

Saha, S., and Coauthors, 2010: The NCEP Climate Forecast System Reanalysis. *American Meteorological Society*, 91, 1015-1057.

Semedo, A., Soares, P. M. M., Lima, D. C. A., Cardoso, R. M., Bernardino, M., Miranda, P. M. A., 2016: The impact of climate change on the global coastal low-level wind jets: EC-EARTH simulations. *Global and Planetary Change*, 137, 88-106.

Shannon, L. V., Agenbag, J. J., Buys, M. E. L., 1987: Large-and mesoscale features of the Angola-Benguela front. *South African Journal of Marine Science*, 5(1), 11-34.

Shannon, L. V., Boyd, A. J., Brundrit, G. B., Taunton-Clark, J., 1986: On the existence of an El Niño-type phenomenon in the Benguela System. *Journal of Marine Research*, 44(3), 495–520.

Soares, P. M. M., Cardoso, R. M., Semedo, A., Chinita, M. J., Ranjha, R., 2014: Climatology of the Iberia coastal low-level wind jet: weather research forecasting model high-resolution results. *Tellus* A, 66, 22377.

Stensrud, D. J., 1996: Importance of low-level jets to climate: a review. *J. Climate*, 9, 1698-1711.

Strub, P. T., Combes, V., Shillington, F. A., Pizarro, O., 2013: Currents and Processes along the Eastern Boundaries. *International Geophysics*, 103, 339-384.

Stull, R. B. (Ed.)., 1988: An Introduction to Boundary Layer Meteorology. *Springer Netherlands.*

Sumaila, U. R., 2016: Socio-economic benefits of Large Marine Ecosystem valuation: The case of the Benguela Current Large Marine Ecosystem. *Environmental Development*, 17, 244-248.

Talley, L. D., Pickard, G. L., Emery, W. J., Swift, J. H., 2011. Descriptive Physical Oceanography: An Introduction (Sixth Edition), *Elsevier*, Boston, 560 pp.

Trenberth, K. E., 1997: The definition of El Niño. *Bulletin of the American Meteorological Society*, 78(12), 2771-2777.

van der Lingen, C. D., Shannon, L. J., Cury, P., Kreiner, A., Moloney, C.L., Roux, J.-P., Vaz-Velho, F., 2006: Resource and ecosystem variability, including regime shifts, in the Benguela Current system. Benguela: Predicting a Large Marine Ecosystem (First Edition), *Elsevier*, Oxford, 147-184.

Wang, B., 2002: Kelvin Waves. Shankar, M. (Ed.), *Elsevier Science Ltd.*, 7p.

Wang, C., 2006: An overlooked feature of tropical climate: Inter-Pacific-Atlantic variability. *Geophysical Research Letters*, 33(12).

Warner, T. T., 2004: Desert Meteorology. *Cambridge*, 595 pp.

Winant, C. D., Dorman, C. E., Friehe, C. A., Beardsley, R. C., 1988: The marine layer off northern California: an example of supercritical channel flow. *J. Atmos. Sci*., 45, 3588 – 3605.

APPENDIX

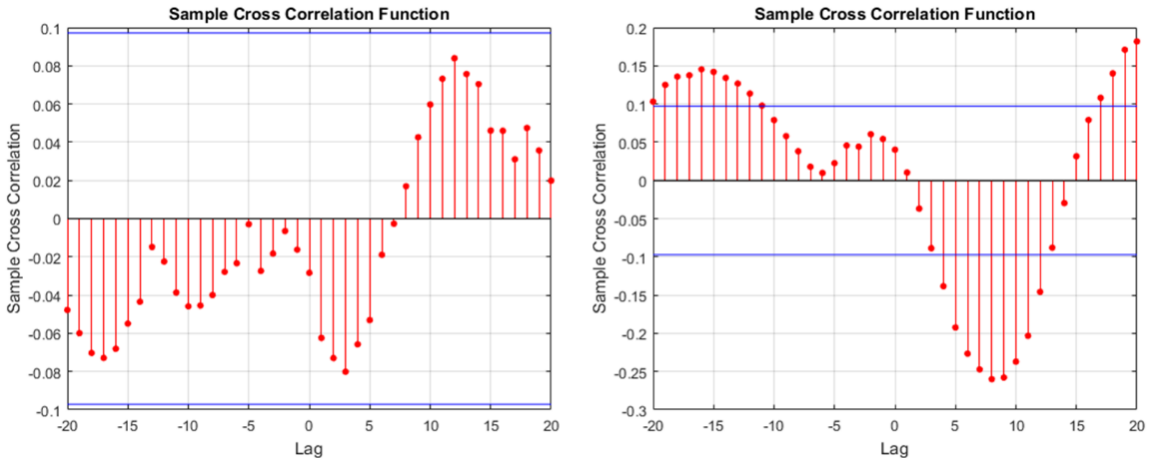

Figure A1 – Cross-correlations between SST Niño 3.4 anomaly and: Benguela surface wind speed anomaly (left), and Benguela SST anomaly (right).

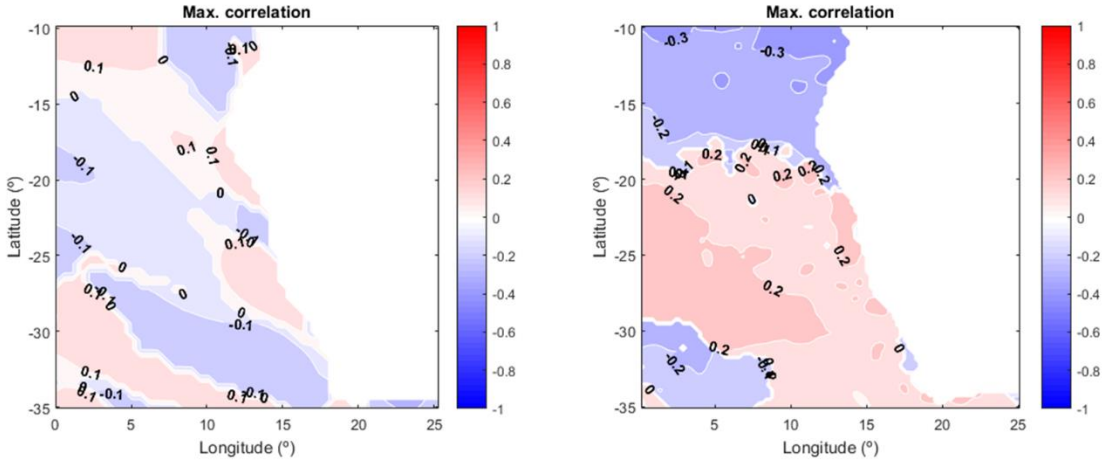

Figure A2 – Maximum correlation between SST Niño 3.4 anomaly and: Benguela surface wind speed anomaly (left), and Benguela SST anomaly (right).

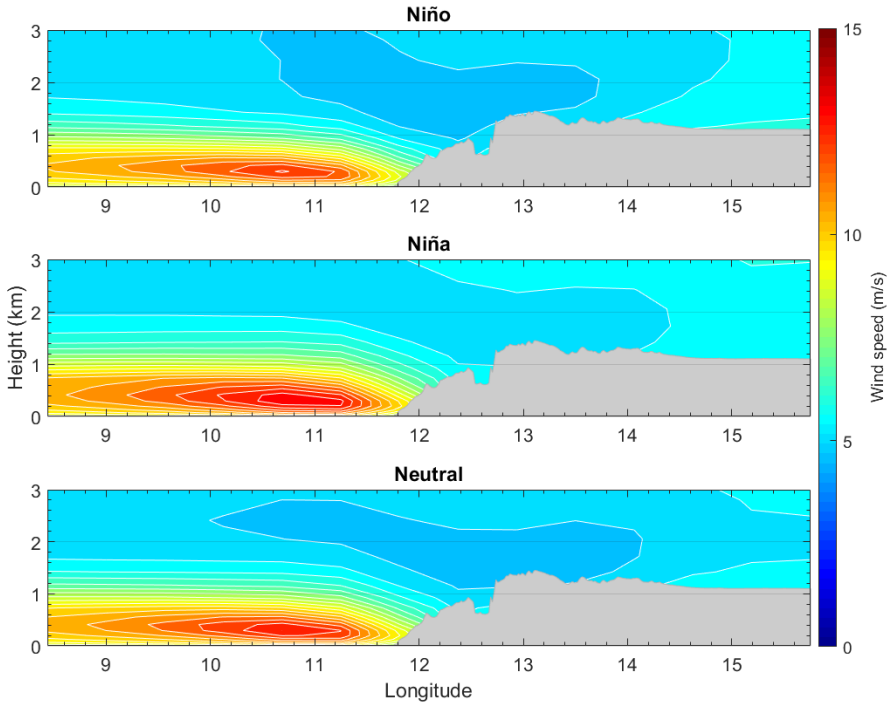

Figure A3 – Vertical distribution of the wind speed intensity for the west–east cross section at the jet northern core, averaged for the cases of strong (top), weak (middle) and neutral (bottom) jet.